Galloway

THE RESPONSE OF THE WATER LEVEL IN A WELL TO ATMOSPHERIC LOADING AND EARTH TIDES: THEORY AND APPLICATION

A DISSERTATION

SUBMITTED TO THE DEPARTMENT OF APPLIED EARTH SCIENCES

AND THE COMMITTEE ON GRADUATE STUDIES

OF STANFORD UNIVERSITY

IN PARTIAL FULFILLMENT OF THE REQUIREMENTS

FOR THE DEGREE OF

DOCTOR OF PHILOSOPHY

By

Stuart Alan Rojstaczer

March 1988

8.3.1.2.3.1

I certify that I have read this thesis and that in my opinion it is fully adequate, in scope and quality, as a dissertation for the degree of Doctor of Philosophy.

(Principal Adviser)

I certify that I have read this thesis and that in my opinion it is fully adequate, in scope and quality, as a dissertation for the degree of Doctor of Philosophy.

I certify that I have read this thesis and that in my opinion it is fully adequate, in scope and quality, as a dissertation for the degree of Doctor of Philosophy.

I certify that I have read this thesis and that in my opinion it is fully adequate, in scope and quality, as a dissertation for the degree of Doctor of Philosophy.

(Civil Engineering)

Approved for the University Committee on Graduate Studies:

Dean of Graduate Studies

every task you undertake
becomes a piece of cake

Mary Poppins

ACKNOWLEDGMENTS

This cake would have never made it into or out of the oven had it not been for the support and influence of many people. Pat Domenico got me started in this business. Irwin Remson magnanimously let me pursue a field of research outside the usual realm of his students in hydrogeology. Duncan Agnew gave me many useful suggestions. Dave Pollard and Dave Freyberg made sure my work was of good quality. Helpful reviews of portions of this dissertation were made by Evelyn Roeloffs, Ed Weeks, Al Moench, Don Bower, John Beavan, Keith Evans and Ken Kipp. Frank Riley, Chris Farrar, Mike Sorey and Mark Clark supplied or aided in the collection of the hydrologic data. John Bredehoeft gave me this project and his enthusiasm and optimism about my work was greatly appreciated.

My friends at Stanford and the U.S.G.S. helped make my work environment unusually amiable. The Friday afternoon basketball crew squelched any hopes I may have had of trading my research career for one in the NBA. My wife, Holly Welstein, and my daughter Claire made sure that all my hours weren't spent lost in space and it is to them that I dedicate my dissertation.

TABLE OF CONTENTS

LIST OF TABLES

LIST OF ILLUSTRATIONS

In the problem of decoding, the most important information we can possess is the knowledge that the message we are reading is not gibberish.

Norbert Wiener

INTRODUCTION

In many wells, the water level fluctuates in response to variations to atmospheric loading and earth tides. The fluctuations are an indicator of the response of pore pressure to rock deformation. When rock is compressed, porosity is reduced and in the absence of any fluid drainage, pore pressure rises. When rock is placed in tension, porosity is increased and in the absence of any fluid sources, pore pressure drops. The strains produced by atmospheric loading and earth tides in rock are small (usually 10^{-7} dilatation or less) and pore pressure response is also small (usually less than 10 millibars pressure). These small variations in rock deformation, while they make measurement of deformation and pore pressure somewhat difficult, are a blessing in disguise. They allow us to examine the response of fluid saturated rock to deformation under conditions where the response is nearly entirely linear and elastic.

If the well is in communication with a rock formation of high horizontal permeability that is completely isolated from the water table, the response of the well is a direct indication of the undrained response of pore pressure to deformation. In this study, well response under these conditions is termed the static-confined

response. Jacob (1940) was the first to recognize that the static-confined response of a well to atmospheric loading was strongly dependent on the porosity and drained compressibility of the rock. Bredehoeft (1967) found that the static-confined responses of a well to atmospheric loading and earth tides could be used to estimate rock porosity and matrix compressibility. Van der Kamp and Gale (1983) refined the analyses of Jacob (1940) and Bredehoeft (1967) to allow the rock grains, as well as the rock matrix, to be compressible. In Chapter 1, I modify the analysis of Van der Kamp and Gale (1983) by including the influence of horizontal deformation on the response of the water level in a well to atmospheric loading. I also apply the theory developed in the chapter to determine rock compressibility and porosity from the response of five wells to atmospheric loading and earth tides.

The response of water wells to earth tides suggests that water wells can be used to monitor small tectonic strains in the earth which occur over periods of hours to months. Johnson et al. (1973; 1974) were the first to exploit the potential of a water well as an indicator of tectonically induced deformation. The principal problems with using water wells a strain meters are: 1) the water table is largely insensitive to rock deformation and any hydraulic communication between the rock formation tapped by the well and the water table serves to dampen well sensitivity; 2) long and short term variations in precipitation also influence the water level in a well and this influence degrades the quality of the strain signal in the well. In Chapter 2, I examine the quality of a water well as a strain meter for strains produced by atmospheric loading and earth tides

which occur over a period of hours to weeks. I develop a theory which describes the response of a well to deformation under conditions where the water table influences well response. I then apply this theory to examine the sensitivities and noise levels of two water wells which were used as strain meters in areas of active deformation and compare their overall quality as strain meters with other conventional indicators of small crustal deformation.

Although water table drainage adversely effects the quality of a water well as a strain meter, this phenomenon when analyzed in detail can be exploited as a hydrologic tool. The insensitivity of the water table to deformation induces vertical fluid flow between the zone of rock tapped by the well and the water table; in the case of atmospheric loading water table insensitivity also induces vertical air flow in the unsaturated zone. The fluid flow in the unsaturated and saturated materials causes the response of a water well to atmospheric loading to be dependent on the frequency of the atmospheric load signal. Fluid flow between the well and the saturated rock can, if the rock has low permeability, also cause the sensitivity of a well to atmospheric loading to be a function of the frequency of the atmospheric load. In Chapter 3, I develop theoretical frequency response curves which describe the influence of air flow and groundwater flow on the sensitivity of a well to atmospheric loading under conditions where the rock tapped by the well is separated from the water table by a partial confining layer. These frequency response curves are dependent on the air diffusivity of the unsaturated zone, the vertical hydraulic diffusivity of the partial confining layer and the permeability of the rock tapped by the

well. I then examine the frequency response of three wells to atmospheric loading and fit the theoretical curves to the observed response. The fit to the data provides an estimate of the saturated and unsaturated fluid flow properties of the rock in hydraulic communication with the well.

In Chapter 4, theoretical frequency response curves are developed which describe the influence of air flow and vertical groundwater flow on the response of wells which tap unconfined aquifers to atmospheric loading. These theoretical curves are compared with the theoretical response under paritially confined conditions and help explain why wells which tap unconfined aquifers can sometimes exhibit a high sensitivity to rock deformation. They can also be used to provide an estimate of the vertical air diffusivity of the unsaturated zone and the vertical permeability of the aquifer.

The overall purpose of all the chapters in this dissertation is to show that the response of a water well to atmospheric loading and earth tides is systematic and has a sound physical basis. When we examine the response of a water wells to these imposed deformations the message we read is not gibberish. The message that the water wells give in response to rock deformation is dependent on the material properties of the rock directly and indirectly tapped by the well. The message can be decoded to determine the hydraulic and mechanical properties of rock. The message can also be decoded to identify small strain events in the earth if these strains occur over periods of hours to weeks.

REFERENCES

Bredehoeft, J. D., Response of well-aquifer systems to earth tides, J. Geophys. Res., 72, 3075-3087, 1967.

Jacob, C. E., The flow of water in an elastic artesian aquifer, Eos Trans. AGU, 21, 574-586, 1940.

Johnson, A. G., R. L. Kovach, and A. Nur, Fluid pressure variations and fault creep in Central California, Tectonophysics, 23, 257-266, 1974.

Johnson, A. G., R. L. Kovach, A. Nur, and J. R. Booker, Pore pressure changes during creep events on the San Andreas Fault, J. Geophys. Res., 78, 851-857, 1973.

Van der Kamp, G. and J. E. Gale, Theory of earth tide and barometric effects in porous formations with compressible grains, Water Resour. Res., 19, 538-544, 1983.

Teach us to sit still

T. S. Eliot

CHAPTER 1

THE STATIC RESPONSE OF THE WATER LEVEL IN AN OPEN WELL TO AREALLY EXTENSIVE DEFORMATION UNDER CONFINED CONDITIONS

ABSTRACT

The static response of the water level in an open well to deformation under confined conditions is dependent on the matrix and solids compressibility, porosity and Poisson's ratio of the formation that the well taps as well as the compressibility of the pore fluid. High sensitivity to earth tides is favored in formations of low porosity and matrix compressibility. High sensitivity to atmospheric loading is favored in formations of high porosity and low matrix compressibility. The material properties which govern the static-confined response of the well also strongly influence vertical fluid flow induced by areally extensive deformation. These material properties can be combined to define two types of specific storage, one which applies under conditions of atmospheric loading and one which applies under conditions of earth-tide induced subsurface fluid flow. Given equal formation material properties, the hydraulic diffusivity which governs fluid flow in response to atmospheric loading will be slightly smaller than the hydraulic diffusivity which governs fluid flow in response to earth tides. If the static-confined

response of water wells to atmospheric loading and earth tides can be observed or inferred, it can be used to obtain approximate in-situ estimates of matrix compressibility and porosity. These estimates can in turn be used to determine the one-dimensional specific storage of the formation. Analysis of the static-confined response of five wells to atmospheric loading and earth-tides indicates that the approach yields reasonable estimates of formation material properties.

INTRODUCTION

Fluctuations in water level due to atmospheric loading, earth tides and seismic events have long been noted in many wells. These fluctuations are principally of interest to geophysicists and hydrologists for two reasons: they indicate that water wells can serve as sensitive indicators of crustal strain; they contain some essential information about the material properties of the rock and/or sediment that they tap. When the response of the water level in a well to areally extensive deformation occurs under conditions where neither well bore storage or water table drainage are of influence, water level changes are a direct reflection of the undrained response of the formation. Following hydrologic convention, we define water level changes under these conditions as the static-confined response. The static-confined response cannot always be expected to be observed in a well. The response to high frequency deformation may be influenced by well bore storage; the response to low frequency deformation may be influenced by water table drainage (see Chapters 2,

3 and 4). However, if it can be observed or inferred, the static-confined response is a useful geophysical and hydrologic parameter. In terms of the application of water wells to geodesy and seismology, the static-confined response represents (in the absence of significant resonance) the maximum sensitivity we can expect to areally extensive strain. It also is an indicator of some material properties of the formation which govern its elastic response and its ability to diffuse fluid pressure. Applications of theoretical models which describe the response of water wells to areally extensive deformation can yield some information on the performance of water wells as strain meters and provide estimates of formation fluid flow and elastic properties.

Many workers have theoretically examined the static-confined response of wells to atmospheric loading and earth tides. Jacob (1940) recognized that the undrained response of rock and sediment to atmospheric loading was dependent on the formation's elastic properties and porosity. Bredehoeft (1967) noted that the undrained response of rock and sediment to earth tides was proportional to the formation's response to atmospheric loading. The analyses of both Jacob (1940) and Bredehoeft (1967) were done in terms of a deforming coordinate system. Relations between areally extensive deformation and formation response in terms of a fixed coordinate system were developed by Robinson and Bell (1971) and Rhoads and Robinson (1979). Van der Kamp and Gale (1983) extended the results of Jacob (1940) and Bredehoeft (1967) to allow for grain compressibility.

The potential of water wells as strain meters has been discussed in detail (Bredehoeft, 1967; Bodvarsson, 1970; see Chapter 2), and some attempts have been made to use the response of the water level in

a well to known areally extensive strains as a strain calibration tool. Johnson et al. (1973; 1974) used the response of a well near the San Andreas fault to atmospheric loading to calibrate its response to creep events. Savage and Gu (1985) noted that long term changes (on the order of several years) in water level in wells near Palmdale, California could be correlated with a geodetically inferred strain event. Sterling and Smets (1971) quantified the response of a well in Belgium to atmospheric loading and earth tides and described its behavior as a strain seismograph. Bower and Heaton (1978) calibrated a well near Ottawa, Canada to the local earth tide and noted that its co-seismic response to the great Alaskan earthquake of 1964 could not readily be explained on the basis of the static strain field produced by the earthquake.

In comparison to the application of water wells as strain meters, considerably more work has been focused on analyzing the static-confined response of wells to atmospheric loading and earth tides in an effort to determine formation material properties. Bredehoeft (1967) showed that it was possible to estimate formation compressibility and porosity on the basis of the undrained response of a formation to atmospheric loading and earth tides. Although the general approach of Bredehoeft (1967) has been seriously questioned (Narasimhan et al., 1984), investigations by Van der Kamp and Gale (1983) and Hsieh et al. (1988) reaffirm its correctness. Analyses of the observed response of water wells to atmospheric loading and earth tides similar to that of Bredehoeft (1967) have been made by others (Robinson and Bell, 1971; Marine, 1975; Rhodes and Robinson, 1979;

Hanson, 1980) in an effort to determine formation elastic properties and/or porosity.

Several assumptions are commonly made in the analysis of wells response to atmospheric loading and earth tides which are often inappropriate. One assumption is that the observed response is independent of frequency and reflects the static-confined response of the formation. If fluid flow influences response, this assumption can lead to a severe underestimation of the undrained sensitivity of the formation to strain (see Chapters 2, 3 and 4). Another assumption is that the matrix compressibility is much greater than the solids compressibility; while this assumption is appropriate for the response of unconsolidated materials it is likely to be inappropriate for most rock (Van der Kamp and Gale, 1983). Finally, a third common assumption is that atmospheric loading induces strictly vertical deformation; this assumption is not always valid and determination of formation material properties based on this assumption can lead to considerable error.

In this paper we remove the above assumptions and analyze the static-confined response of water wells to atmospheric loading and earth tides in theory and in practice. We examine the sensitivity of wells to earth tides and tectonic strain using the results of Van der Kamp and Gale (1983) which incorporate grain compressibility. We then examine the theoretical response of wells to atmospheric loading through the formalism of Rice and Cleary (1976) which describes (in a distilled form) the poro-elastic theory of Biot (1941); this response differs from that given by Van der Kamp and Gale (1983) because of the incorporation of the effects of horizontal deformation. As a result

of this modification we find that the elastic parameter which governs vertical fluid flow in response to areally extensive strain (the specific storage) differs for atmospheric-loading and earth-tide induced strains. We then apply the theoretical results to the response of five wells to strain and correct for the influence of fluid flow in order to obtain in-situ estimates of rock compressibility, porosity and the specific storage of the formation.

STATIC-CONFINED RESPONSE OF WELLS TO CUBIC STRAIN

Before we examine the response of wells to earth tides and atmospheric loading, it is useful to examine the response of wells to cubic strain. If we take extension to be positive, the relation between cubic strain, ϵ_r, and water level under static-confined conditions can be obtained from the effective stress relation of Nur and Byerlee (1971):

$$\epsilon_r = \beta (\bar{\sigma} + \alpha P) \qquad (1)$$

where β is the drained matrix compressibility, $\bar{\sigma}$ is the mean stress (1/3 the sum of the principal stresses), α is the fraction of rock strain taken up by the pore space under drained conditions (Biot and Willis, 1957) and P is the pore pressure. Nur and Byerlee (1971) relate α to the drained compressibility of the matrix, β , and the solid grains, β_u, through the following relation:

$$\alpha = 1 - \beta_u/\beta \qquad (2)$$

The relation between the mean stress and the pore pressure is (Skempton, 1954; Bishop, 1966):

$$P = -B\sigma \tag{3}$$

where B is :

$$B = \frac{(\beta - \beta_u)}{(\beta - \beta_u) + \phi(\beta_f - \beta_u)} \tag{4}$$

and β_f is the fluid compressibility. We employ the notation of Green and Wang (1986) in the above and subsequent derivations. As noted by Green and Wang (1986), the above definition of B assumes that the rock matrix is homogeneous and all the pore space is interconnected. Substituting equation 2 into 1 and dividing by ρg yields the following relation between water level and cubic strain:

$$W = \frac{-\alpha\epsilon_r}{\rho g[\phi(\beta_f - \beta_u) + \beta_u \alpha]} \tag{5}$$

The dependence of the static-confined response of water wells to an imposed cubic strain, ϵ_r, on material properties is shown in Figure 1-1. Water well sensitivity is given in terms of a static-confined dilatational efficiency, DE', which represents the amount of water level drop in centimeters per cubic nanostrain extension:

$$DE' = -W/\epsilon_r \tag{6}$$

As shown in the figure, water well sensitivity is largely independent of matrix compressibility unless matrix compressibility is very low. High dilatational efficiency is favored for low porosity formations. We can generally expect wells which tap formations with porosity less than 0.25 to have a static-confined dilatational efficiency of at least 0.05 cm/nε. Since water level monitoring equipment which can resolve water level changes on the order of 0.1 cm is readily available, it is possible in the absence of fluid flow influences to detect changes in dilatation on the order of 1 nanostrain in most wells. As noted by others (Bredehoeft, 1967; Bodvarsson, 1970), such a high level of sensitivity makes water wells attractive as strain meters. However, as will be shown below, it is not always possible for earth tides and tectonic strain to generate significant cubic strains near the earth's surface under confined conditions.

STATIC-CONFINED RESPONSE TO EARTH TIDES

Water well response to earth tides are of value because the areal strains produced by earth tides can be approximately determined from theoretical calculations (Beaumont and Berger, 1975; Berger and Beaumont, 1976). Because the areal strain is approximately known, the response of water wells to earth tides serves as a strain calibration tool. It is commonly assumed that at typical well depths the vertical stresses induced by earth tides are so small that they can be ignored (Bredehoeft, 1967), and we make the same assumption. This assumption essentially states that earth tide deformation occurs under conditions of plane stress. Under conditions of plane stress, the relation

between water level and a known areal strain, ϵ_{2r}, can be obtained from the results of Van der Kamp and Gale (1983):

$$W = -3\epsilon_{2r}(1-2\nu)\gamma'/(\rho g\beta\ (1+\nu)) \qquad (7)$$

where γ' is the negative of the ratio of pore pressure to vertical stress under conditions of undrained, one-dimensional, vertical strain:

$$\gamma' = \frac{B(1+\nu)}{3(1-\nu)-2\alpha B(1-2\nu)} \qquad (8)$$

and ν is the drained Poisson's ratio of the formation.

The static-confined response of a water well to an areal dilatation, ϵ_{2r}, is shown in Figure 1-2. The response is expressed in terms of the static-confined <u>areal</u> dilatational efficiency, DE'_a, of the well which represents the water level drop in centimeters per areal nanostrain extension (the areal nanostrain is the sum of the principal horizontal strains):

$$DE'_a = -W/\epsilon_{2r} \qquad (9)$$

Like the response of a water well to cubic strain, high sensitivity is favored by low porosity; unlike the response of water well to cubic dilatation, the sensitivity is a strong function of matrix compressibility. High matrix compressibilities are indicative of low well sensitivity. The reason for this inverse relation between

compressibility and well sensitivity is due to the substantial vertical deformation induced by the presence of the pore fluid when horizontal strain is imposed under undrained, plane stress conditions. For high compressibility materials, the undrained Poisson's ratio approaches 0.5 and the volumetric change produced by the imposed horizontal strain approaches 0.

Since it might be expected that deep wells would tap relatively stiff, low porous rock, the results shown in Figure 1-2 are in accordance with the observation of Roeloffs (1987) that earth tide sensitivity tends to increase with well depth. If we use earth tide sensitivity as an indicator of sensitivity to tectonic strain, the implication of Figure 1-2 for the use of water wells as strain meters is clear: independent of any fluid flow considerations, installation of water wells for strain monitoring purposes should be done in stiff, low porous formations. Wells which tap highly compressible rock and/or sediment can expected to be relatively insensitive to tidal and tectonic strains. It is useful to examine the response of a typical formation to earth tides in order to infer what may be expected in terms of strain sensitivity. Given a matrix compressibility of 1×10^{-11} cm^2/dyne and a porosity of 0.10, a well will have a static-confined areal dilatational efficiency of 0.06 cm/nε. This sensitivity is greater than the static-confined areal dilatational efficiency of the wells examined later in this study; the formations these wells tap possess higher compressibility and/or porosity than the values given above.

STATIC-CONFINED RESPONSE TO ATMOSPHERIC LOADING

The strains induced by atmospheric pressure are quite different from those induced by earth tides and tectonic events: they are produced under conditions where both vertical stresses and horizontal stresses are significant (Farrell, 1972; Rabbel and Zschau, 1985). In an open well, atmospheric pressure exerts a stress directly on the water in the well; it also exerts a stress directly on the water table at low frequencies (Yusa, 1969; Weeks, 1979). The quantity most easily estimated concerning atmospheric pressure effects on the near surface is the imposed vertical load. The response of a water well to changes in atmospheric pressure is:

$$W = P/\rho g + \sigma_a/\rho g \qquad (10)$$

where P is the pore pressure and σ_a is the atmospheric load (extension is positive). Equation 10 assumes that the well is in quasi-static equilibrium with the pore pressure and is open to the atmosphere; as a result, any changes in pore pressure which are different than changes in atmospheric pressure must result in a change in water level in the well.

For static-confined conditions, the pore pressure response to atmospheric loading can be derived from the formalism of Rice and Cleary (1976). The relations for stress and strain can be written as:

$$\epsilon_{ij} = \beta\left[\frac{(1+\nu)}{3(1-2\nu)}\sigma_{ij} - \frac{\nu}{1-2\nu}\sigma\delta_{ij} + \frac{\alpha}{3}P\delta_{ij}\right] \qquad (11)$$

Under conditions where the near surface is composed of rock or stiff sediment, areally extensive surface loading near the surface of the

earth induces horizontal strains, ϵ_{11} and ϵ_{22}, which are 1/2 the vertical strain (Farrell, 1972):

$$\epsilon_{11} = \epsilon_{22} = 1/2\epsilon_{33} \tag{12}$$

The change in vertical stress is equal to the atmospheric load:

$$\sigma_{33} = \sigma_a \tag{13}$$

Insertion of equations 12 and 13 into 11 yields the following relation between the pore pressure within the formation and the atmospheric load:

$$P = -\gamma\sigma_a \tag{14}$$

where γ is:

$$\gamma = \frac{2B(1+\nu)}{3 - (1-2\nu)\alpha B} \tag{15}$$

It should be noted that γ has been termed the loading efficiency by Van der Kamp and Gale (1983). Their definition of this surface loading efficiency differs from that given by equation 15 because they assume that areally extensive surface stresses induce one-dimensional vertical strain. This assumption is appropriate only under conditions where the formation of interest is highly compressible relative to the underlying formations (Kuo, 1969). For the wells examined in a

subsequent section of this chapter, the assumption of one-dimensional strain is inappropriate. Insertion of equation 14 into equation 10 yields the relation between water level changes and atmospheric loading under static-confined conditions:

$$W = (1 - \gamma)\sigma_a/\rho g \qquad (16)$$

In order to examine how water well response to atmospheric loading changes as a function of material properties under static-confined conditions we examine the static-confined barometric efficiency of a well, BE', which is defined as (Jacob, 1940):

$$BE' = W\rho g/\sigma_a \qquad (17)$$

Figure 1-3 shows the static-confined barometric efficiency of a well as a function of compressibility and porosity. The response to changes in atmospheric loading, like the response to areal dilatation, is a strong function of compressibility with low compressibility favoring high sensitivity; unlike the response to dilatation, water level response to atmospheric loading is favored by high porosity. For formations with matrix compressibility exceeding about 3×10^{-10} cm^2/dyne, the static-confined barometric efficiency is so low that that the response to atmospheric loading may be difficult to detect in a well; earth tide sensitivities are also low for high compressibility formations. As a result of this lack of sensitivity, it may be difficult to determine the elastic properties of the formation based on well response to areally extensive deformation if matrix

compressibility is high. This problem is addressed in further detail elsewhere (Hsieh et al., 1988).

Figure 1-4 shows the difference between the theoretical barometric efficiency given here and that determined from the loading efficiency, γ', of Van der Kamp and Gale (1983). Including the effects of horizontal deformation causes the static-confined barometric efficiency of a well which taps a formation of a given matrix compressibility and porosity to be considerably smaller. Differences between the two theoretical responses are greatest when matrix compressibility is on the order of 10^{-11} cm^2/dyne.

MATERIAL PROPERTIES GOVERNING VERTICAL FLUID FLOW IN RESPONSE TO AREALLY EXTENSIVE DEFORMATION

The preceding sections indicate that the static-confined response of the water level in a well to deformation is often dependent on the matrix and solids compressibility, the Poisson's ratio and the porosity of the formation. It is worthwhile to examine how these material properties govern fluid flow. As noted above, the static-confined response of the well is a reflection of the undrained response of the formation. We can, however, fully expect that fluid flow will influence water well response. If we assume that formations are of large extent laterally and the frequency of the deformation is low enough that well bore storage effects are negligible, then the influence of the horizontal component of fluid flow can be neglected. Vertical fluid flow may occur due to water table drainage (see Chapters 3 and 4) or vertical variations in formation elastic

properties (Bower and Heaton, 1978; Gieske and de Vries, 1985). The response of pore pressure to changes in mean rock stress can be derived from the results of Biot (1941) and Nur and Byerlee (1971) and can be written in the form (Van der Kamp and Gale, 1983):

$$kV^2P = S'\frac{\partial}{\partial t}(P-B\sigma) \qquad (18)$$

where k is the hydraulic conductivity and S' is a measure of the elastic response of the fluid saturated rock or 'three dimensional specific storage':

$$S' = \rho g[(\beta - \beta_u) + \phi(\beta_f - \beta_u)] \qquad (19)$$

Under conditions of one-dimensional vertical fluid flow, equation 19 can be rewritten by noting that the mean stress, σ, is solely a function of the cubic strain, ϵ_r, and the local pore pressure. Utilizing equation 7, fluid flow in response to areally extensive deformation induced under conditions of plane stress (such as that caused by earth tides) can be written as:

$$D' \frac{\partial^2 P}{\partial z^2} = \frac{\partial P}{\partial t} + 2\mu\gamma' \frac{\partial \epsilon_{2r}}{\partial t} \qquad (20)$$

where D' is a hydraulic diffusivity for imposed horizontal strains under conditions of plane stress:

$$D' = k\left\{\rho g \left[\alpha\beta_r\left(1 - \frac{2\alpha(1-2\nu)}{3(1-\nu)}\right) + \phi(\beta_f - \beta_u)\right]\right\}^{-1} \qquad (21)$$

and μ is the shear modulus.

Utilizing equation 14, fluid flow induced by areally extensive atmospheric loading is governed by:

$$D\frac{\partial^2 P}{\partial z^2} = \frac{\partial P}{\partial t} + \gamma\frac{\partial \sigma_a}{\partial t} \qquad (22)$$

where D is a hydraulic diffusivity under conditions of areally extensive imposed surface stress:

$$D = k\left\{\rho g \left[\alpha\beta_r\left(1 - \frac{\alpha(1-2\nu)}{3}\right) + \phi(\beta_f - \beta_s)\right]\right\}^{-1} \qquad (23)$$

Equations 20 and 22 indicate that the hydraulic diffusivity which governs fluid flow under conditions of earth-tide induced strain differs from the hydraulic diffusivity which governs atmospheric-loading induced fluid flow. The difference is that fluid pressure influences horizontal deformation under conditions of atmospheric loading but does not influence horizontal deformation under conditions of earth-tide induced strain. The hydraulic diffusivity, D', is identical to the term k/S_s developed by Van der Kamp and Gale (1983) where S_s is their one dimensional specific storage coefficient:

$$S_s = \rho g \left[\alpha\beta\left(1 - \frac{2\alpha(1-2\nu)}{3(1-\nu)}\right) + \phi(\beta_f - \beta_u)\right] \qquad (24)$$

As noted by Van der Kamp and Gale (1983), the one-dimensional specific storage coefficient is the elastic property of the formation assumed by hydrologists to govern fluid flow.

The hydraulic diffusivity which governs fluid flow induced by atmospheric loading, D, differs from that given by Van der Kamp and Gale (1983) because, as noted earlier, they assumed that atmospheric loading induces vertical deformation only. Following hydrologic convention, we define D as the ratio k/S_a where S_a is the specific storage under conditions of surface loading: .

$$S_a = \rho g \left[\alpha\beta \left(1 - \frac{\alpha(1-2\nu)}{3}\right) + \phi(\beta_f - \beta_u)\right] \qquad (25)$$

Because S_a is by definition larger than S_s, pressure diffusion driven by atmospheric loading will (all material properties being equal) be dampened relative to pressure diffusion driven by earth tides.

The above relations indicate that the same material properties which govern the static-confined sensitivity of a well to atmospheric loading and earth tides also influence fluid flow. If these material propertes can be identified from the response of a well to known areally extensive deformation, the specific storages S'and S_s (parameters of interest to hydrologists) can also be determined.

DETERMINATION OF IN-SITU FORMATION MATERIAL PROPERTIES FROM THE STATIC-CONFINED RESPONSE OF A WELL TO ATMOSPHERIC LOADING AND EARTH TIDES

As has been noted by others (Bredehoeft, 1967; Hsieh et al., 1988), it is possible in theory to estimate formation elastic properties and porosity if the static-confined response of a well to atmospheric loading and earth tides can be determined or inferred. In the analysis of Bredehoeft (1967), solids compressibility was assumed to be zero and atmospheric loading was assumed to induce one-dimensional strain only. Under these conditions, the matrix compressibility and porosity of the formation can be directly determined from the static-confined response if the Poisson's ratio of the formation can be estimated. Because we have included the effects of solids compressibility and three dimensional deformation induced by atmospheric loading, determination of matrix compressibility and porosity, while similar in approach, becomes more complex.

The relation of matrix compressibility to the static-confined barometric efficiency, BE', and areal dilatational efficiency, DE'_a, of the well can be obtained from equations 7 and 14:

$$\lim_{\substack{\beta \\ 3\epsilon \to 1}} = 0$$

$$\beta = \frac{3(1-2\nu)(1-BE')[3-(1-2\nu)\alpha B]}{2\rho g DE'_a(1+\nu)[3(1-\nu)-2\alpha B(1-2\nu)]} \qquad (26)$$

$$DE = \left[\frac{C}{C} \quad \frac{}{\beta}\right] \qquad \lim_{\substack{\nu \\ \beta \to \beta_s}} = \qquad \lim_{\substack{DE \\ \varepsilon_c \to 1}} = \frac{C \to 0}{\beta \to \beta_s}$$

Equation 26 indicates that determination of matrix compressibility requires a priori estimates of solids and fluid compressibility, Poisson's ratio and the loading coefficient B of the formation. Rearrangement of equation 4 also indicates that estimation of formation porosity requires a priori estimates of solids and fluid compressibility and loading coefficient B as well as estimates of matrix compressibility:

$$\phi = \frac{(\beta - \beta_u)(1-B)}{\beta_f - \beta_u} \qquad (27)$$

The relation of the loading coefficient, B, to the static-confined barometric efficiency, BE', can be obtained from equation 15:

$$B = \frac{3(1-BE')}{2(1+\nu) + \alpha(1-BE')(1-2\nu)} \qquad (28)$$

Equations 26 and 28 can be used iteratively to determine matrix compressibility if the static-confined barometric efficiency, areal dilatational efficiency, Poisson's ratio and solids compressibility are known. An initial guess of matrix compressibility is used to derive an initial estimate of α and B. These values are then used to determine a new value of matrix compressibility. New estimates of α and B are then determined for reinsertion into equation 26; this iterative procedure continues until closure is achieved. Once closure is achieved, it is possible to determine porosity from equation 27.

Equations 26-28 were used to make estimate of the formation matrix compressibility and porosity tapped by five wells. These wells are described in Table 1-1. All five have been monitored for purposes of detecting tectonic strain. Three of the wells - TF, GD, and JC - are located near Parkfield, California. Two of the wells - SC2 and LKT - are located near Mammoth Lakes, California. The observed dilatational efficiencies in response to the O_1 and M_2 tide and the inferred static-confined barometric and areal dilatational efficiencies for these wells are shown in Table 1-2.

The observed areal dilatational efficiencies were determined by cross-spectral estimation of the water level, atmospheric load and theoretical earth tide time series (see Appendix). The tidal areal strain time series at each site was determined from the theoretical tidal potential with no correction made for ocean loading, topographic or geologic effects. The static-confined responses of these wells were inferred by a procedure outlined in the Appendix which adjusted for any influence of water table drainage on water well response.

Figure 1-5 shows the barometric efficiencies of the five wells as a function of frequency. As is discussed in detail elsewhere (see Chapters 2, 3 and 4), these barometric efficiencies which were determined by cross-spectral estimation can be a strong function of frequency. The frequency dependence is prominent at three wells - GD, TF and JC - and can be readily explained by the influence of water table drainage. Water table drainage also influences the areal dilatational efficiency and may at least partially explain the difference betwween the M_2 and O_1 observed areal dilatational efficiencies at these wells. The O_1 efficiency may be slightly less sensitive because water table drainage influences will generally cause relatively more attenuation at this frequency. Ignoring water table influences at the three Parkfield wells would lead to considerable difficulty in determining formation material properties. First, it would be difficult to determine the static-confined barometric efficiencies for the wells since the static-confined response is never observed in the frequency range analyzed. Second, use of the observed areal dilatational efficiencies would lead to an error in the estimation of static-confined strain sensitivity. At two of the

Parkfield wells - TF and JC - the difference between the observed and inferred sensitivity is slight; regardless of whether the inferred or observed response is used in equation 26, the material properties determined from the analysis will be about the same. At well GD, however, the difference between the inferred and observed response is considerable. Use of the observed areal dilatational efficiency at GD in equation 26 will yield estimates of matrix compressibility and porosity which will likely be too high.

Table 1-3 shows the material properties of the formations estimated from the analysis. In order to make estimates of matrix compressibility and porosity one needs to know the solids compressibility and Poisson's ratio of the formation and the compressibility of the pore fluid. The matrix compressibilities and porosities given in Table 1-3 were determined by assuming a solids and fluid compressibility of 2×10^{-12} cm^2/dyne and 4.4×10^{-11} cm^2/dyne, respectively, and a Poisson's ratio of 0.25 for all formations. The inferred M_2 static-confined areal dilatational efficiency was used in all calculations. Although independent confirmation of matrix compressibility is lacking, the estimates made from the well responses are reasonable compared with laboratory measurements of compressibility of rock (Haas, 1981). The estimates for formation porosity are also within the realm of expected values (Wolff, 1981). Also included in Table 1-3 are estimates of the specific storages, S_s and S_a, determined from the estimated matrix compressibilities and porosities through the use of equations 24 and 25. The one-dimensional specific storages, S_s, are generally about 1.3 times greater than the loading storages, S_a, indicating that horizontal

deformation has a slight effect on fluid flow induced by atmospheric loading for the formations examined.

Although the estimates of matrix compressibility and porosity for these wells are reasonable, it is worth briefly examining the possible errors involved in making these estimates. The largest sources of potential error are the assumptions that the theoretical tidal potential can be used to adequately describe the areal strain at each location and that the Poisson's ratio of each formation is 0.25. The results of Beaumont and Berger (1975) and Berger and Beaumont (1976) suggest that earth tide strain estimates based on the theoretical tidal potential can sometimes be in error by as much as ±50% due to the influence of ocean loading, topographic and geologic effects. Equations 26-28 indicate that estimates of matrix compressibility and porosity are roughly inversely proportional to the static-confined areal dilatational efficiency. If the theoretical tidal strain is 1/2 the actual tidal strain, estimates of matrix compressibility and porosity will be roughly be too small by a factor of 2; conversely if the theoretical tidal strain is twice the actual tidal strain, the estimates will be too large by a factor of about 1/2. Clearly, if tidal strains can be measured or if estimates of tidal strain can be made incorporating the effects of ocean loading and geologic and topographic effects the error involved in estimating formation material properties can be significantly reduced.

Variations in Poisson's ratio can also lead to significant variations in estimates of formation material properties. Inspection of equations 26-28 indicates that the principal influence of the Poisson's ratio on the estimates of matrix compressibility and

porosity is contained in the term $(1-2\nu)/(1+\nu)$. If the actual Poisson's ratio of the formation is 0.35, estimates of matrix compressibility and porosity based on a Poisson's ratio of 0.25 will be roughly to large by a factor of two. If the actual Poisson's ratio is 0.15, estimates will be roughly too small by factor of 1/3. These rough error estimates indicate that the material properties estimated for the wells in Table 1-3, while reasonable, are approximate values only.

CONCLUSIONS

The static-confined response of the water level in a well to areally extensive deformation provides both a first order measure of well strain sensitivity and a means to measure in-situ formation material properties. In the absence of fluid flow influences, formations can be expected to be sensitive to induced horizontal deformation such as that produced by earth tides and tectonic strain if they are relatively stiff and are of low porosity. Open wells can be expected to be sensitive to atmospheric loading if they tap formations which are relatively stiff and are of high porosity.

Although knowledge of the static-confined response of wells is useful, it is not always observable. In three of the wells examined in this paper (GD, TF and JC) the inferred static-confined response to strain is different than the observed response. If fluid flow influences water well response, it is possible to underestimate the static-confined sensitivity of a well to deformation. Estimates of

formation material properties directly based on the observed response of a well to deformation can be in error.

Even if the static-confined response of a well can be observed or inferred, use of water well response to atmospheric loading and earth-tides can be expected to provide only approximate values of matrix compressibility, porosity and specific storage. The values determined from well response may be in error as much as ±50%. While estimates of porosity which have such a potential for error are likely of limited utility, rough estimates of matrix compressibility and specific storage are often of use to geophysicists and hydrologists.

APPENDIX: DETERMINATION OF THE STATIC-CONFINED RESPONSE OF THE WELLS TO ATMOSPHERIC LOADING AND EARTH TIDES

The static-confined response of the wells to atmospheric loading and earth tides was inferred by fitting the observed response of these wells to theoretical models which describe the influence of water table drainage on well sensitivity. The observed response was determined from cross spectral estimation of the water level, atmospheric load and earth tide time series (Bendat and Piersol, 1986). The power spectra and cross spectra for the water well record, the local atmospheric load and the earth tide strain were determined using the Blackman-Tukey algorithm. The transfer functions between water level, atmospheric load and earth tides were determined by solving the following system of equations at each frequency:

$$\begin{vmatrix} BB & BT \\ TB & TT \end{vmatrix} \begin{vmatrix} HB \\ HT \end{vmatrix} = \begin{vmatrix} BW \\ TW \end{vmatrix} \qquad (A1)$$

where BB and TT denote the power spectra of the atmospheric pressure and earth tides respectively, BT and TB denote the cross spectrum and complex conjugate of the cross spectrum between atmospheric loading and earth tides, BW and TW denote the cross spectra between atmospheric loading and water level and earth tides and water level respectively, and HB and HT denote the transfer functions between water level and atmospheric loading and water level and earth tides respectively.

For the wells examined, solution of equation A1 provided high coherence (coherence greater than 0.85) estimates of the transfer function between water level and atmospheric load in the frequency band of 0.08 to 2 cycles/day; it also provided transfer function estimates between water level and earth tides at the peak tidal frequencies (M_2 and O_1). The transfer function between water level and atmospheric load was then fit to a theoretical solution which is governed by equation 22 and describes the influence of water table drainage on water well response (see Chapters 2, 3 and 4). The barometric efficiency at which the theoretical solution indicated fluid flow influences were negligible was inferred to be the static-confined barometric efficiency. The transfer functions of the wells examined in this paper and the details on fitting the transfer functions to the theoretical solutions are given elsewhere (see Chapters 2, 3 and 4).

The inferred static-confined dilatational efficiencies were determined by an iterative process. First the fit of the atmospheric load transfer function was used to determine the vertical hydraulic diffusivity governing fluid flow due to atmospheric loading, D (equation 23). Estimates were then made of the loading storage, S_a, based on the inferred static-confined barometric efficiency and the observed M_2 dilatational efficiency to determine the hydraulic conductivity, k, in equation 23. This hydraulic conductivity was then inserted into equation 21 along with an initial estimate of, S_s, to provide an estimate of the one dimensional hydraulic diffusivity, D'. The estimated value of D' was inserted into a theoretical solution to equation 20 which describes the influence of water table drainage on well response to earth tides (see Chapters 2 and 4). The degree of attenuation or amplification of response indicated by the theoretical solution was used to obtain new estimates of the inferred static-confined areal dilatational efficiencies. A new estimate of the loading storage, S_a, was made based on the new M_2 dilatational efficiency and the process was repeated until closure was achieved. Further details on inferring strain response can be found in Chapter 2.

REFERENCES

Beaumont, C., and J. Berger, An analysis of tidal strain observations from the United States of America: I. The homogeneous tide, Bull. Seismol. Soc. Am., 66, 1821-1846, 1976.

Bendat, J. S., and A. G. Piersol, Random Data: Analysis and Measurement Procedures, John Wiley and Sons, New York, 566pp., 1986.

Berger J., and C. Beaumont, An analysis of tidal strain observations from the United States of America: II. The inhomogeneous tide, Bull. Seismol. Soc. Am., 66, 1821-1846, 1976.

Biot, M. A., General theory of three-dimensional consolidation, J. Appl. Phys., 12, 155-164, 1941.

Biot, M. A., and D. G. Willis, The elastic coefficients of the theory of consolidation, J. Appl. Mech., 24, 594-601, 1957.

Bishop, A. W., Soils and soft rocks as engineering materials, Inaug. Lect. Imp. Coll. Sci. Techno., 6, 189-213, 1966.

Bodvarsson, G., Confined fluids as strain meters, J. Geophys. Res., 75, 2711-2718, 1970.

Bower, D. R., and K. C. Heaton, Response of an aquifer near Ottawa to tidal forcing and the Alaskan earthquake of 1964, Can. J. Earth Sci., 15, 331-340, 1978.

Bredehoeft, J. D., Response of well-aquifer systems to earth tides, J. Geophys. Res., 72, 3075-3087, 1967.

Farrell, W. E., Deformation of the earth by surface loads, Rev. Geophys. Space Phys., 10, 761-797, 1972.

Gieske, A., and de Vries, J. J., An analysis of earth-tide-induced groundwater flow in eastern Botswana, J. Hydrol., 82, 211-232, 1985.

Green D. H., and H. F. Wang, Fluid pressure response to undrained compression in saturated sedimentary rock, Geophys., 51, 948-956, 1986.

Haas, C. J., Static stress-strain relationships, in Touloukian, Y. S., W. R. Judd, and R. F. Roy, eds., Physical properites of rocks and minerals, McGraw-Hill, New York, 123-176, 1981.

Hanson, J. M., Reservoir response to tidal and barometric effects, Geotherm. Resour. Counc. Trans., 4, 337-340, 1980.

Hsieh, P. A., J. D. Bredehoeft and S. A. Rojstaczer, Response of well-aquifer systems to earth tides--problem revisited, Water Resour. Res., in press, 1988.

Jacob, C. E., The flow of water in an elastic artesian aquifer, Eos Trans. AGU, 21, 574-586, 1940.

Johnson, A. G., R. L. Kovach, and A. Nur, Fluid pressure variations and fault creep in Central California, Tectonophysics, 23, 257-266, 1974.

Johnson, A. G., R. L. Kovach, A. Nur, and J. R. Booker, Pore pressure changes during creep events on the San Andreas Fault, J. Geophys. Res., 78, 851-857, 1973.

Kuo, J. T., Static response of a multilayered medium under inclined surface loads, J. Geophys. Res., 74, 3195-3207, 1969.

Marine, I. W., Water level fluctuations due to earth tides in a well pumping from slightly fractured rock, Water Resour. Res., 11, 165-173, 1975.

Narasimhan, T. N., B. Y. Kanehiro, and P. A. Witherspoon, Interpretation of earth tide response of three deep, confined aquifers, J. Geophys. Res., 89, 1913-1924, 1984.

Nur, A., and J. D. Byerlee, An exact effective stress law for elastic deformation of rock with fluids, J. Geophys. Res., 76, 6414-6419, 1971.

Rabbel, W. and J. Zschau, Static deformations and gravity changes at the earth's surface due to atmospheric loading, J. Geophys., 56, 81-99, 1985.

Rhoads, G. M., Jr., and E. S. Robinson, Determination of aquifer parameters from well tides, J. Geophys. Res., 84, 6071-6082, 1979.

Rice, J. R., and M. P. Cleary, Some basic stress diffusion solutions for fluid saturated elastic porous media with compressible constituents, Rev. Geophys. Space Phys., 14, 227-241, 1976.

Robinson, E. S., and Bell R. T., Tides in confined well-aquifer systems, J. Geophys. Res., 76, 1857-1869, 1971.

Roeloffs, E. A., Hydrologic precursors: a critical review, U. S. Geological Survey Open-File Rept., 87-591, 1987.

Savage, J. C., and Gu G., The 1979 Palmdale, California strain event in retrospect, J. Geophys. Res., 90, 10301-10309, 1985.

Skempton, A. W., The pore-pressure coefficients A and B, Geotechnique, 4, 143-147, 1954.

Sterling, A., and E. Smets, Study of earth tides, earthquakes and terrestial spectroscopy by analysis of the level fluctuations in a borehole at Heibaart (Belgium), Geophys. J. R. Astr. Soc., 23, 225-242, 1971.

Van der Kamp, G. and J. E. Gale, Theory of earth tide and barometric effects in porous formations with compressible grains, Water Resour. Res., 19, 538-544, 1983.

Weeks, E. P., Barometric fluctuations in wells tapping deep unconfined aquifers, Water Resour. Res., 15, 1167-1176, 1979.

Wolff, R. G., Porosity, permeability, distribution coefficients and dispersivity, in Touloukian, Y. S., W. R. Judd, and R. F. Roy, eds., Physical properites of rocks and minerals, McGraw-Hill, New York, 45-82, 1981.

Yusa, Y., The fluctuation of the level of the water table due to barometric change, Geophys. Inst. Spec. Contrib., Kyoto Univ., 9, 15-28, 1969.

Table 1-1: Description of wells.

Well Id.	Location	Open Interval (meters)	Rock type
GD	Parkfield, CA	18-88	Granodiorite
TF	Parkfield, CA	152-177	Marine sediments
JC	Parkfield, CA	147-153	Diatomaceous sandstone and siltstone
SC2	Mammoth Lakes, CA	66-70	Fractured basalt
LKT	Mammoth Lakes, CA	152-296	Largely rhyolite

Table 1-2: Atmospheric and tidal responses of the wells

Well Id.	Inferred BE'	Observed tidal sensitivities (cm/nc)		Inferred DE'_a (cm/nc)	
		M_2	O_1	M_2	O_1
GD	0.10	0.030	0.024	0.038	0.034
TF	0.37	0.034	0.029	0.033	0.030
JC	0.67	0.028	0.022	0.027	0.021
SC2	0.74	0.013	0.007	0.013	0.007
LKT	0.48	0.034	0.031	0.034	0.031

Table 1-3: Material properties and specific storages estimated from analysis.

Well Id.	Matrix compress. β (cm^2/dyne x 10^{-11})	Porosity	Specific storage (cm^{-1} x 10^{-6}) S_s	S_s
GD	2.7	0.04	1.6	2.3
TF	1.0	0.13	1.5	1.0
JC	1.1	0.14	1.1	1.3
SC2	1.8	0.27	2.1	2.4
LKT	1.5	0.13	1.3	1.8

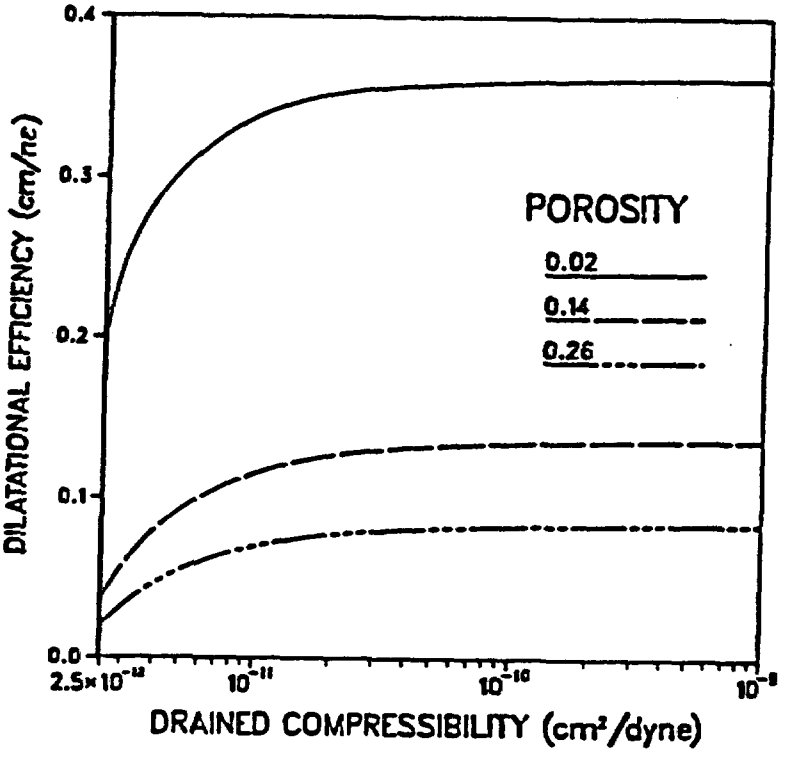

Figure 1-1: Static-confined dilatational efficiency of a well as a function of matrix compressibility and porosity. Solids and fluid compressibility assumed to be 2 x 10^{-12} cm^2/dyne and 4.4 x 10^{-11} cm^2/dyne respectively.

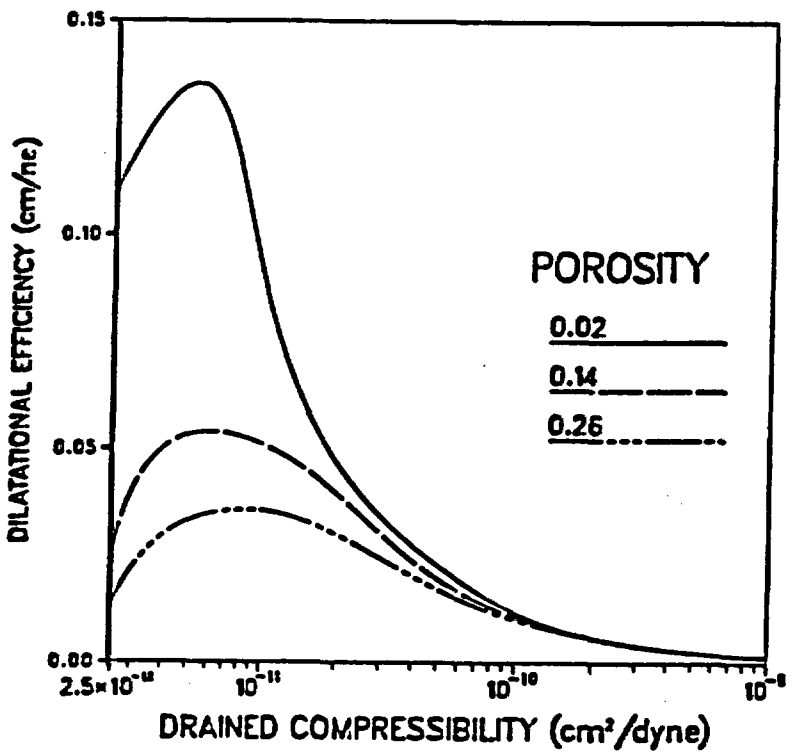

Figure 1-2: Static-confined areal dilatational efficiency of a well as a function of matrix compressibility and porosity. Solids and fluid compressibility assumed to be 2 x 10^{-12} cm^2/dyne and 4.4 x $10^{-11}cm^2$/dyne respectively. Poisson's ratio assumed to be 0.25.

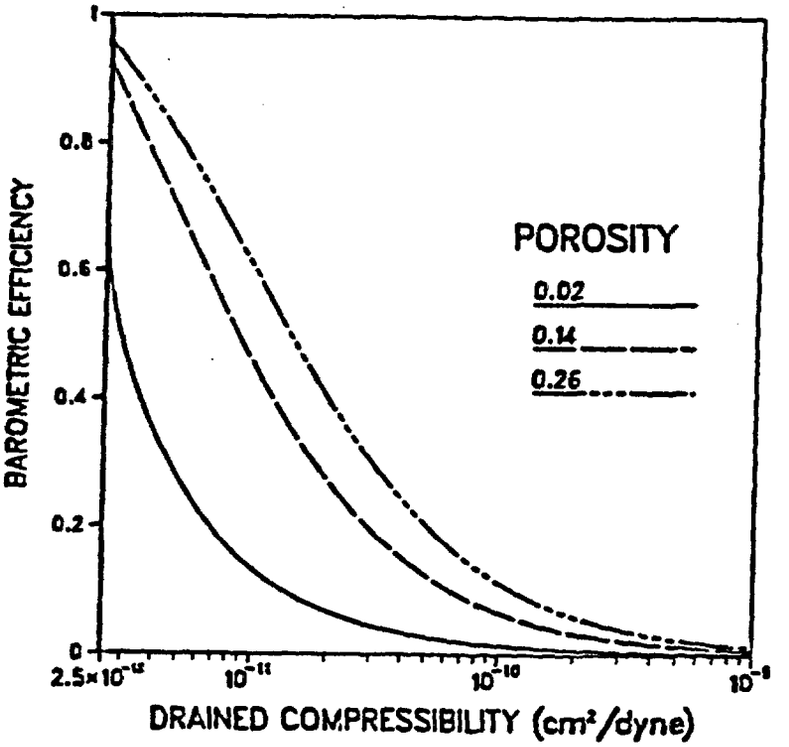

Figure 1-3: Static-confined barometric efficiency of an open well as a function of matrix compressibility and porosity. Solids and fluid compressibility assumed to be 2 x 10^{-12} cm^2/dyne and 4.4 x 10^{-11} cm^2/dyne respectively. Poisson's ratio assumed to be 0.25.

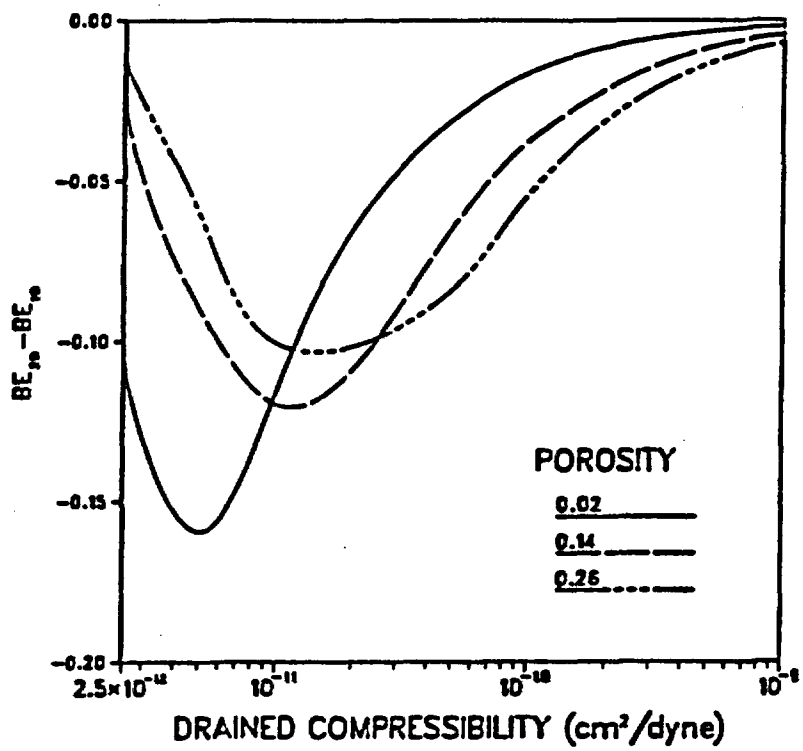

Figure 1-4: Difference between static-confined barometric efficiency including horizontal deformation (denoted as BE_{3D}) and static-confined barometric efficiency for vertical deformation only (denoted as BE_{1D}) as a function of matrix compressibility and porosity. Solids and fluid compressibility assumed to be 2×10^{-12} cm²/dyne and 4.4×10^{-11} cm²/dyne respectively. Poisson's ratio assumed to be 0.25.

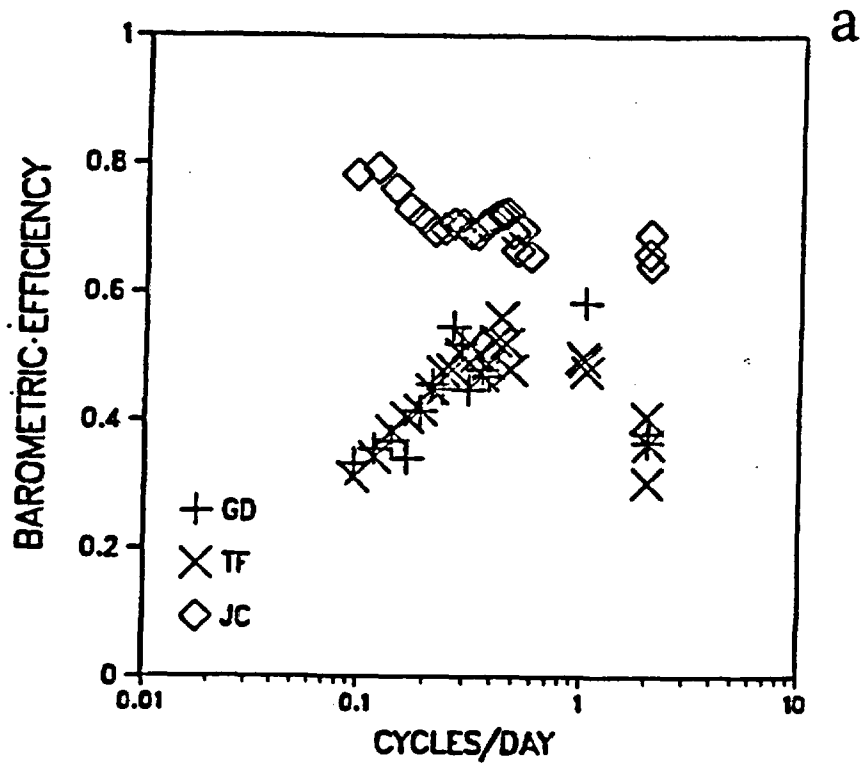

Figure 1-5: Barometric efficiencies of the Parkfield wells (a) and Mammoth Lakes wells (b) as a function of frequency.

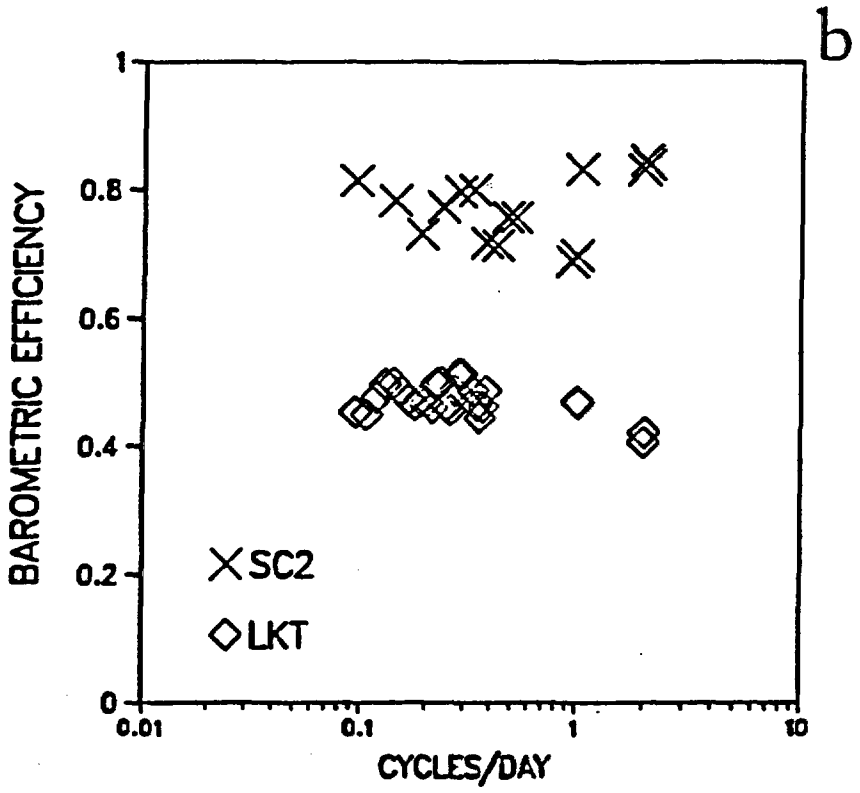
b
BAROMETRIC EFFICIENCY
1
0.8
0.6
0.4
0.2
0
0.01
0.1
1
10
CYCLES/DAY
SC2
LKT

How can we know the dancer from the dance?

W. B. Yeats

CHAPTER 2

INTERMEDIATE PERIOD RESPONSE OF WATER WELLS TO CRUSTAL STRAIN: SENSITIVITY AND NOISE LEVEL

ABSTRACT

The response of water wells to earth tides indicates that they can be sensitive to small crustal strains. Groundwater flow induced by the presence of the water table can significantly attenuate this sensitivity. The attenuation of strain sensitivity as a function of frequency can be inferred from the response of water wells to atmospheric loading. For the wells examined in this study, significant attenuation due to water table effects can occur when strains accumulate gradually over periods of days to weeks. Even if this attenuation is present, however, wells can still be used as accurate strain meters over this range in period. At a frequency of 2.5 cycles/day, the noise level of the water level records examined is slightly above -130 db relative to 1 strain^2/Hz. In the frequency band of 0.025 to 2.5 cycles/day, the noise level of the raw water level records examined increases 25 db per decade decrease in frequency. Much of this noise is due to the influence of atmospheric pressure. When the effects of atmospheric pressure are removed from the record, the noise level is reduced to 20 db per decade for

frequencies above 0.08 cycles/day, a rate typical of high quality strain meters. Below a frequency of 0.08 cycles/day, the water level records show a rate of noise increase of roughly 35 db per decade, a change which may reflect the influence of precipitation. For periods slightly less than a month, the two wells examined possess a higher accuracy than can be obtained from the best geodetic distance measurements.

INTRODUCTION

Although it is well known that water wells respond systematically to small strains induced by earth tides and atmospheric pressure fluctuations (Jacob, 1940; Bredehoeft, 1967; Van der Kamp and Gale, 1983), the use of water wells for the purpose of monitoring tectonically induced strain has been largely qualitative. There have been very few successful attempts to calibrate water level fluctuations in response to known tectonic events in terms of strain and/or compare a water well's response to other strain measurements. Sterling and Smets (1971) include a power spectrum from a water well's response to a seismic event which indicates that in the frequency band of 10^{-4} to 10^{-2} Hz a well can be highly sensitive to dilatation. Johnson et al. (1973, 1974) monitored water levels from 1971 to 1973 in a well located near the Almaden Winery within 10 m of the surface trace of the San Andreas fault; they found that water level fluctuations of several centimeters which lasted from hours to several days were associated with creep events. Based upon the response of their well to atmospheric loading, Johnson et al. were

also able to infer the mean stress at the well induced by the associated creep events. Wesson (1981) and Roeloffs and Rudnicki (1984) have analyzed one of the water level - creep events observed by Johnson et al. and have found that the water level fluctuation is qualitatively consistent with the magnitude of the creep event. The same well observed by Johnson et al. showed correlations with two creep events during 1975-1976 (Mortensen et al., 1977); water level fluctuations of 3 centimeters were associated with creep induced strains of approximately 10^{-7}.

The response of the water well near the Almaden Winery suggests that water wells can measure tectonic strain. There are, however, some inherent problems with using water wells as strain meters. These problems can be separated into two broad classes: those that are strictly related to the bulk material properties of the rock or sediment in direct communication with the well; those that are due primarily to groundwater flow.

The principal problem related to bulk material properties is that the sensitivity of a well to strain is highly dependent on the porosity and elastic properties of the rock or sediment with which it is in hydraulic communication. A well in communication with rock or sediment which is highly compressible and porous cannot be expected to be highly sensitive to tectonic strain. This point is discussed in Chapter 1.

Many other problems with using water wells as strain meters are due primarily to the influence of groundwater flow. The principal problem related to groundwater flow is that the water level in a well responds to hydrology as well as strain. A year of above average

rainfall will likely cause a low frequency rise in water level; conversely, a year of below average rainfall will likely cause a low frequency drop in water level. The hydrologic influences of rainfall can be viewed as noise placed upon any strain signal which might be present in the water well record and interpretation of changes in water level as being solely the result of strain will have some inherent error.

Groundwater flow can cause another significant problem inherent in the use of water wells as strain meters; it may reduce strain sensitivity, and restrict the usefulness of water wells to a narrow frequency band. Figure 2-1 shows an idealized cross section of a well in communication with saturated rock undergoing strain and indicates three potential ways for groundwater flow to reduce strain sensitivity. The first source is the limited hydraulic communication between the well and the saturated rock; if the well is to be a gage of pore pressure, changes in pore pressure must be accompanied by flow into or out of the borehole. For strains above some limiting frequency (which depends on the borehole geometry and the material properties of the saturated rock), groundwater flow will be too slow to allow the full pore pressure signal to be seen in the well. Fortunately, this can usually be mitigated by placing a packer beneath the water surface so that only small volumes of fluid must move in and out of the borehole to change fluid pressure within the well.

The second source of sensitivity reduction due to groundwater flow is flow from (in the case of strain being compressional) or to (in the case of strain being extensional) the strain induced pore pressure disturbance to a region which is either undergoing slight or

no strain or to a region which is undergoing strain which is opposite in sense. For strains of tectonic origin, the wavelengths of the pressure disturbance are likely on the order of kilometers so that this problem is likely to take place only at very low frequencies. The third source of sensitivity deterioration is vertical flow from or to the water table. Since the water table is particularly insensitive to crustal strain (Bredehoeft, 1967), any hydraulic communication between the water table and the zone of saturated rock monitored can cause significant attenuation of the strain signal. Water wells are typically in communication with rocks which are less than 200 m below the water table, and we might expect that this source would begin to operate at frequencies higher than those of the second source. Because the second and third sources of sensitivity attenuation described above are directly due to large scale dissipation of pore pressure within rock, their effects cannot be mitigated.

The problem of noise in the water level signal has not been quantitatively examined, but the problems of strain sensitivity related to groundwater flow have been studied previously in some detail. Sensitivity attenuation because of fluid flow into and out of the well has been extensively examined (Cooper et al., 1965; Bodvarrson, 1970; Johnson, 1973; Gieske, 1986); it will only be peripherally discussed here and is discussed in detail in Chapter 3. The influence of the water table on attenuation has been examined by Johnson (1973) and Johnson and Nur (unpublished manuscript, 1978); these studies theoretically examined this influence assuming that the

unsaturated zone above the water table did not significantly influence water table response.

This study examines: the influence of groundwater flow to the water table on the sensitivity of water wells as strain meters; the noise levels of water wells in comparison with other strain meters. The influence of groundwater flow on attenuation of sensitivity is examined by: extending the theoretical work of Johnson (1973) and Johnson and Nur (unpublished manuscript, 1978) to include the influence of the unsaturated zone above the water table on atmospheric pressure induced strains; applying these theoretical results to the response of two wells to atmospheric loading in order to examine how groundwater flow influences strain sensitivity as a function of frequency. The comparative performance of water wells as strain meters is assessed by calibrating two wells to known strains and examining how noise levels, in terms of strain, increase with decreasing frequency.

OVERVIEW OF WELLS TO BE EXAMINED

Figure 2-2 shows the water level record for the two wells which are examined here. These wells were chosen because: they are located in areas which have been the focus of many crustal deformation studies over the past decade; and they exhibit the largest amplitude response to the strain induced by earth tides of any of the wells monitored in these areas over the time shown. The hydrograph labeled LKT is the water level record from a well in the Long Valley caldera near Mammoth Lakes, California; the hydrograph labeled TF is the record from a well

near the San Andreas fault near Parkfield, California. Both areas are being monitored (with water wells and more conventional strain instruments) in the hope of detecting strains precursory to a tectonic event. Within Long Valley, the possible tectonic event is a major earthquake or a volcanic eruption (Cockerham and Pitt, 1984; Savage and Clark, 1982; Miller, 1985). Near Parkfield, the historic record points to the strong possibility that a magnitude 6 earthquake will take place near Parkfield by 1993 (Bakun and McEvilly, 1984).

If any tectonic event within Long Valley or Parkfield is to be successfully predicted using strain meters it must be preceded by strains which are large enough to be detected with strain instrumentation and have a character which is noticeably different from any background strain that may be present within the region. The water level records at LKT and TF over the second half of 1985 both show a long term decline in water level; this low frequency decline is at least partially due to the relative lack of precipitation in central California over the winter of 1984-1985, but even if this decline was solely due to tectonic strain it would be difficult to utilize such low frequency behavior as a precursor to a major tectonic event. Superimposed upon the trend are deviations on the order of centimeters and which appear nearly at the same time in both wells. These fluctuations of period of several days to several weeks are (as we shall see later) in the frequency range in which we can expect to use these water wells as sensitive and relatively noise free strain meters and they are largely due to strains induced by atmospheric loading. Finally, there are high frequency fluctuations (on the order

of a cycle/day) which are largely due to atmospheric pressure and earth tide induced strains and are about a centimeter in amplitude.

The above qualitative discussion of the water well records can be brought into somewhat sharper focus by examining the power spectra of the water level records shown in Figure 2-3. Both wells have considerable power in the semi-diurnal and diurnal frequency band due to earth tides and atmospheric loading. Power levels continue to increase at lower frequencies. This increase in power with decreasing frequency is typical of any continuously monitored strain instrument (Agnew, 1986) although the rate of power increase with decreasing frequency is a function of the instrumentation and background strain rate.

Figure 2-3 also shows the power spectra of atmospheric pressure at TF and LKT over the second half of 1985. Comparison of the atmospheric pressure power spectra with the water level power spectra at TF and LKT indicates many similarities. There is substantial power in the semi-diurnal and diurnal band and a strong increase in power with decreasing frequency. At LKT the power spectra of atmospheric pressure and water level have a character which in the frequency band of 0.1 to 0.8 cycles/day is nearly identical. The power spectra of atmospheric pressure and water level at TF are relatively less similar.

In a later section, I quantitatively examine the influence of atmospheric loading on the response of these wells. The response of these water wells to earth tide induced strains while not the primary focus of this study is used to quantitatively calibrate water level fluctuations in terms of strain.

INFLUENCE OF THE WATER TABLE ON THE SENSITIVITY OF WATER WELLS TO AREALLY EXTENSIVE STRAINS

As has been previously noted, we cannot expect the response of a water well to strain to be independent of frequency. At low frequencies, the response of a well will be dominated by the influence of the water table and, as a result, will be negligible. At higher frequencies, the influence of the water table will be weaker and we can expect that (until frequencies are so high that flow into the borehole becomes a difficulty) sensitivity will increase with frequency. I assume, for the purposes of this study, that borehole flow (either due to high permeability or to the installation of a packer) does not significantly attenuate strain sensitivity in the frequency range of interest. When the frequency of the imposed strain is high enough to effectively isolate pore pressure from water table influences, I follow hydrologic convention and call the response of the water well the <u>static-confined response.</u> In this section I examine the response of water wells to periodic crustal strains and stresses as a function of frequency; in the following section I will apply these theoretical results to the observed frequency response of LKT and TF.

In order to examine the influence of the water table on water well response, we need to determine how pore pressure changes in response to periodic deformation. In Chapter 1, it is shown that time-dependent, pore pressure response to laterally extensive and uniform deformation depends upon whether the deformation is an imposed

areal strain or an imposed surface load. Under conditions of one-dimensional vertical fluid flow, the response of pore pressure, P, at typical well depths to areal strain (sum of the principal horizontal strains), ϵ_{2r}, imposed by earth tides and broad-scale tectonic deformation is governed by:

$$D' \frac{\partial^2 P}{\partial z^2} = \frac{\partial P}{\partial t} + C \frac{\partial \epsilon_{2r}}{\partial t} \qquad (1)$$

where D' is a hydraulic diffusivity for imposed horizontal strains under conditions of plane stress (Van der Kamp and Gale, 1983):

$$D' = k\left\{\rho g \left[\alpha\beta\left(1 - \frac{2\alpha(1-2\nu)}{3(1-\nu)}\right) + \phi(\beta_f - \beta_u)\right]\right\}^{-1} \qquad (2)$$

C is a measure of the sensitivity of pore pressure to imposed areal dilatation (Van der Kamp and Gale, 1983):

$$C = \frac{2\mu B(1+\nu)}{3(1-\nu) - 2\alpha B(1-2\nu)} \qquad (3)$$

B is a coefficient which relates mean stress to pore pressure under undrained conditions (Skempton, 1954; Rice and Cleary, 1976):

$$B = \frac{(\beta - \beta_u)}{(\beta - \beta_u) + \phi(\beta_f - \beta_u)} \qquad (4)$$

and α is the fraction of rock strain taken up by the pore space under drained conditions (Biot and Willis, 1957; Nur and Byerlee, 1971):

$$\alpha = 1 - \beta_u/\beta \tag{5}$$

It should be noted that ρ is the fluid density, g is gravity, k is the hydraulic conductivity, β is the rock matrix compressibility, ν is Poisson's ratio, ϕ is the porosity, β_f is the fluid compressibility, β_u is the rock grain compressibility and μ is the shear modulus.

Under conditions of one-dimensional vertical fluid flow in response to areally extensive surface loading (such as that produced by atmospheric loading), pore pressure response at typical well depths is described by:

$$D \frac{\partial^2 P}{\partial z^2} = \frac{\partial P}{\partial t} + \gamma \frac{\partial \sigma_a}{\partial t} \tag{6}$$

where D is a hydraulic diffusivity under conditions of areally extensive imposed surface stress (see Chapter 1):

$$D = k\left\{\rho g \left[\alpha\beta\left(1 - \frac{\alpha(1-2\nu)}{3}\right) + \phi(\beta_f - \beta_u)\right]\right\}^{-1} \tag{7}$$

γ is the near-surface response of pore pressure to surface loading under undrained conditions (see Chapter 1):

$$\gamma = \frac{2B(1+\nu)}{3 - (1-2\nu)\alpha B} \tag{8}$$

and σ_a is the surface load.

Equations 1 and 6 indicate that pore pressure response to imposed areal strain and surface loading are both described by diffusion

equations which contain a source term. As is noted in Chapter 1, the essential difference is that the source term in the case of imposed areal strain has (due to the hydraulic diffusivity, D', being slightly larger than the hydraulic diffusivity, D, for equal bulk material properties) a weaker influence on time dependent changes in pore pressure. The diffusion equations given above are an accurate description of pore pressure response as long as we can assume that, in the frequency range of interest, there is no lateral pore pressure dissipation; under this condition, the deformation and state of stress at a point are independent of far-field pore pressure (Biot, 1941; Rice and Cleary, 1976). We also assume that material properties are uniform throughout the vertical column of interest. It should be noted that the hydraulic diffusivities D' and D are a strong function of hydraulic conductivity, k, and are also a strong inverse function of rock matrix compressibility.

Figure 2-4 shows two problems of interest with regard to the influence of the water table. In the first problem, the rock is subject to a periodic areal strain $A\cos(\omega t)$, the water table is at zero pressure and the well is an accurate gage of pore pressure; this is an idealized description of the response of pore pressure to broad-scale tectonic and earth tide induced strains. The second problem is an idealized description of the water well response to atmospheric loading: the rock is subject to a periodic vertical stress $A\cos(\omega t)$ and areal strain, ϵ_{2r}, is one half the cubic strain ϵ_r (Farrell, 1972); the water table is subject to a pressure $-AG\cos(\omega t-\theta)$ where G and θ account for the attenuation and phase shift of the atmospheric pressure due to diffusion of air through the unsaturated zone above

the water table; the water in the well is subject to a periodic pressure $-A\cos\omega t$ and the relation between water level and pore pressure is (see Chapter 3):

$$W = (A\cos\omega t + P)/\rho g \qquad (9)$$

Since fluid flow is one-dimensional, both problems outlined above are readily solved analytically.

Frequency response of a well to imposed horizontal strain

The response of a water well to imposed periodic areal strain is given by (Appendix A):

$$W = [AC\exp(-\sqrt{\bar{Q}'})\cos(\omega t - \sqrt{\bar{Q}'}) - AC\cos(\omega t)]/\rho g \qquad (10)$$

where A is the amplitude of the dilatation and Q' is a dimensionless frequency:

$$Q' = z^2\omega/2D' \qquad (11)$$

This result is qualitatively similar to the frequency dependent response of water wells to strain given by Johnson (1973) and Johnson and Nur (unpublished manuscript, 1978). The major differences between their analogous solution and that given here are due to their approximation of the water table as a spherically shaped boundary. Equation 11 indicates that the most important parameter governing

sensitivity as a function of frequency is, z, the depth from the water table. Hydraulic diffusivity is also an important factor with low diffusivity favoring low attenuation at a given frequency. As was previously noted, hydraulic diffusivity is a strong inverse function of rock compressibility and as a result, low attenuation at low frequency is favored for highly compressible rock. Conversely, sensitivity due to horizontal loading under static-confined conditions is strongly favored by low compressibility (Van der Kamp and Gale, 1983; see Chapter 1). Thus, high sensitivity under static-confined conditions to strains produced by horizontal loading will be accompanied by a relatively rapid attenuation with decreasing frequency.

The gain and phase of the sensitivity to dilatation are plotted as a function of the dimensionless frequency, Q', in Figure 2-5 under the assumption that the static-confined sensitivity of the well to rock strain (static-confined areal dilatational efficiency) is 0.05 cm water level drop per areal nanostrain (ppb). The figure indicates that attenuation and phase shift with decreasing frequency is a gradual process. Attenuation and phase shift begin to significantly deviate from the static-confined response when the dimensionless frequency decreases to a value of 10. Between a dimensionless frequency of 1 and 10, the strain signal is slightly amplified relative to static-confined conditions; near complete attenuation of the strain signal takes place for strains with dimensionless frequency 0.001 or less.

We can gain some understanding of how an average well will respond to crustal strain by assuming some values for diffusivity and

depth from the water table. Given a well tapping rock with a vertical permeability of 10 millidarcies (the average permeability of non-argillaceous materials inferred for the crust (Brace 1980; Brace, 1984)), a compressibility of 10^{-11} cm^2/dyne, a porosity of 0.10, and a well depth (relative to the water table) of 100 m, the dimensionless frequency will have a value greater than 10 for strains with frequency greater than 20 cycles/day. This result indicates that, for reasonable material properties and geometries, the water table can have a strong influence on strain sensitivity in the frequency range of practical interest.

Frequency response of a well to atmospheric loading

The response of a well to atmospheric loading is considerably different than that given above. These differences are due to the stress placed upon the earth's surface and the diffusion of the load through the air phase of the unsaturated zone (Weeks, 1979) Water level response to periodic fluctuations in atmospheric loading is given by (Appendix B):

$$W = [(-M+\gamma)A\exp(-\sqrt{\bar{Q}})\cos(\omega t-\sqrt{\bar{Q}}) - (\gamma-1)A\cos(\omega t) - NA\exp(-\sqrt{\bar{Q}})\sin(\omega t-\sqrt{\bar{Q}})]/\rho g \qquad (12)$$

where M and N are:

$$M = \frac{2\cosh(\sqrt{\bar{R}})\cos(\sqrt{\bar{R}})}{\cosh(2\sqrt{\bar{R}})+\cos(2\sqrt{\bar{R}})}$$

(13)

$$N = \frac{2\sinh(\sqrt{\bar{R}})\sin(\sqrt{\bar{R}})}{\cosh(2\sqrt{\bar{R}})+\cos(2\sqrt{\bar{R}})}$$

Q and R are dimensionless frequencies referenced to fluid diffusivity, D, and air diffusivity, D_a, respectively.:

$$Q = z^2\omega/2D$$

$$R = L^2\omega/2D_a \qquad (14)$$

and L is the depth from the earth's surface to the water table. The gain (barometric efficiency, BE) and phase of the response of a water well to atmospheric pressure fluctuations is shown in Figure 2-6 for a well with a surface loading efficiency, γ, of 0.5.

The response is plotted as a function of two dimensionless parameters: dimensionless frequency, Q, and the ratio of dimensionless frequencies R and Q. The dimensionless ratio, R/Q, is a measure of the time taken for atmospheric pressure changes to reach the water table versus the time taken for water table effects to significantly influence water well response.

For values of R/Q less than 0.0001, the water table is fully influenced by atmospheric pressure changes at dimensionless frequency, Q, and the response of the water well to atmospheric loading is functionally identical (except for a phase shift of 180°) to the response to strains which are applied directly to the solid phase alone. Under these conditions, the attenuation of sensitivity to

tectonic or earth tide induced strains can be inferred from the air pressure response once an allowance is made for the slightly different hydraulic diffusivity which governs fluid flow. For values of R/Q greater than 0.1, there is significant attenuation and phase shift of the atmospheric pressure signal at the water table; under these conditions we can expect that, over a frequency band whose width and location is a strong function of R/Q, the water well response will be significantly amplified relative to the static-confined response. When R/Q is greater than 10, we can expect a water well to respond significantly to atmospheric loading in a frequency band where response to tectonic or earth tide induced strains are strongly attenuated. Hence, the response of a water well to atmospheric loading, when R/Q is significantly greater than 0, is not indicative of how the sensitivity to tidal or tectonic strains attenuates with frequency.

Although it is not possible, based upon the response to air pressure, to directly infer how the sensitivity of water wells will attenuate in response to imposed strain when R/Q is 0.1 or greater, the air pressure response gives us an indirect means to determine how wells respond to tectonic strain. The material and fluid flow properties of the rock and/or sediment which control well response can be determined by fitting the atmospheric pressure response of the well to the theoretical response (equation 12 or B12). These elastic and fluid flow properties can then be used in conjunction with the theoretical response to imposed areal strain (equation 10 or A7) to infer how sensitivity to tectonic strain attenuates with frequency. In the following section, I examine the atmospheric pressure response

of LKT and TF to see if any air diffusion effects are present and use the atmospheric pressure response to infer how these wells respond to tectonic strain.

BEHAVIOR OF WATER WELLS AS STRAIN METERS IN PRACTICE

The previous section focused on the theoretical behavior of water wells in response to strain. In theory, water wells may suffer from relatively rapid attenuation of sensitivity in a frequency range which is of practical interest for purposes of deformation monitoring. In this section I examine the behavior of two wells, LKT and TF, to earth tide and atmospheric pressure induced strains to determine whether the previous theoretical results have any merit in practice. We also try to examine the overall noise levels of these wells as a function of frequency. The wells, as previously noted, exhibited the highest sensitivity to earth tides of all the wells monitored for tectonic strain in the Long Valley caldera and near Parkfield, California in the second half of 1985 and it might be expected that the sensitivity and noise levels of these wells are close to the best response we can expect from wells which are no more than 300 m deep.

The depth and near-hole lateral permeabilities of these two wells are shown in Table 2-1. Both wells are isolated from the near surface to a depth in excess of 100 m. The depth to water is about 20 m at both LKT and TF; if near-hydrostatic conditions prevail at these wells, then this depth indicates the depth to the water table at both sites. The lateral permeabilities of the rock in direct hydraulic communication with these wells were inferred from a slug test (Kipp,

1985) and pumpage data from LKT and TF, respectively. These permeabilities are high in relation to the range of permeabilities which have been measured or inferred for the crust (Brace, 1980) indicating that hydraulic communication between the well and rock is relatively good. The borehole diameter is roughly 15 cm at both wells.

At each site, atmospheric pressure and water level were measured with silicon strain bridge transducers 4 times per hour. The water level and atmospheric pressure records over the time interval shown in Figure 2-2 contain 2% and 5% gaps at LKT and TF respectively; these gaps range from 1/2 hour to a few days in length. The method by which these gaps in the time series were filled is described in Appendix C. The tidal areal strain time series at each site was determined from the theoretical tidal potential with no corrections made for ocean loading, topographic or geologic effects. The results of Beaumont and Berger (1975) and Berger and Beaumont (1976) suggest that the amplitude of actual tidal dilatation agrees with those determined from the homogeneous earth tide with an error of about ±50%.

The relation of water level to crustal strains induced by atmospheric pressure and earth tides was determined by cross-spectral estimation (Appendix D). Table 2-2 indicates the response of these wells to the M_2 and O_1 earth tides in terms of their areal dilatational efficiency (water level drop in centimeters per areal nanostrain) and phase. Their response to the M_2 tide in terms of areal dilatational efficiency is identical; for both sites the dilatational efficiency with regard to the M_2 component of the tidal potential is about 0.034 cm water level drop per areal nanostrain.

The dilatational efficiency of the O_1 tide is slightly lower, particularly at TF. At TF, this slightly greater difference in amplitude may be partly due to water table influences which (as is shown below) significantly attenuate strain sensitivity in the frequency band of interest (0.025 to 2.5 cycles/day). Phase differences at LKT and TF between the O_1 and M_2 tidal constituents are slight. The constituents at LKT are both roughly -10° out of phase with the response that would be expected if the phase of the tidal dilatation could be precisely determined from the theoretical tidal potential; at TF, the phase of the O_1 and M_2 tidal constituents are both roughly +10° out of phase with the theoretical response. The phase shift of both constituents as well as the small difference in dilatational efficiency between the M_2 and O_1 constituents at LKT are likely due to local inhomogeneities and/or ocean loading effects. At TF, the phase shift of both constituents is likely due to a combination of local inhomogeneities, ocean loading effects and water table influences.

The response of LKT to atmospheric loading is shown in Figure 2-7. The phase is generally flat and near 0° out to a frequency of 0.02 cycles/day. The admittance or barometric efficiency begins to show some attenuation below a frequency of 0.05 cycles/day. This attenuation may not reflect any water table influence; rather it may be the result of some error in the estimate of barometric efficiency at low frequencies. Bendat and Piersol (1986) give error estimates for the admittance and phase determined from cross-spectral estimation. For this study the 95% confidence interval for admittance or barometric efficiency, BE, for LKT is given by:

$$BE_{.95} = BE \pm 1.2\sqrt{(1-\Gamma^2)}BE \qquad (15)$$

where Γ is the coherence. Figure 2-8 shows the coherence squared, as a function of frequency for LKT. At frequencies less than 0.05 cycles/day, the coherence squared is substantially less than 1 and the error bounds on barometric efficiency are greater than ±.27. A flat barometric efficiency of .48 (the mean value of the barometric efficiency for frequencies greater than 0.05 cycles/day) over the entire frequency range examined is thus not inconsistent with the admittance values and is consistent with the general frequency insensitivity of the phase. Alternatively, the attenuation which begins to occur at frequencies less than 0.05 cycles/day is a real physical phenomenon, presumably due to the influence of the water table.

The fit to the data, based on the assumption that there is some water table influence in the observed frequency band is also shown in Figure 2-7. The best fit to the data is achieved with a static-confined barometric efficiency of .45 (γ=.55), a value for dimensionless frequency Q of 30.0ω, and a value for dimensionless frequency R of 5.9ω where frequency ω is in units of cycles/day. The value for Q indicates that the observed M_2 and O_1 tidal responses are not influenced by water table drainage. The value for the static-confined barometric efficiency given by this fit combined with the dilatational efficiency estimate for the M_2 tide shown in Table 2-2 allow us to calculate (see Chapter 1) a compressibility for the rock in communication with the well. Assuming a Poisson's ratio of .25,

the drained rock matrix compressibility is 1.5×10^{-11} cm^2/dyne. Given this compressibility and assuming that the depth to water is indicative of the depth to the water table, it is also possible to estimate the vertical permeability of the zone between the water table and the uppermost depth that the well is in hydraulic communication with saturated rock. This permeability is 0.6 millidarcies which is considerably below the lateral permeability given in Table 2-1; the difference indicates that either moderately low permeability layers exist above the monitored zone or that there is considerable anisotropy in the permeability of the rock and sediment above the zone monitored. It should be noted that this inferred permeability is a maximum permeability based upon the assumption that the attenuation indicated at low frequencies is a real phenomenon. If significant attenuation is not present in the entire frequency band analyzed, vertical permeability would be lower.

The elastic and fluid flow properties determined from the response of LKT to atmospheric loading are used to infer how this well responds to crustal strains (Figure 2-9; note that we assume that the attenuated response to atmospheric loading reflects a real physical phenomenon). In terms of attenuation of sensitivity, it is not considerably different from the atmospheric pressure response. This correspondence indicates that the water table is largely in phase with the pressure disturbance. The inferred sensitivity remains high when frequencies are less than 0.001 cycles/day. Unfortunately, it will be shown below that while sensitivity remains high for low frequency response, the noise level at very low frequencies is also high.

The response of TF to atmospheric loading is shown in Figure 2-10. This response has a signature which indicates that water table influences are present throughout the observed frequency band. The relative lack of ambiguity in this signal is evident in the coherence squared for the transfer function (Figure 2-8) which is near 1 for frequencies in excess of 0.06 cycles/day. The response to atmospheric pressure has a maximum at about 0.5 cycles/day. It might be suspected that decreasing sensitivity with increasing frequency above the frequency of 0.5 cycles/day would be at least partially due to limited groundwater flow into and out of the borehole; this source of attenuation is unlikely because it is inconsistent with the near flat dilatational sensitivity for the semi-diurnal and diurnal tidal constituents shown in Table 2-2 and is also inconsistent with the phase of the atmospheric pressure response. Rather, this decreasing sensitivity at higher frequencies is likely due to air diffusion effects which amplify the atmospheric pressure response in the frequency band of 0.2 to 2 cycles/day. As Figure 2-6 indicates, such a response would be theoretically possible if the dimensionless numbers, R and Q, were of the same magnitude.

The best fit to the data is given with a static-confined barometric efficiency of 0.37 (γ=.63) and a value for both Q and R of 2.2ω where frequency is in terms of cycles/day. The fit to the atmospheric loading response indicates that water table drainage also influences tidal strain response at frequencies less than about 5 cycles/day. The value for Q' which is consistent with the atmospheric loading response is 1.7ω. Fitting the strain response to the observed M_2 dilatational efficiency given in Table 2-2 yields a static-confined

areal dilatation efficiency of 0.033 cm/nε. These values of static-confined barometric efficiency and areal dilatational efficiency indicate that the drained rock matrix compressibility for the rock in direct communication with the well bore is 1.9×10^{-11} cm²/dyne (see Chapter 1). Given this compressibility, the vertical permeability above the well is estimated to be 10 millidarcies, a value which is only slightly less than the lateral permeability inferred from pumping data, indicating that the material above and within the zone monitored is largely homogeneous and isotropic with respect to permeability.

The inferred response to tectonic strain is shown in Figure 2-9. In terms of attenuation of sensitivity, it is considerably different from the atmospheric pressure response. The inferred response to strain approaches static-confined conditions at a frequency of 2.5 cycles/day but the static-confined response is never fully observed in the frequency band analyzed. Below a frequency of 0.001 cycles/day, where strain sensitivity is about 1/10 the inferred static-confined response, strain sensitivity asymptotically approaches zero.

The raw and filtered (atmospheric loading effects removed) strain spectra for LKT and TF are shown in Figure 2-11. These strain spectra were derived by: 1) obtaining power spectral densities for the water level records in terms of cm² per cycle/day; 2) converting these spectra into units of strain²/Hz through the use of the estimated static confined areal dilatational efficiencies for the wells (0.034 cm/nε for LKT and 0.033 cm/nε for TF); 3) adjusting the strain spectra, when necessary, to account for any unambiguous frequency dependent changes in dilatational efficiency inferred from the response to atmospheric loading; 4) normalizing the spectra relative

to 1 strain^2/Hz and converting to a decibel scale. The spectral estimates TF were adjusted upwards to account for the observed decreasing sensitivity with period by essentially adding 8 db per decade decrease in frequency to the slopes of the strain spectra for frequencies less than 1 cycle/day; since the observed attenuation at LKT is slight and ambiguous in the frequency band examined here, no adjustments in the strain spectra were made. The raw strain spectra at LKT and TF are very similar and increase at a rate of roughly 25 db per decade decrease in frequency, a rate that is slightly high compared to the best dilatometers (Johnston et al., 1986) but is comparable to the behavior of some laser strain meters (Beavan and Goulty, 1977). The M_2 tide at both wells is roughly 20 db above the background noise level.

Considerable reduction in noise level can be achieved by filtering or removing the effects of barometric pressure on water level response. These effects were removed in two ways. In the first method the fit of the observed frequency response shown in Figures 2-7 and 2-10 was assumed to be the transfer function between water level and atmospheric pressure. This transfer function was then multiplied with the Fourier transform of the atmospheric pressure record and the resultant frequency response was then inverted into the time domain and subtracted from the water level time series. In the second method a single coefficient between the water level record and the atmospheric pressure record was found by linear regression of the two time series (the coefficient was .48 for LKT and .35 for TF); the atmospheric pressure record was then simply multiplied by this

coefficient and the resultant time series was then subtracted from the water level record.

At LKT, there is little difference between the strain spectra for the time series obtained with regression and the frequency dependent transfer function in the frequency range of interest. The lack of difference between the two strain spectra is due to the relatively flat response to air pressure in the frequency range of interest; as a result, it is operationally similar to the filter which assumes a simple linear relationship between water level and atmospheric pressure.

At TF, there is substantial difference between the strain spectra determined with the regression coefficient and the frequency dependent transfer function because there is considerable attenuation and phase shift of the atmospheric pressure signal.

Both filtered records at LKT and the record filtered with a frequency dependent transfer function at TF yield strain spectra whose slope increase at a rate of roughly 20 db per decade in frequency in the frequency band of 0.08 to 2.5 cycles per day. This is comparable to the rate of increase seen in the raw strain spectra of high quality strain instruments (Agnew, 1986; Beavan and Goulty, 1977; Johnston et al., 1986). Presumably, one could also remove the effects of atmospheric pressure from other strain instruments as well to decrease the rate at which noise levels increase. For instruments which measure horizontal strain only, however, the reduction in noise rate achieved by removing atmospheric loading effects would be slightly less than that for water wells since the sum of the principal horizontal strains induced near the earth's surface by atmospheric

loading is approximately 1/2 the cubic strain (Farrell, 1972). The similarity in rate of noise increase between water wells and other strain instruments suggests that either the effects of precipitation on the water level record are slight in this frequency band or are not significantly greater than other strain meters (Takemoto, 1983). Below 0.08 cycles/day, the slope of the corrected strain spectra increase significantly at both sites to about 35 db per decade. This slope increase may be due to the influence of precipitation, but the limited amount of data present for frequencies less than 0.1 cycles/day in these strain spectra make any analysis of low frequency behavior ambiguous.

Following the approach of Agnew (1987), we compare the strain response shown in Figure 2-11 with standard electronic distance measurement response by transforming standard error estimates for distance measurements into strain spectra. When the strain spectrum of the water well exceeds the strain spectrum of the distance measurement, the water well is less accurate; when the strain spectrum of the well is less then the strain spectrum of the distance measurement, the water well is more accurate. The most accurate electronic distance measurement currently available is obtained with a two color laser device (Linker et al., 1986). The standard error for a two color distance measurement taken over a baseline of 10 km is 1.2 x 10^{-7}. If 10 km length distance measurements were made to determine areal dilatation with a two color geodimeter once a day, the resultant strain spectrum would be (in the absence of a tectonic signal) a flat -83 db, relative to 1 strain^2/Hz. The raw and corrected strain spectra for both wells are well below this noise level until

frequencies are less than 0.04 cycles/day indicating that these wells are quite capable of outperforming existing distance measurement capability over the time span of days to weeks.

CONCLUSIONS

The results given here suggest that theoretical models which describe the response of water wells to air pressure and tectonic strain can be used, in conjunction with cross-spectral estimation, to yield some valuable information on the influence the water table has on strain sensitivity. When the water table is weakly isolated from air pressure changes, the attenuation of the air pressure response of water wells is qualitatively similar to the attenuation of the earth tide and tectonic strain response. Well sensitivity in both cases gradually attenuates with decreasing frequency due to the presence of the water table and the frequency at which significant attenuation begins to take place is a strong function of well geometry and rock material properties. For wells open to rock in excess of 100 m below the water table, attenuation of sensitivity will be slight at periods of days to weeks if the rock above the open interval has a vertical permeability of 0.1 md or less and a compressibility of 1×10^{-11} cm^2/dyne.

The wells examined here are most useful as strain meters over a limited frequency band. Both exceed the accuracy of standard distance measurement techniques for strains with periods of days to weeks; at longer periods, electronic distance measurements can have superior performance. At TF, increasing noise with increasing period

appears to be the result of decreasing strain sensitivity in the presence of a 15 to 20 db per decade increase in the water level power spectrum. At LKT, the increasing noise appears to be largely due simply to a 20 to 25 db per decade increase in the water level spectrum.

The noise levels of these wells, in the frequency band of 0.08 to 2.5 cycles/day are not substantially different from the noise levels of other continuous strain meters; this correspondence indicates that if precipitation influences these wells in this frequency band, it does so at a level which is not significantly different than its influence on other strain instruments. If tectonic events are preceded by strains on the order of 10^{-8} which take place over periods of less than a month, they can be detectable in water wells which are sensitive to strain.

APPENDIX A: SOLUTION TO THE RESPONSE OF A WELL TO A PERIODIC DILATATION WHICH DOES NOT DIRECTLY PRESSURIZE THE WELL OR WATER TABLE

The solution to the response of a well to periodic dilatation is obtained by solving for the pore pressure response to periodic dilatation. We assume that the well is an accurate gage of the average pore pressure of the saturated rock with which it is in communication and assume that the open interval of the well is very small relative to the change in pore pressure with depth. Pore pressure response to a periodic dilatation, $A\cos\omega t$, is governed by the equation:

$$D' \frac{\partial^2 P}{\partial z^2} = \frac{\partial P}{\partial t} - CA\omega \sin\omega t \qquad (A1)$$

Equation A1 was obtained from equation 1 by substituting $A\cos\omega t$ for ϵ_{2r}. This equation must be solved subject to the boundary conditions:

$$P(0,t) = 0$$

$$P(\infty,t) = -AC\cos\omega t \qquad (A2)$$

where z=0 is taken to be the water table. No initial condition is imposed because we seek the periodic steady-state solution. This problem is easily solved by employing complex notation. Taking P to be complex:

$$P(z,t) = F(z)\exp(i\omega t) \qquad (A3)$$

and substituting in equation A1 we obtain:

$$F'' = \frac{i\omega F}{D'} + \frac{i\omega CA}{D'} \qquad (A4)$$

$$F(0) = 0$$

$$F(\infty) = -AC$$

where, ", implies double differentiation and all exponential terms have been divided out. Equation A4 is a second order inhomogeneous ordinary differential equation. Its particular solution, F_p, is:

$$F_p = -AC \tag{A5}$$

Its homogeneous solution, F_h, is:

$$F_h = ACexp(-(i+1)\sqrt{\bar{Q}'}) \tag{A6}$$

where Q' is defined in equation 11. Summing equations A5 and A6, the solution in terms of gain and phase is:

$$\text{Gain} = |P/AC| = \sqrt{(J^2+K^2)} \tag{A7}$$
$$\text{Phase} = \text{Tan}^{-1}(K/J)$$

where J and K are:

$$J=exp(-\sqrt{\bar{Q}'})cos(\sqrt{\bar{Q}'}) - 1$$
$$K=exp(-\sqrt{\bar{Q}'})sin(\sqrt{\bar{Q}'}) \tag{A8}$$

Since the well is assumed to be an accurate gauge of pore pressure in the frequency band of interest, water level changes are related to pore pressure changes by $W=P/\rho g$ and the solution in terms of water level change per change in strain can be obtained from equation A7 by multiplying the gain by $C/\rho g$. The solution in the real domain is given in equation 10.

APPENDIX B: SOLUTION TO THE RESPONSE OF A WELL TO PERIODIC FLUCTUATIONS IN ATMOSPHERIC PRESSURE

The solution for the response of a well to periodic fluctuations in atmospheric pressure is obtained, as in Appendix A, by solving for the pore pressure response. In Appendix A, it was assumed that the water table (z=0) was always at zero pressure; this is not the case for periodic fluctuations in atmospheric pressure and before pressure at depth can be known, the water table pressure must be determined. The water table response to periodic fluctuations in atmospheric pressure is determined through the use of a diffusion equation for flow of air through unsaturated porous materials (Buckingham, 1904; Weeks, 1979):

$$D_a \frac{\partial^2 P_a}{\partial z^2} = \frac{\partial P_a}{\partial t} \qquad \text{(B1)}$$

subject to the following boundary conditions:

$$P_a(-T,t) = A\cos\omega t$$
$$P_a(T,t) = A\cos\omega t \qquad \text{(B2)}$$

where P_a is the air pressure. The boundary -T is taken to be the earth's surface; the zone from depth 0 to depth T is simply an artifice to assure that at the water table, z=0, there is no air flux. As in Appendix A, we seek the periodic steady state solution:

$$P_a(z,t) = F(z)\exp(i\omega t) \qquad \text{(B3)}$$

Substitution of B3 into equations B1 and B2 yields the following second order homogeneous differential equation with transformed boundary conditions:

$$F'' = \frac{i\omega F}{D_a} \qquad (B4)$$

$$P_a(-T,t) = P_a(T,t) = A$$

The solution for the air pressure at the water table is obtained by solving equation B4 at z=0:

$$P_a = M\cos(\omega t) + N\sin(\omega t) \qquad (B5)$$

where M and N are given in equation 13. The pore pressure at the water table is $-P_a$.

With the pressure at the water table known, the solution to pore pressure response to a periodic atmospheric pressure fluctuation, $A\cos\omega t$, is obtained from the following modified version of equation 6:

$$D\frac{\partial^2 P}{\partial z^2} = \frac{\partial P}{\partial t} - \gamma A\omega\sin\omega t \qquad (B6)$$

The appropriate boundary conditions are:

$$P(0,t) = -M\cos(\omega t) - N\sin(\omega t)$$

$$P(\infty,t) = -A\gamma\cos\omega t \qquad (B7)$$

We again take P to be complex:

$$P(z,t) = F(z)\exp(i\omega t) \tag{B8}$$

and substituting into equation B6 we obtain:

$$F'' = \frac{i\omega}{D}F + \frac{i\omega\gamma A}{D} \tag{B9}$$

$$F(0) = (-M+iN)$$

$$F(\infty) = -A\gamma$$

where, ", implies double differentiation and all exponential terms have been divided out. Equation B9 is a second order inhomogeneous ordinary differential equation. Its particular solution, F_p, is:

$$F_p = -A\gamma \tag{B10}$$

Its homogeneous solution, F_h, is:

$$F_h = (-M+iN+\gamma)A\exp(-(i+1)\sqrt{\bar{Q}}) \tag{B11}$$

The sum of equations B10 and B11 multiplied by exp(iωt) yield the solution to pore pressure response to periodic changes in atmospheric pressure. The response in terms of water level within the well can be obtained (as in equation 9) by adding Acosωt to the real part of the

solution and dividing by ρg. The solution for water well pressure, P_w, in terms of gain and phase is given by:

$$\text{Gain} = |P_w/A| = \sqrt{(U^2+V^2)} \qquad \text{(B12)}$$
$$\text{Phase} = \text{Tan}^{-1}(V/U)$$

where U and V are:

$$U=(-M+\gamma)\exp(-\sqrt{Q})\cos(\sqrt{Q}) + N\exp(-\sqrt{Q})\sin(\sqrt{Q}) - (\gamma-1)$$
$$V=(-M+\gamma)\exp(-\sqrt{Q})\sin(\sqrt{Q}) - N\exp(-\sqrt{Q})\cos(\sqrt{Q}) \qquad \text{(B13)}$$

The solution in the real domain in terms of water level is given in equation 12.

APPENDIX C: METHOD BY WHICH GAPS WERE FILLED IN THE WATER LEVEL AND ATMOSPHERIC PRESSURE RECORD

Gaps in the water level and atmospheric pressure record over the time period examined were filled by an iterative process. The gaps were originally filled by linear interpolation. A finite impulse response high pass filter (Otnes and Enochson, 1978) with a cutoff frequency of 10^{-6} Hz was then applied to the water level and atmospheric pressure data to remove any long term trends. The autocovariance with a maximum length of 40 days was then calculated for each time series. Gaps were then filled with a symmetric linear filter of length 120 with weights determined from the structure of the autocovariance and the distance between the interpolated point and the

nearest data point. The spacing between each value used in the filter was eight data points (two hours) and weights were calculated by solving the following system of linear equations:

$$\begin{bmatrix} \sigma^2 & C1\dagger 2 & .. & C1\dagger 60 & 1 \\ C2\dagger 1 & \sigma^2 & .. & C2\dagger 60 & 1 \\ .. & .. & .. & .. & 1 \\ C60\dagger 1 & .. & .. & \sigma^2 & 1 \\ 1 & 1 & 1 & 1 & 0 \end{bmatrix} \begin{bmatrix} w_1 \\ w_2 \\ .. \\ w_{60} \\ \mu \end{bmatrix} = \begin{bmatrix} C1\dagger' \\ C2\dagger' \\ .. \\ C60\dagger' \\ 1 \end{bmatrix} \qquad (C1)$$

where σ^2 is the variance, μ is the mean, Ci†j is the autocovariance between the ith data value and the jth data value used in the interpolation, w_i is the weight of the ith data point in the filter and Ci†' denotes the autocovariance for the length between the interpolated point and the ith nearest data value. This linear system of equations provides an estimate of the interpolated value for which the estimation variance is at a minimum (Journel and Huijbregts, 1978). The estimation variance is σ_e^2 is defined as:

$$\sigma_e^2 = \sigma^2 + \mu - \Sigma w_i Ci\dagger' \qquad (C2)$$

Once the gaps were interpolated using the system of equations given in equation C1, the residual time series (the original time series with linearly interpolated gaps minus the high pass filtered time series with linearly interpolated gaps) was added to the new time series to preserve the long term trend.

APPENDIX D: METHOD BY WHICH THE TRANSFER FUNCTIONS OF WATER LEVEL TO EARTH TIDES AND ATMOSPHERIC PRESSURE WERE DETERMINED

The relation of water level to earth tides and atmospheric pressure at the wells in the frequency domain was obtained by solving the following complex system of equations for every frequency (Bendat and Piersol, 1986):

$$\begin{bmatrix} BB & BT \\ TB & TT \end{bmatrix} \begin{bmatrix} HB \\ HT \end{bmatrix} = \begin{bmatrix} BW \\ TW \end{bmatrix} \qquad (D1)$$

where: BB and TT denote the power spectra of the atmospheric pressure and earth tides respectively; BT denotes the cross spectrum between atmospheric pressure and earth tides; TB denotes the complex conjugate of the cross spectrum between atmospheric pressure and earth tides; BW and TW denote the cross spectra between atmospheric pressure and water level and earth tides and water level, respectively; and HB and HT denote the transfer function between water level and atmospheric pressure and water level and earth tides respectively. The power spectra and cross spectra were obtained for the time series of interest by using the Blackman-Tukey procedure (Bendat and Piersol, 1986) after removing the mean and long term trend from the time series. This procedure is computationally inefficient because it requires that the autocorrelation or cross-correlation function be calculated in the real domain in order to obtain spectral quantities; it was used because the frequencies of interest are low relative to the length of the data set. The spectral estimates obtained from the Blackman-Tukey procedure are smoothed using a Hanning window (Otnes and Enochson, 1978).

At TF, the long term trend was removed with a high pass finite impulse response filter (Otnes and Enochson, 1978) with a cutoff frequency of 10^{-6} Hz. Spectral estimates were then obtained using a maximum correlation length of 20 days. At LKT, the time series for water level, atmospheric pressure and earth tides were lengthened to include the first half of 1986 and the data were decimated to 2 samples per hour; the time series was lengthened to see whether any attenuation of sensitivity could be unambiguously identified at low frequencies. The long term trend was removed with a high pass finite impulse response filter with a cutoff frequency of 5×10^{-8} Hz. Spectral estimates were obtained using a maximum correlation length of 40 days.

The barometric and dilatational efficiency as a function of frequency are simply the gains of the transfer functions HB and HT respectively. The phase relations given for LKT and TF are the phase of the transfer functions. The multiple coherence squared, Γ^2, of the transfer functions as a function of frequency is obtained from the following spectral estimates (Otnes and Enochson, 1978):

$$\Gamma^2 = \frac{(WB \times TT - WT \times TB)BW + (WT \times BB - WB \times BT)TW}{(TT \times BB - TB \times BT)WW} \quad (D2)$$

where WB and WT denote the complex conjugates of BW and TW respectively and WW is the water level power spectrum. This coherence squared is a measure of the ability of a linear relationship of water level to atmospheric pressure and earth tides to account for the water level power.

REFERENCES

Agnew, D. C., On noise levels in deformation measurements: comparison in the frequency domain, U. S. Geol. Surv. Open File Rep., 87-591, 838-844, 1987.

Agnew, D. C., Strainmeters and tiltmeters, Rev. Geophys., 24, 579-624, 1986.

Bakun, W. H., and T. V. McEvilly, Recurrence models and Parkfield, California earthquakes, J. Geophys. Res., 89, 3051-3058, 1984.

Beaumont, C., and J. Berger, An analysis of tidal strain observations from the United States of America: I. The homogeneous tide, Bull. Seismol. Soc. Am., 66, 1821-1846, 1976.

Beavan, R. J., and N. R. Goulty, Earth strain observations made with the Cambridge laser strainmeter, Geophys. J. R. Astr. Soc., 48, 293-305, 1977.

Bendat, J. S., and A. G. Piersol, Random Data: Analysis and Measurement Procedures, John Wiley and Sons, New York, 566pp., 1986.

Berger J., and C. Beaumont, An analysis of tidal strain observations from the United States of America: II. The inhomogeneous tide, Bull. Seismol. Soc. Am., 66, 1821-1846, 1976.

Biot, M. A., General theory of three-dimensional consolidation, J. Appl. Phys., 12, 155-164, 1941.

Biot, M. A., and D. G. Willis, The elastic coefficients of the theory of consolidation, J. Appl. Mech., 24, 594-601, 1957.

Bodvarsson, G., Confined fluids as strain meters, J. Geophys. Res., 75, 2711-2718, 1970.

Brace, W. F., Permeability of crystalline rock: new in situ measurements, J. Geophys. Res., 89, 4327-4330, 1984.

Brace, W. F., Permeability of crystalline and argillaceous rocks, Int. J. Rock Mech. Min. Sci., 17, 241-251, 1980.

Bredehoeft, J. D., Response of well-aquifer systems to earth tides, J. Geophys. Res., 72, 3075-3087, 1967.

Buckingham, E., Contributions to our knowledge of the aeration of soils, Bull. 25, 52pp., U. S. Dept. Agr. Soils Bur., Washington, D. C., 1904.

Cockerham, R. S., and A. M. Pitt, Seismic Activity in Long Valley caldera area, California: June 1982 through July 1984, U. S. Geol. Surv. Open-File Rep., 84-939, 493-526, 1984.

Cooper, H. H. Jr., J. D. Bredehoeft, I. S., Papadopulos, and R. R. Bennett, The response of well-aquifer systems to seismic waves, J. Geophys. Res., 70, 3915-3926, 1965.

Farrell, W. E., Deformation of the earth by surface loads, Rev. Geophys. Space Phys., 10, 761-797, 1972.

Gieske, A., On phase shifts and periodic well fluctuations, Geophys. J. R. Astr. Soc., 86, 789-799, 1986.

Jacob, C. E., The flow of water in an elastic artesian aquifer, Eos Trans. AGU, 21, 574-586, 1940.

Johnson, A. G., Pore pressure changes associated with creep events on the San Andreas Fault, Ph.D. thesis, Dept. of Geophysics, Stanford University, 177pp., 1973.

Johnson, A. G., R. L. Kovach, and A. Nur, Fluid pressure variations and fault creep in Central California, Tectonophysics, 23, 257-266, 1974.

Johnson, A. G., R. L. Kovach, A. Nur, and J. R. Booker, Pore pressure changes during creep events on the San Andreas Fault, J. Geophys. Res., 78, 851-857, 1973.

Johnston, M. J. S., R. D. Borcherdt, and A. T. Linde, Short- period near-source strain field for an earthquake near San Juan Bautista, California, J. Geophys. Res., 91, 11497-11502, 1986.

Journel, A. G., and C. J. Huijbregts, Mining Geostatistics, Academic Press, New York, 599pp., 1978.

Kipp, K. L. Jr., Type curve analysis of inertial effects in the response of a well to a slug test, Water Resour. Res., 21, 1397-1408, 1985.

Linker, M. F., J. O. Langbein, and A. McGarr, Decrease in deformation rate observed by two-color laser ranging in Long Vally caldera, Science, 232, 213-216, 1986.

Miller, C. D., Holocene eruptions at the Inyo volcanic chain, California - implications for possible eruptions in Long Valley caldera, Geology, 13, 14-17, 1985.

Mortensen, C. E., R. C. Lee, and R. O. Burford, Observations of creep-related tilt, strain and water-level changes on the central San Andreas Fault, Bull. Seismol. Soc. Am., 67, 641-649, 1977.

Nur, A., and J. D. Byerlee, An exact effective stress law for elastic deformation of rock with fluids, J. Geophys. Res., 76, 6414-6419, 1971.

Otnes, R. K., and L. Enochson, Applied Time Series Analysis, John Wiley and Sons, New York, 449pp., 1978.

Rice, J. R., and M. P. Cleary, Some basic stress diffusion solutions for fluid saturated elastic porous media with compressible constituents, Rev. Geophys. Space Phys., 14, 227-241, 1976.

Roeloffs, E., and J. W. Rudinicki, Coupled deformation - diffusion effects on water-level changes due to propagating creep events, Pageoph., 122, 560-582, 1984.

Savage, J. C., and M. M. Clark, Magmatic resurgence in Long Valley caldera, California: possible cause of the 1980 Mammoth Lakes earthquakes, Science, 217, 531-533, 1982.

Skempton, A. W., The pore-pressure coefficients A and B, Geotechnique, 4, 143-147, 1954.

Sterling, A., and E. Smets, Study of earth tides, earthquakes and terrestial spectroscopy by analysis of the level fluctuations in a borehole at Heibaart (Belgium), Geophys. J. R. Astr. Soc., 23, 225-242, 1971.

Takemoto, S, Effect of meterological and hydrological changes on ground strains, Bull. Disaster Prev. Res. Inst. Kyoto Univ., 31, 211-237, 1983.

Van der Kamp, G. and J. E. Gale, Theory of earth tide and barometric effects in porous formations with compressible grains, Water Resour. Res., 19, 538-544, 1983.

Weeks, E. P., Barometric fluctuations in wells tapping deep unconfined aquifers, Water Resour. Res., 15, 1167-1176, 1979.

Wesson, R. L., Interpretation of changes in water level accompanying fault creep and implications for earthquake prediction, J. Geophys. Res., 86, 9259-9267, 1981.

Table 2-1: Description of wells examined. Local permeability refers to the permeability near the borehole.

WELL ID	LOCATION	OPEN INTERVAL (m)	LOCAL PERMEABILITY
LKT	Long Valley,CA	152-296	2×10^{4} millidarcies
TF	Parkfield, CA	152-177	2×10^{1} millidarcies

Table 2-2: Tidal response of wells examined. Gain expressed in terms of centimeters of water level drop per areal nanostrain. Phase expressed in degrees.

WELL ID	O_1 GAIN	O_1 PHASE	M_2 GAIN	M_2 PHASE
LKT	0.0314	-183.8	0.0337	-189.4
TF	0.0293	-171.1	0.0337	-171.8

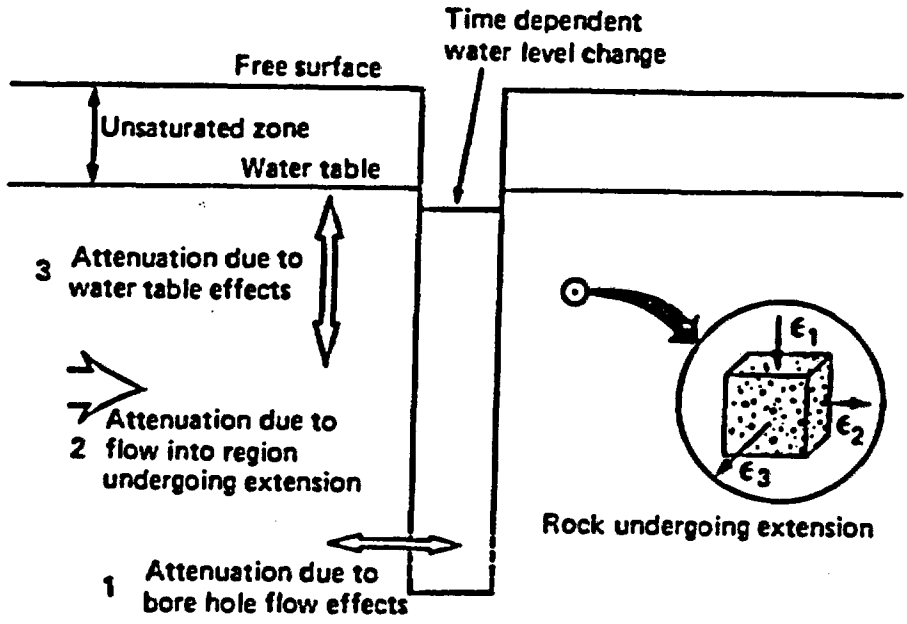

Figure 2-1: Cross-section of well response to deformation and principal sources of attenuation of well response.

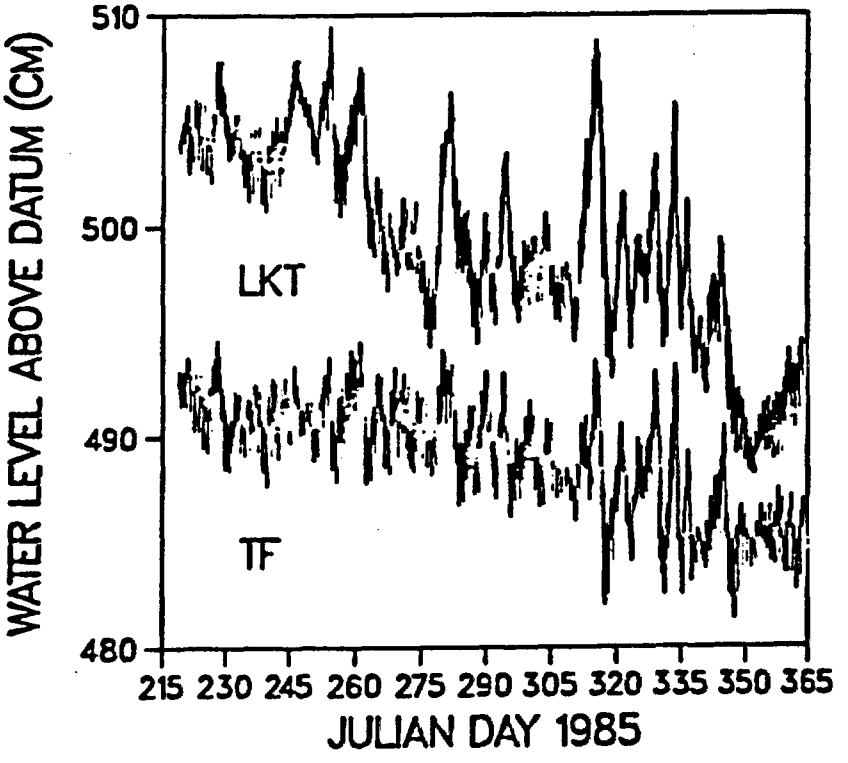

Figure 2-2: Water level record at LKT and TF during the second half of 1985.

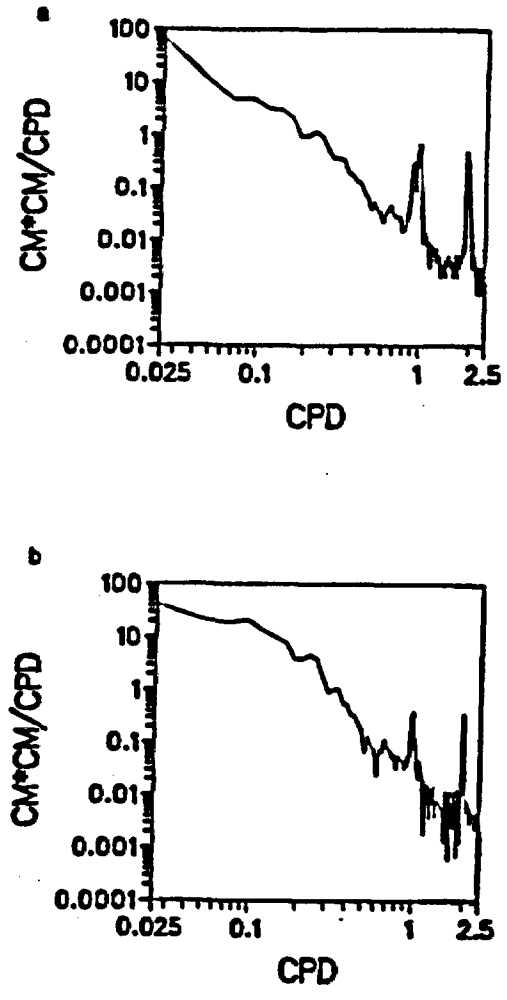

Figure 2-3: Power spectral densities for water level (a) and atmospheric pressure (b) at LKT; power spectral densities for water level (c) and atmospheric pressure (d) at TF. The abbreviation 'CPD' in the figures denotes cycles per day.

c

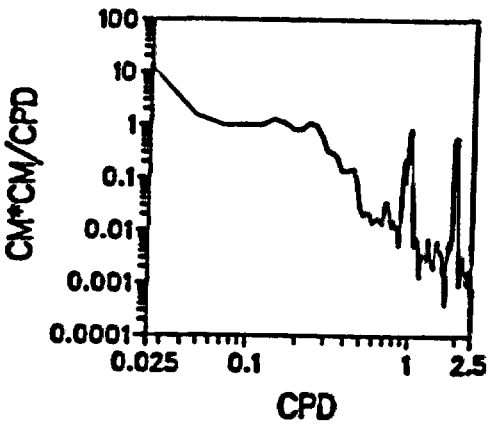
100
10
1
0.1
0.01
0.001
0.0001
CM*CM/CPD
0.025
0.1
1
2.5
CPD

d

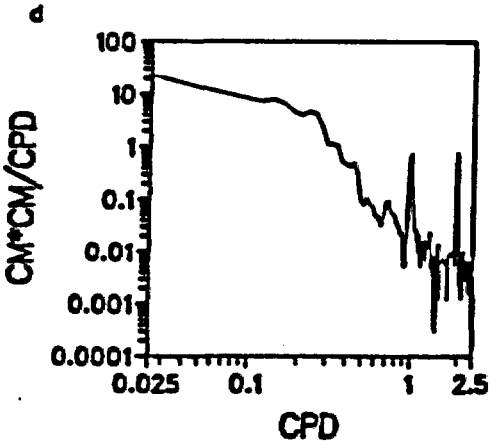
100
10
1
0.1
0.01
0.001
0.0001
CM*CM/CPD
0.025
0.1
1
2.5
CPD

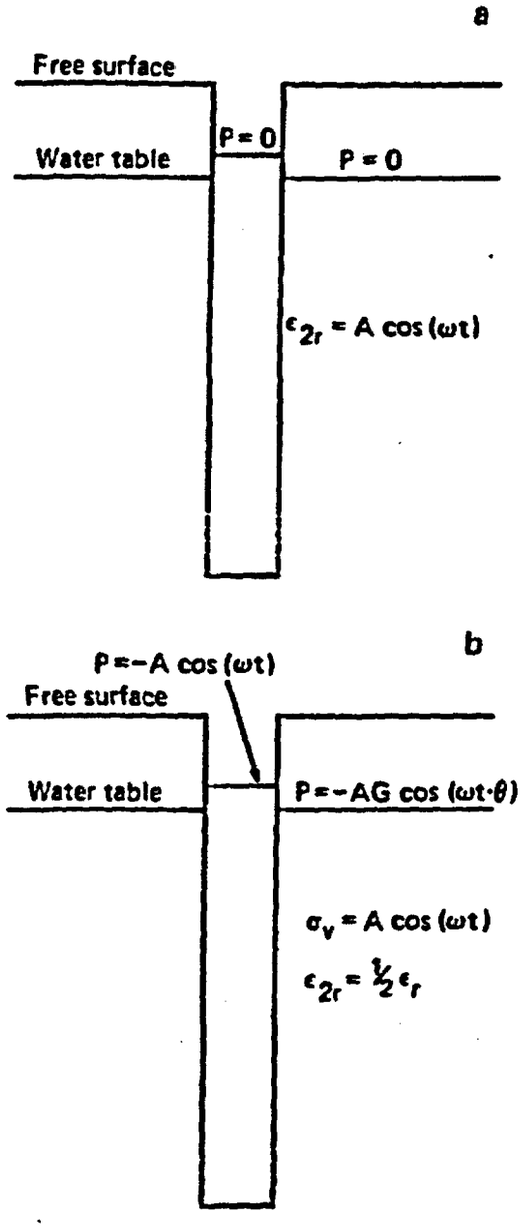

Figure 2-4: a) Idealized model of response of well to areally extensive periodic strain; b) Idealized model of response of well to areally extensive periodic atmospheric pressure changes.

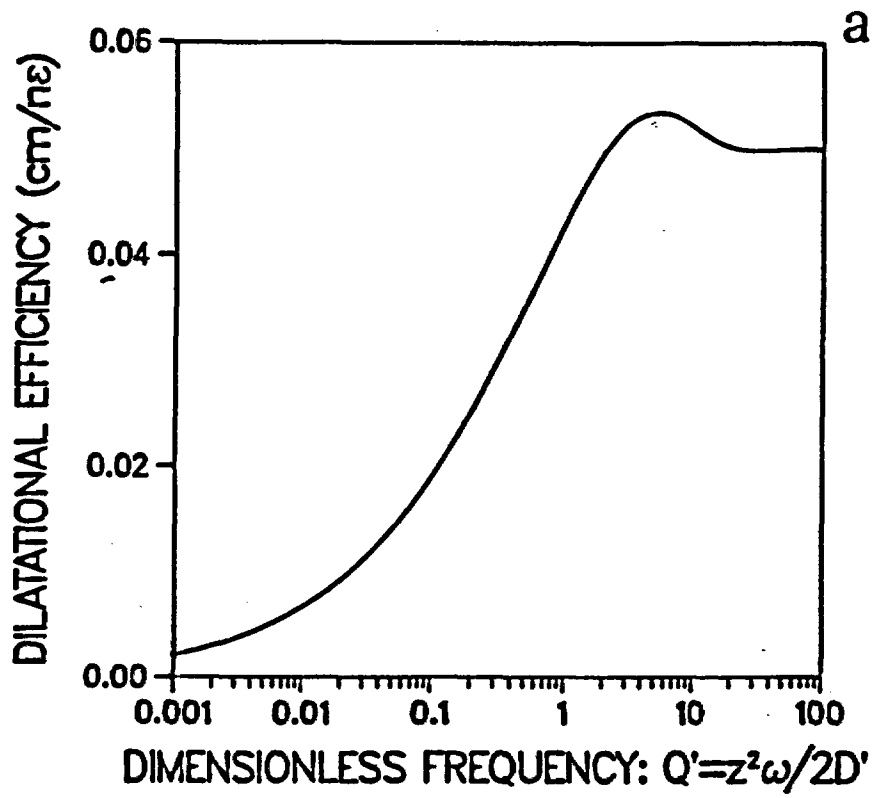

Figure 2-5: Response of well to areally extensive periodic strains in terms of areal dilatational efficiency (cm water level drop per areal nanostrain) (a) and phase (b). Static-confined areal dilatational efficiency is 0.05 cm/nε.

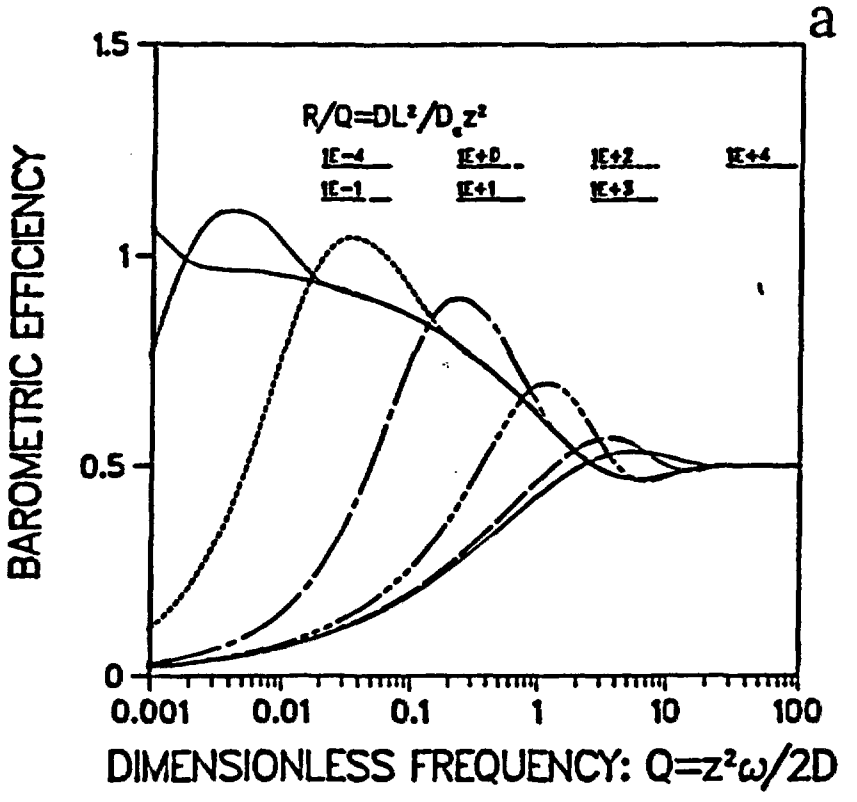

Figure 2-6: Barometric efficiency (a) and phase (b) of response to atmospheric pressure as a function of frequency and R/Q. Static-confined barometric efficiency is 0.5.

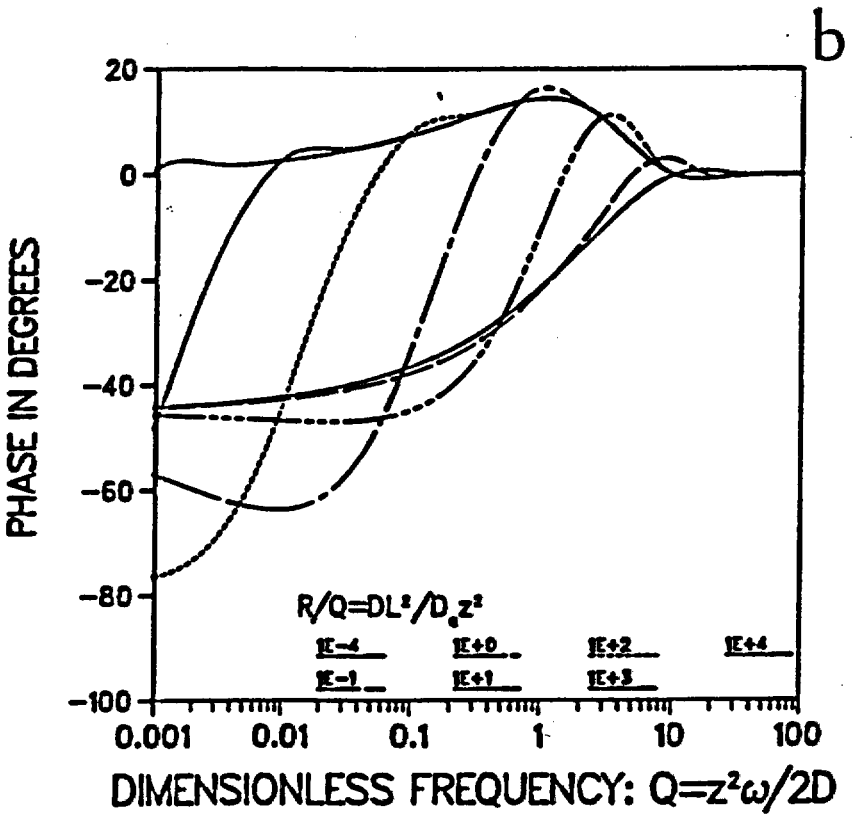
b
20
0
-20
-40
-60
-80
-100
PHASE IN DEGREES
R/Q=DL²/D_eZ²
1E-4
1E-3
1E+0
1E+1
1E+2
1E+3
1E+4
0.001
0.01
0.1
1
10
100
DIMENSIONLESS FREQUENCY: Q=z²ω/2D

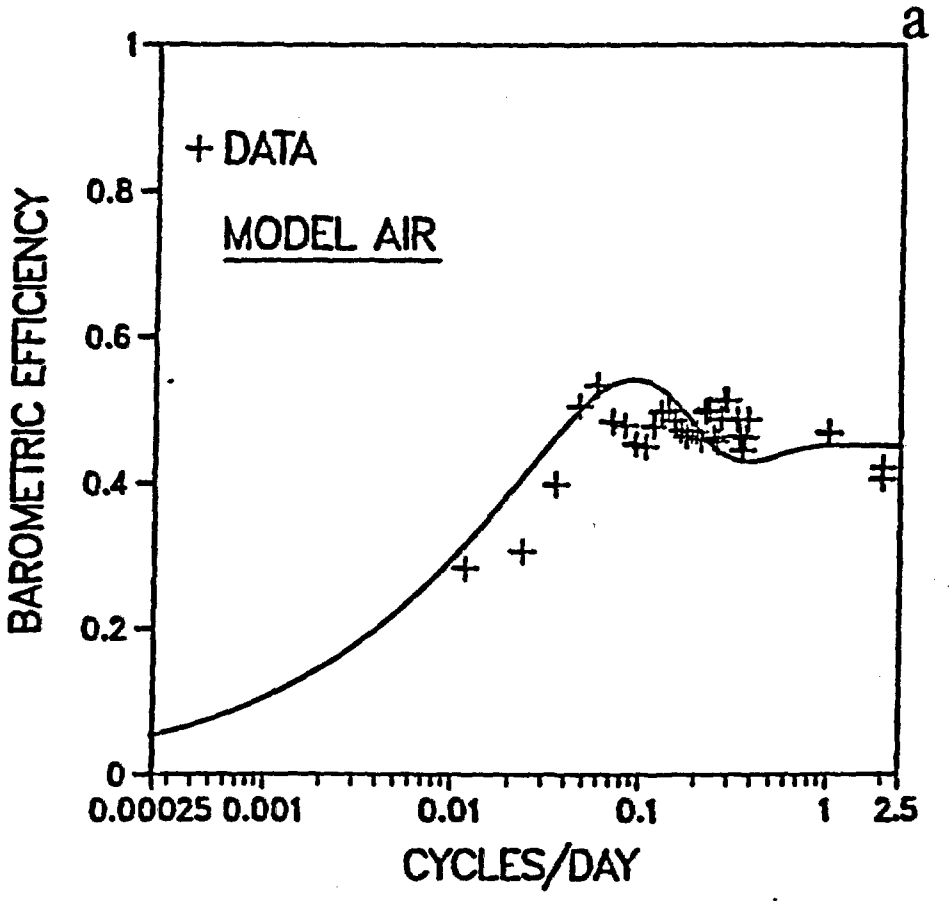

Figure 2-7: Response of LKT to atmospheric pressure in terms of barometric efficiency (a) and phase (b). Fit to data is solid line denoted as 'MODEL AIR'.

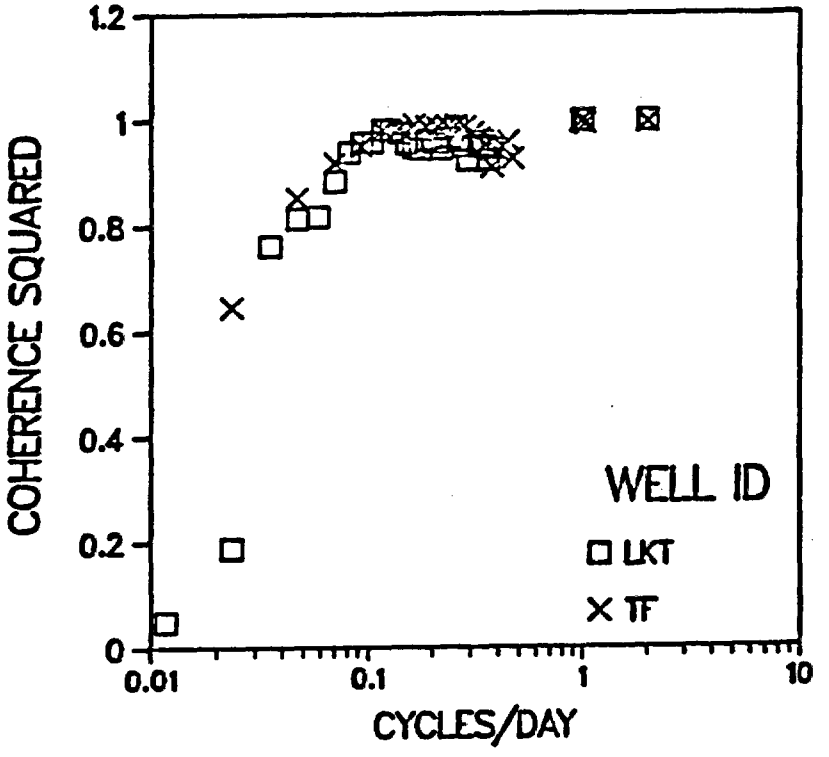

Figure 2-8: Multiple coherence squared for relation of water level to atmospheric pressure and earth tides at LKT and TF.

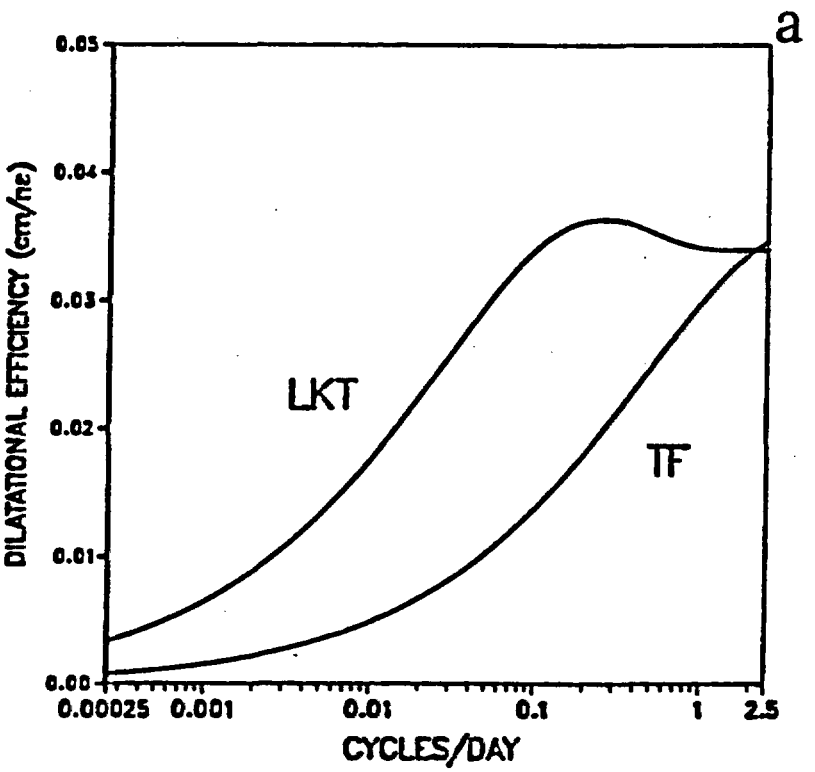

Figure 2-9: Inferred strain response of LKT and TF in terms of areal dilatational efficiency (a) and phase (b).

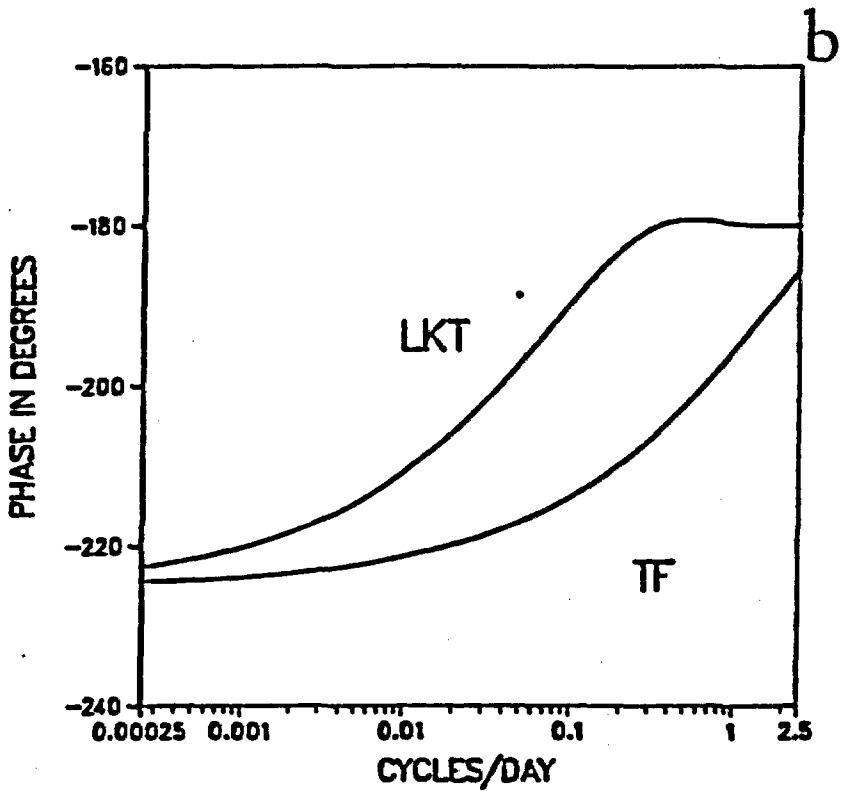
b
-160
-180
-200
-220
-240
PHASE IN DEGREES
LKT
TF
0.00025
0.001
0.01
0.1
1
2.5
CYCLES/DAY

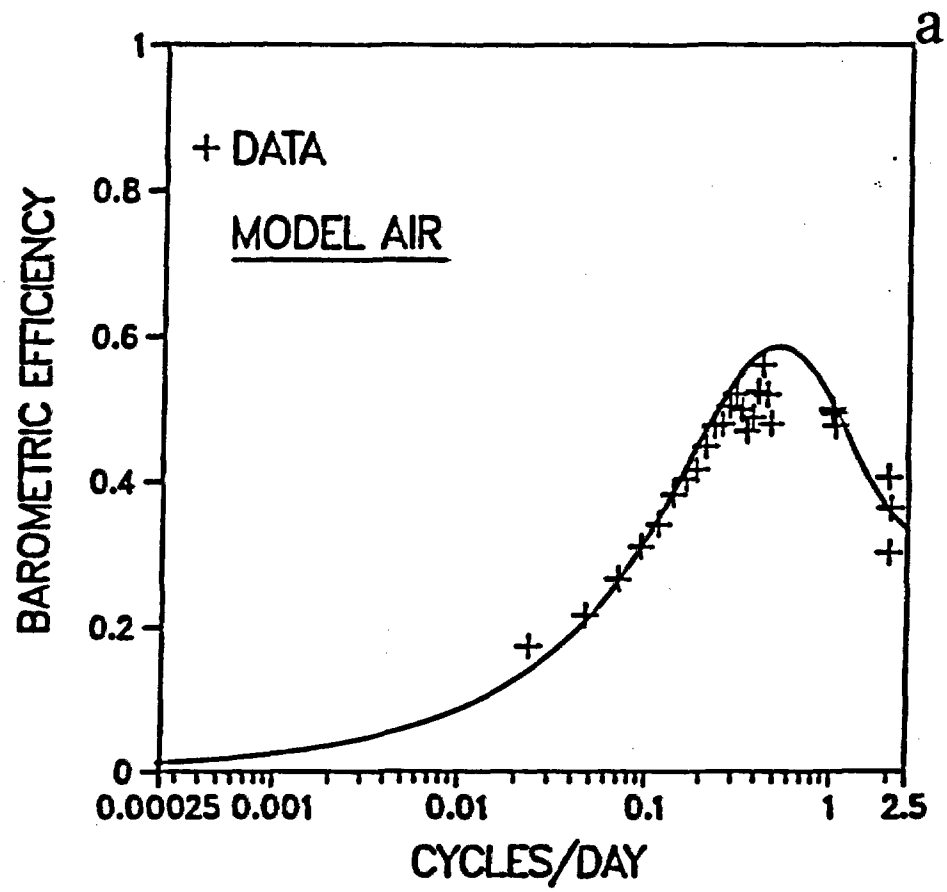

Figure 2-10: Response of TF to atmospheric pressure in terms of barometric efficiency (a) and phase (b). Fit to data is solid line denoted as 'MODEL AIR'.

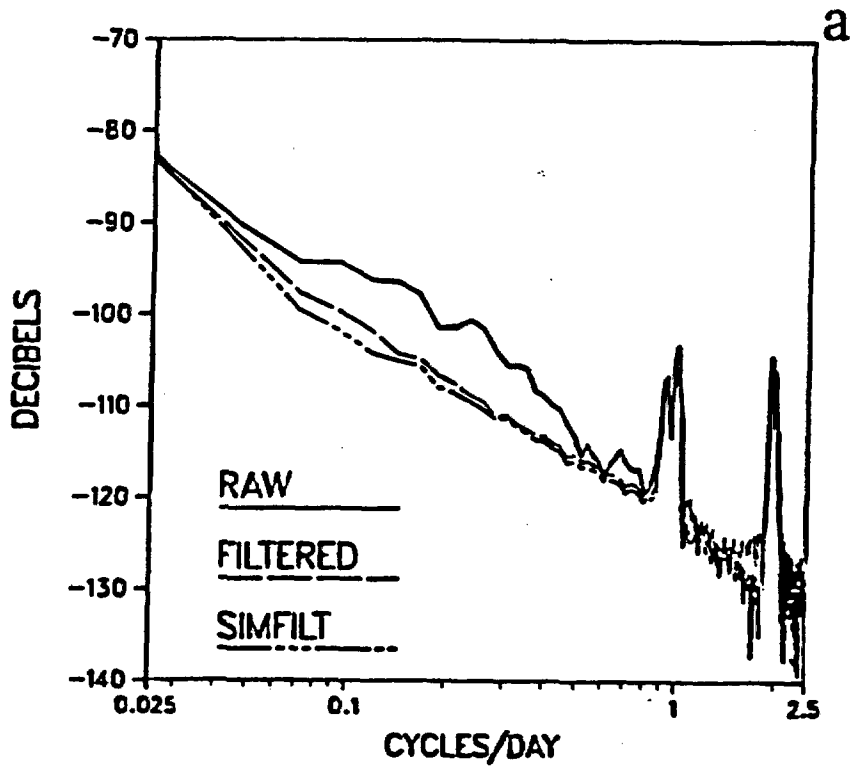

Figure 2-11: Power spectral densities at LKT (a) and TF (b) normalized to 1 strain^2/Hz. 'RAW' curve is water level record without atmospheric pressure effects removed. 'FILTERED' curve is water level record with atmospheric pressure effects removed with a frequency dependent transfer function. 'SIMFILT' curve is water level record with atmospheric pressure effects removed with a filter of length one.

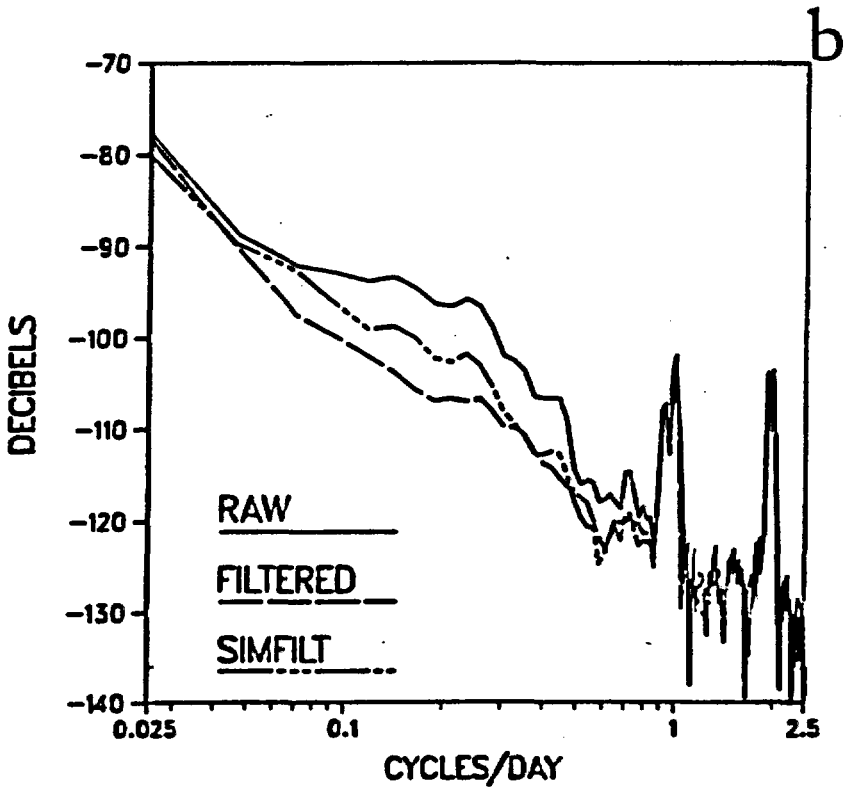
b
-70
-80
-90
-100
-110
-120
-130
-140
DECIBELS
RAW
FILTERED
SIMFILT
0.025
0.1
1
2.5
CYCLES/DAY

Such waltzing was not easy

Theodore Roethke

CHAPTER 3

DETERMINATION OF FLUID FLOW PROPERTIES FROM THE RESPONSE OF THE WATER LEVEL IN AN OPEN WELL TO ATMOSPHERIC LOADING: PARTIALLY CONFINED CONDITIONS

ABSTRACT

The water level in a well that taps a partially confined aquifer is often sensitive to atmospheric loading. The magnitude and character of this response is partly governed by: the well radius; the lateral hydraulic diffusivity of the aquifer; the thickness and vertical pneumatic diffusivity of the unsaturated zone; and the thickness and vertical hydraulic diffusivity of the saturated zone overlying the aquifer. These key elements can be combined into five dimensionless parameters which partly govern the phase and attenuation of the response. In many cases, the response of a well to atmospheric loading can be broken up into a high, intermediate and low frequency response. The high frequency response is governed largely by the well radius and lateral diffusivity of the aquifer. The intermediate frequency response is governed by the surface loading efficiency of the aquifer. The low frequency response is governed by the vertical pneumatic diffusivity and thickness of the unsaturated zone and the vertical hydraulic diffusivity and thickness of the saturated material

above the aquifer. Cross-spectral estimation is used to fit the response to atmospheric loading of three water wells to the theoretical curves in order to yield estimates of three of the key dimensionless parameters. These estimates then are used to make estimates or place bounds on the vertical pneumatic diffusivity of the unsaturated zone, the lateral permeability of the aquifer, and the composite vertical hydraulic diffusivity of the overlying saturated materials.

INTRODUCTION

The water level in a well is often sensitive to atmospheric loading. Figure 3-1 compares a hydrograph of one of the wells to be examined in detail to local barometric pressure and tidal strain. The well responds inversely to barometric pressure changes, a phenomenon first rigorously examined by Jacob (1940). The well also responds to tidal strains (compression is positive). If the aquifer is perfectly confined and has high lateral transmissivity, the response of a water well to atmospheric loading and earth tides will be a direct indication of the undrained response of the aquifer to imposed deformation. Under these conditions, changes in atmospheric pressure are related to changes in the water level of the well by a simple linear coefficient called the barometric efficiency (Jacob, 1940) or static-confined barometric efficiency (see Chapter 1); changes in earth-tide induced strain are related to changes in water level by a simple linear coefficient sometimes called the static-confined dilatational efficiency (see Chapter 1). If these coefficients are

known or can be inferred, it is theoretically possible to determine the elastic properties and porosity of the aquifer (Bredehoeft, 1967; Van der Kamp and Gale, 1983; see Chapter 1).

Aquifers, however, are never perfectly confined and their transmissivity can range in value over many orders of magnitude. Hence, the response of a water well to atmospheric loading and earth tides may not always be a direct indication of the undrained, or static-confined, response of the aquifer. In Chapter 2, I discuss the response of aquifers to earth tides and tectonic strain under conditions of partial drainage or partial confinement. The focus of this paper is on the response of water wells to atmospheric loading.

Figure 3-2a conceptually shows that air flow and groundwater flow can influence the response of a well to atmospheric loading. When atmospheric pressure changes slowly, air flow through the unsaturated zone and groundwater flow between the aquifer and the water table cause the aquifer response to be partially drained. When atmospheric pressure changes take place rapidly, aquifer response may be nearly undrained, but radial groundwater flow into and out of the well can strongly attenuate water well response if lateral aquifer transmissivity is low. These deviations from the undrained, or confined, water well response cause the barometric efficiency of a well to be a function of the length of time or frequency over which the atmospheric pressure change takes place.

It is instructive to examine the idealized response of the well-aquifer system shown in Figure 3-2a to a step change in atmospheric load ΔP. Initially, the aquifer and partial confining layer are pressurized instantaneously via grain to grain contact due to the

change in surface load. The pressure is changed by an amount $\gamma''\Delta P$ in the confining layer and $\gamma\Delta P$ in the aquifer, where γ'' and γ are the surface loading efficiencies of the partial confining layer and the aquifer respectively (see Chapter 1). In contrast to the aquifer and the partial confining layer, the pressure change at the water surface of the open well is ΔP. The pressure change at the water table, due to its high storage is negligible. There are thus four imbalances in pressure potential due to the step change in atmospheric load which induce fluid flow: 1) vertical air flow induced by the pressure imbalance ΔP between the earth's surface and the water table; 2) vertical groundwater flow induced by the pressure potential imbalance $\gamma''\Delta P$ between the water table and the confining layer; 3) vertical groundwater flow induced by the pressure potential imbalance $(\gamma''-\gamma)\Delta P$ between the confining layer and the aquifer; 4) lateral groundwater flow induced by the pressure potential imbalance $(1-\gamma)\Delta P$ between the open water well and the aquifer.

All of these four imbalances induced by the step load will be established instantaneously. If the surface loading efficiencies γ and γ'' are nearly equal, then groundwater flow induced by the pressure imbalance $(\gamma''-\gamma)\Delta P$ will be negligible and we are left with three significant pressure potential imbalances. In this paper, I assume that γ'' equals γ. This essentially restricts the analysis to conditions where the confining layer and aquifer possess similar elastic properties and porosities or the aquifer is very thin and possesses a high vertical permeability relative to its lateral permeability.

The remaining three pressure imbalances caused by the step change in atmospheric load can (under certain conditions which will be examined below) cause water well response to occur in four distinct phases. The qualitative water well response to the step load is shown in Figure 3-2b. The qualitative pressure change in the unsaturated zone, partial confining layer and aquifer during each of the four phases is shown in Figure 3-2c. Initially (phase 1), water flows out of the well into the aquifer driven by the pressure potential imbalance between the well and the aquifer. The water level in the well eventually drops by an amount $(1-\gamma)\Delta P/\rho g$ at which point the well is in equilibrium with the undrained response of the aquifer (phase 2). The water well response temporarily forms a plateau whose width is governed by the length of time it takes for groundwater flow to the water table to influence the pressure of the aquifer.

If the unsaturated zone is thick or possesses little air permeability, the pressure potential at the water table does not change for a substantial period of time. The confining layer and eventually the aquifer, however, gradually depressurize due to groundwater flow to the water table and the water level in the well drops in response to this change in aquifer pressure potential (phase 3). The aquifer continues to depressurize and the water level in the well drops an additional $\gamma\Delta P/\rho g$ so that the total water level change is $\Delta P/\rho g$. Once air pressure begins to increase at the water table, however, a new pressure imbalance between the water table and the aquifer is created. Water moves back into the aquifer and partial confining layer. The water level in the well increases in response to this increase in aquifer pressure (phase 4) and eventually returns

to its original static position once air pressure at the water table, the atmospheric load and the aquifer pressure are in static equilibrium.

Although examination of the response of a water well to step changes in deformation is useful for illustrative purposes, it is more quantitatively tractable to examine the response to periodic changes. Numerous studies have examined the response of wells to areally extensive deformation as a function of frequency. Cooper et al. (1965) and Bodvarsson (1970) theoretically examined the high frequency response of water wells to deformation under the assumption that the aquifer was hydraulically isolated from the water table in the frequency range of interest. Johnson (1973) and Johnson and Nur (unpublished manuscript, 1978) examined the theoretical response of water wells to deformation as a function of frequency under the assumptions that: the unsaturated zone did not influence the response; inertial effects within the well were negligible; the water table could be idealized as a spherically shaped boundary. Yusa (1969) and Weeks (1979) examined the response of water table wells to atmospheric loading due to the influence of the unsaturated zone under the assumption that the fluid pressure change at the water table was the average pressure change of the aquifer and that lateral transmissivity was high enough to allow for unattenuated groundwater flow between the aquifer and the borehole. Morland and Donaldson (1984), Gieske (1986) and Hsieh et al. (1987) have examined the response of water wells to deformation induced by earth tides and/or atmospheric loading under the assumption that water table influences and inertial effects were negligible.

This study extends the results noted above by unifying many aspects of the different theoretical models. I theoretically examine the response of water wells to atmospheric loading by including the influences of: groundwater flow between the borehole and the aquifer; groundwater flow between the aquifer and the water table; and air flow between the land surface and the water table through the unsaturated zone. I examine the theoretical response of water wells to atmospheric loading as a function of frequency under conditions where the well taps a partially confined aquifer. This theoretical model is applied to the response of three water wells to atmospheric loading inferred from cross-spectral estimation (Bendat and Piersol, 1986) to yield an estimate or place bounds on the following fluid flow parameters: pneumatic diffusivity of the unsaturated zone; vertical hydraulic diffusivity of the partial confining layer; and lateral permeability of the aquifer. It should be noted that the results shown here have many similarities to the response of wells tapping water table aquifers (see Chapter 4).

THEORETICAL RESPONSE OF WELLS IN PARTIALLY CONFINED AQUIFERS TO PERIODIC ATMOSPHERIC LOADING

The response of a water well to atmospheric loading can be conveniently broken up into five processes: 1) mechanical loading of the aquifer due to the surface load; 2) pressurization at the water surface of the open well due to the air load; 3) flow of air between the earth's surface and the water table; 4) flow of groundwater between the water table and the aquifer; 5) flow of groundwater

between the aquifer and the borehole. In order to make the analysis analytically tractable I make some simplifying assumptions about these processes. I assume that the undrained response of the aquifer and the partial confining layer to surface loading are the same; this essentially assumes that the compressibility, porosity and Poisson's ratio are vertically and laterally uniform. I make the assumption that air flow between the earth's surface and the water table and groundwater flow in the partial confining layer, owing to the lateral extent of the atmospheric load, is vertical. I also make the assumption, common to the analysis of partially confined aquifers (Hantush, 1955, 1960; Neuman and Witherspoon, 1969a), that groundwater flow between the aquifer and the borehole is horizontal. These assumptions allow me to uncouple the three dimensional nature of the problem into three flow problems, two of which have a strictly vertical component of flow and one of which has a strictly radial component of flow in the aquifer and vertical component of flow within the partial confining layer: 1) vertical air flow between the earth's surface and the water table; 2) vertical groundwater flow between the water table and the aquifer; 3) horizontal groundwater flow between the aquifer and the borehole with concomitant 'leakance' (Jacob, 1946) from the overlying partial confining layer.

Vertical flow between the earth's surface and the water table

Periodic vertical flow of air between the earth's surface and the water table is governed by a simple diffusion equation (Buckingham, 1904; Weeks, 1979):

$$D_a \frac{\partial^2 P_a}{\partial z^2} = \frac{\partial P_a}{\partial t} \qquad (1)$$

subject to the following boundary conditions:

$$P_a(-T,t) = A\cos(\omega t) \qquad (2a)$$

$$P_a(T,t) = A\cos(\omega t) \qquad (2b)$$

where P_a is the air pressure, D_a is the air diffusivity, and A and ω are the amplitude and frequency respectively of the pressure wave. The boundary -T is taken to be the earth's surface; the water table is at a depth of 0 and the zone from depth 0 to depth T is an artifice to assure that at the water table there is no air flux. The solution for air pressure at the water table (z=0) is given by (see Chapter 2):

$$P_a = (M-iN)A\exp(i\omega t) \qquad (3)$$

where M and N are:

$$M = \frac{2\cosh(\sqrt{\bar{R}})\cos(\sqrt{\bar{R}})}{\cosh(2\sqrt{\bar{R}})+\cos(2\sqrt{\bar{R}})} \qquad (4a)$$

$$N = \frac{2\sinh(\sqrt{\bar{R}})\sin(\sqrt{\bar{R}})}{\cosh(2\sqrt{\bar{R}})+\cos(2\sqrt{\bar{R}})} \qquad (4b)$$

and R is a dimensionless frequency referenced to air diffusivity, D_a, and the depth, L, from the earth's surface to the water table:

$$R = L^2\omega/2D_a \qquad (5)$$

Carslaw and Jaeger (p. 105, 1959) give the solution of equation 1 subject to the boundary conditions of equation 2 strictly in terms of phase and gain.

It should be noted that the inverse of the dimensionless frequency, R, is analogous to the dimensionless time 1/u well known in well hydraulics. The difference is that time has been replaced by frequency, the diffusivity of the aquifer has been replaced by the air diffusivity of the unsaturated zone and the radial distance from the well has been replaced by the thickness of the unsaturated zone.

Vertical flow between the water table and the aquifer

Groundwater flow between the water table and the aquifer under partially confined conditions is assumed to be strictly vertical and occurs strictly within the partial confining layer overlying the aquifer. The governing equation for pore pressure response due to periodic atmospheric loading can be obtained from Chapter 1 (compression is taken to be positive):

$$D\frac{\partial^2 P}{\partial z^2} = \frac{\partial P}{\partial t} + \omega\gamma A \sin\omega t \qquad (6)$$

where D is the vertical hydraulic diffusivity of the partial confining layer under conditions where the principal components of horizontal strain are 1/2 the vertical strain, P is the pore pressure change in excess of hydrostatic and γ is the surface loading efficiency. The surface loading efficiency is the ratio of change in pore pressure to change in surface load under undrained conditions. The surface loading efficiency, γ, is qualitatively the same as the loading efficiency given by Van der Kamp and Gale (1983) and the tidal efficiency given by Jacob (1940). The difference is the γ given here incorporates the influence of horizontal deformation. The source term in equation 6 is due to the essentially instantaneous transmission of the surface load via grain to grain contact to the subsurface.

If I take compressive stresses to be positive, the appropriate boundary conditions are:

$$P(0,t) = M\cos(\omega t) + N\sin(\omega t) \qquad (7a)$$

$$P(\infty,t) = A\gamma\cos(\omega t) \qquad (7b)$$

where I again take z=0 to be the water table. The water table boundary condition is the solution of equation 3. The solution of equation 6 subject to boundary conditions given in equation 7 is (see Chapter 2):

$$P = (M+iN-\gamma)A\exp(-(i+1)\sqrt{0.5qS'})\exp(i\omega t) + A\gamma\exp(i\omega t) \qquad (8)$$

where S' is the storage of the confining layer under conditions of surface loading and q is a dimensionless frequency referenced to the vertical hydraulic conductivity of the partial confining layer, K', and the distance, b', between the water table and the top of the aquifer (ie. the thickness of the partial confining layer):

$$q = b'\omega/K' \tag{9}$$

It should be noted that the term 0.5qS' is the dimensionless frequency Q used in a later section and defined as:

$$Q = qS'/2 = b'^2\omega/2D \tag{10}$$

where D is the vertical hydraulic diffusivity of the partial confining layer under conditions of surface loading.

Flow between the borehole and the aquifer

Groundwater flow between the borehole and the aquifer is driven by the difference between the water level in the well and the aquifer pressure in terms of head. Flow within the aquifer, as previously noted, is assumed to be strictly horizontal and the influence of the partial confining layer is described by a leakance term. Under these conditions, the governing equation is (Jacob, 1946):

$$\frac{\partial^2 s}{\partial r^2} + \frac{1}{r}\frac{\partial s}{\partial r} - \frac{K' s}{Kbb'} = \frac{S_s}{K}\frac{\partial s}{\partial t} \tag{11}$$

subject to the following boundary conditions (Cooper et al., 1965):

$$s(\infty,t) = 0 \tag{12a}$$

$$\lim_{r\to 0} r\frac{\partial s}{\partial r} = \frac{\omega r_w^2 x_0 \sin\omega t}{2Kb} \tag{12b}$$

where s is the drawdown within the aquifer caused by a periodic volumetric discharge within the well, K is the hydraulic conductivity of the aquifer, b is the thickness of the aquifer, S_s is the specific storage of the aquifer under conditions of no horizontal deformation, r_w is the radius of the well and x_0 is the amplitude of the water level fluctuation within the well casing produced by the volumetric discharge. This periodic steady state problem is solved in the Appendix. The solution for the drawdown at the well just outside the well screen, s_w, is:

$$s_w = i0.5Wx_0K_0\left\{[W^2(S^2+1/q^2)]^{0.25}\exp[i0.5(\tan^{-1}(qS)]\right\}\exp(i\omega t) \tag{13}$$

where K_0 is the modified Bessel function of the second kind of order zero (Olver, 1972; Tranter, 1968), S is simply, $S_s b$, the storage of the aquifer and W is:

$$W = \frac{\omega r_w^2}{Kb} \tag{14}$$

It should be noted that W is a dimensionless frequency (analogous to the inverse of dimensionless time used in well hydraulics) and 1/q is the conventional leakance of well hydraulics divided by frequency.

The solution given by equation 13 assumes that: 1) the water table does not change in response to periodic discharge from the well; 2) the partial confining layer has negligible storage; 3) pore pressure changes induced by the fluctuating water level induce only vertical deformation; 4) the well is a line source. In essence equation 13 is the same solution given by Hantush and Jacob (1955) for aquifer response to pumpage under conditions of leakance; the difference is that the well discharges at a periodic rate rather than at a constant rate. Neuman and Witherspoon (1969b) have examined the error involved in assumptions 1 and 2. Their results indicate that confining layer storage and changes in water table height can be ignored when the dimensionless parameter $\sqrt{W/q}$ and a dimensionless parameter β are less than 0.01 where β is defined as:

$$\beta = \frac{r_w}{4b}\sqrt{\frac{K'S_s'}{KS_s}} \tag{15}$$

In equation 15, S_s' is the specific storage of the confining layer under conditions of no horizontal deformation. Since confining layer permeabilities will be less than aquifer permeabilities and the well

radius will be significantly less than the thickness of the confining layer and the aquifer, the dimensionless terms $\sqrt{W/q}$ and β will almost always be less than 0.01. These results indicate that changes in water table height do not significantly influence aquifer response and that the specific storage of the partial confining layer, although it does influence vertical flow (see equation 8), does not significantly influence horizontal flow in the aquifer.

The assumption that pore pressure changes induced by well discharge do not induce horizontal deformation is a standard assumption in groundwater hydraulics. Gambolati (1974) examined the error in this assumption and found that (in the absence of leakance) drawdown accompanying well discharge is not significantly influenced by horizontal deformation when the well taps an aquifer whose thickness is less than 1/2 its average depth.

Response of a well to atmospheric loading--general case

The response of a well to atmospheric loading can be obtained, in the absence of inertial effects, by combining the solutions given in equations 8 and 13. Since we are concerned only with slowly varying water level fluctuations, inertial effects in the borehole can be ignored and the relation between the amplitude of the water level fluctuation in the well, x_0, and the amplitude of the atmospheric load, A, is:

$$x_0 = - A/\rho g + P_0/\rho g - s_0 \qquad (16)$$

where P_0 is the far field pore pressure of the aquifer (pore pressure at a radial distance where the influence of the well is negligible), P, divided by exp(iωt) and s_0 is the drawdown at the well, s_w, divided by exp(iwt):

$$P_0 = P\exp(-i\omega t) \tag{17a}$$

$$s_0 = s_w\exp(-i\omega t) \tag{17b}$$

Equation 16 describes the response of the well in the frequency domain and states that the change in water level in the well plus the atmospheric load (in terms of equivalent change in water level) equals the far field pore pressure (in terms of equivalent water level) minus the drawdown at the well.

It is useful to write equation 16 in terms of the gain or barometric efficiency, BE, and the phase, θ, of the response:

$$BE(\omega) = \left|\frac{x_0\rho g}{A}\right| = \left|\frac{P_0 - A - s_0\rho g}{A}\right| \tag{18a}$$

$$\theta(\omega) = \arg(x_0\rho g/A) \tag{18b}$$

where the brackets in equation 18a denote the modulus of the complex function; and 'arg' in equation 18b denotes the inverse tangent of the ratio of the imaginary component to the real component of the complex

function. Equation 18a describes the ratio of the amplitude of the water level fluctuation to the amplitude of the atmospheric load (in terms of equivalent water level). Equation 18b describes the phase shift between the atmospheric load wave and the water level fluctuation. Under conditions where the confining layer has zero permeability and the aquifer transmissivity is high, P_0 would be equal to the surface loading efficiency and the barometric efficiency, BE, would simply be one minus the surface loading efficiency, γ. The phase shift would be a flat -180° for all observable frequencies of the atmospheric wave. However, under conditions where the confining layer has a finite permeability and the aquifer transmissivity is low, both the barometric efficiency and the phase will be a strong function of frequency.

In this study, barometric efficiency depends on frequency. As defined in Chapter 1, the value for efficiency that reflects the undrained response of the aquifer is termed the static-confined barometric efficiency. Equations 8, 13 and 18 indicate that the barometric efficiency, BE, and phase, θ, of the response are a function of 6 dimensionless parameters: 1) R, the dimensionless unsaturated zone frequency; 2) q, the dimensionless confining layer frequency; 3) S', the storage of the confining layer; 4) S, the storage of the aquifer; 5) γ, the surface loading efficiency of the partial confining layer and aquifer; and 6) W, the dimensionless aquifer frequency.

The barometric efficiency and phase of the response of the water well are shown in Figure 3-3 as a function of dimensionless aquifer

frequency, W, and the ratio of dimensionless confining layer frequency, qS'/2 or Q, to W. In Figure 3-3, R is assumed to be much less than Q (R/Q=0.0001), S and S' are 0.0001, and the static-confined barometric efficiency of the aquifer is 0.5. These constraints allow us to examine water well response under conditions where the aquifer has typical elastic properties and unsaturated zone effects, due either to a shallow water table or a high air diffusivity, are negligible. The assumption of negligible unsaturated zone effects will be relaxed in a subsequent section. The dimensionless ratio Q/W is a measure of the frequency above which there is significant attenuation and phase shift due to limited groundwater flow between the borehole and the aquifer relative to the frequency below which the water table significantly influences aquifer pressure. When Q/W is large, a frequency band exists over which there is little attenuation and phase shift in water well response. When Q/W is small, we can expect that the water well response will show significant attenuation and phase shift (relative to -180^{0}) for all frequencies. Because unsaturated zone effects have been neglected, the response shown is qualitatively similar to the theoretical response given by Johnson (1973) and Johnson and Nur (unpublished manuscript, 1978); the major difference between this set of theoretical curves and their results is due to their approximation that the water table is a spherically shaped boundary which encloses a spherically shaped aquifer.

For values of Q/W much less than 1000, the static-confined barometric efficiency is never observed. Barometric response is attenuated with concomitant phase shift throughout the entire frequency range. Physically, values of Q/W less than 100 indicate

conditions where the water table has a strong influence on water well response over a wide frequency band; the aquifer becomes isolated from water table influences only when frequencies are so high, relative to aquifer transmissivity, that limited groundwater flow between the aquifer and the borehole cause significant attenuation of response.

For values of Q/W greater than 1000, three distinct stages of response can be observed: an intermediate frequency response, a low frequency response, and a high frequency response. At intermediate frequencies, air pressure response forms a plateau in both phase and barometric efficiency that increases in width with increasing values of Q/W. This response is analogous to the plateau shown during stage 2 in Figure 3-2. In this frequency band, the static-confined barometric efficiency is observed and there is little phase shift between the atmospheric pressure wave and the water well response (the phase shift of -180° is due to the inverse relation between water level and atmospheric pressure). Physically, water table influences are negligible in this frequency band and the aquifer transmissivity is high enough to allow for well response to be unattenuated. It should be noted that overlapping the low and intermediate frequency band, barometric response slightly exceeds the static-confined barometric efficiency. There is no analog to this slight amplification in the response of a water well to step changes in atmospheric load. The amplification of response is due to resonance: the influence of the water table is slight, but it has a phase shift that weakly reinforces the nearly confined water well response.

In the low frequency band, the response is distinguished by increasing attenuation and phase advance with decreasing frequency.

This response is analogous to stage 4 in Figure 3-2: as frequency decreases, water table influences become more significant and the barometric efficiency asymptotically approaches 0. It should be noted that stage 3 noted in Figure 3-2 (barometric efficiency achieving a value of 1 due to early water table influences) does not appear in Figure 3-3. This is because unsaturated zone effects are assumed to be negligible.

In the high frequency band, the response is characterized by increasing attenuation and phase lag with increasing frequency. This response is analogous to stage 1 in Figure 3-2. At these frequencies, aquifer transmissivity is low enough to limit groundwater flow between the aquifer and the borehole and as frequency increases the response asymptotically approaches 0.

Figure 3-4 shows the influence that the storage of the confining layer and aquifer have on the response. In Figures 3-4a and 3-4b storage for both the confining layer and the aquifer are 0.01; in Figures 3-4c and 3-4d, they are 1×10^{-6}. Both sets of response curves are qualitatively similar to the response curves in Figure 3-3. As in Figure 3-3, the response can be compartmentalized into three frequency bands for values of Q/W greater than 1000. At low frequencies, the sensitivity to storage is negligible for a fixed value of Q/W. This lack of sensitivity is due to the minor amount of well drawdown at low frequencies. At high frequencies, decreasing storage causes greater attenuation and phase shift, a phenomenon which will be considered in detail in the following section.

It is useful to determine, given typical aquifer and confining layer properties and geometries, whether the parameter Q/W can realistically have a value of greater than 1000. Given an aquifer thickness of 30 m and hydraulic conductivity of 2×10^{-6} cm/sec, a confining layer hydraulic conductivity of 10^{-7} cm/sec and specific storage 3×10^{-6} cm^{-1}, and a well radius of 10 cm, the dimensionless parameter Q/W has a value of approximately $1xb'^2$ where b' is in meters. For Q/W to exceed 1000 under these conditions, confining layer thickness must be in excess of 30 m. This result indicates that in many instances the parameter Q/W will be greater than 1000 and water well response can be broken up into three distinct frequency bands. In the following sections I examine the high frequency band and low frequency band in detail.

High frequency response

In the high frequency band, the well is isolated from water table and unsaturated zone influences. As a result, aquifer pressure, P_0, is a constant and the dimensionless frequency q is effectively infinite. The barometric efficiency and phase of the response are described by:

$$BE(\omega) = \left| \frac{\gamma - A - \varepsilon_0 \rho g}{A} \right| \qquad (19a)$$

$$\theta(\omega) = \tan^{-1}[\mathrm{Im}[\gamma\text{-}A\text{-}\varepsilon_0\rho g]/\mathrm{Re}[\gamma\text{-}A\text{-}\varepsilon_0\rho g] \qquad (19b)$$

where Im and Re denote the imaginary and real parts of the argument respectively. Since aquifer pressure is related to the amplitude of the pressure wave by a constant, γ, water well attenuation and phase shift depend on only two out of the six dimensionless parameters: W and S. Of these two parameters, only the dimensionless aquifer frequency, W, strongly influences response. Figure 3-5 shows the barometric efficiency and phase of the water well response as a function of W and S. Because water table influences are negligible, the solution given here is nearly identical to the solution given by Cooper et al. (1965) for the steady state response of a well which taps a confined aquifer to periodic deformation at frequencies where inertial effects are insignificant. The only differences are that the phase has been shifted by -180° due to the inverse relation between air pressure and water level and the amplitude of the response has been multiplied by the static-confined barometric efficiency (1-γ). As noted by Hsieh et al. (1987), the solution given by Cooper et al. indicates that the phase is only weakly dependent on aquifer storage, with less phase lag and attenuation slightly favored by high values of aquifer storage.

For all values of aquifer storage, S, large attenuation and phase shift occur only after dimensionless frequency, W, exceeds a value of 0.1. Thus the absence of any observable attenuation and phase shift with increasing frequency in a well's response places a lower bound on aquifer transmissivity if the radius of the well is known and the

influence of the water table is slight in the frequency band of interest.

Low frequency response

In the low frequency band, the well is in equilibrium with aquifer pressure and the well drawdown, s_0, can be assumed to be zero. The barometric efficiency and phase are described by:

$$BE(\omega) = \left|P_0/A-1\right| \tag{20a}$$

$$\theta(\omega) = \tan^{-1}(\mathrm{Im}(P_0/A-1)/\mathrm{Re}(P_0/A-1)) \tag{20b}$$

Since barometric efficiency and phase are strictly a function of aquifer pressure, P_0, water well response is dependent on only three of the dimensionless parameters: γ (one minus the static-confined barometric efficiency), Q and R.

Figure 3-6 shows the response of a water well in the low frequency band as a function of dimensionless confining layer frequency Q and dimensionless unsaturated zone frequency R. The static-confined barometric efficiency is 0.5. The solution shown in the figure is nearly identical to a solution discussed elsewhere (see Chapter 2); the only differences are that, following hydrologic convention, phase shift is negative with phase lag and compression is

defined as positive. This is a special case of the complete solution given in equation 18.

In summary, water well response in the low frequency band is a strong function of both R and Q. When the ratio R/Q is less than 10^{-4} the unsaturated zone has little influence on response and the barometric efficiency, which exhibits slight resonance at the high end of the frequency band, generally attenuates with decreasing frequency; the phase shows a nearly monotonic phase advance with decreasing frequency. For large values of R/Q, however, barometric efficiency exceeds the confined response over much of the frequency band analyzed. The increasing barometric efficiency with decreasing frequency is analogous to stage 3 in Figure 3-2. As previously noted, the response is caused by water table influence under conditions where the water table is strongly isolated from air pressure changes at the surface. For large values of R/Q, the phase lags slightly behind the air pressure over much of this frequency band.

Figure 3-7 shows the influence of the surface loading efficiency, γ, on well response. For aquifers with a loading efficiency of 0.20 (static-confined barometric efficiency of 0.80), the amplitude of the response is considerably higher than that shown in Figure 3-6 (static-confined barometric efficiency and γ equal 0.50), at dimensionless frequencies less than 1. The phase, in comparison to Figure 3-6, shows little in the way of a phase lag. For aquifers with a loading efficiency of 0.80 (static-confined barometric efficiency of 0.20), the amplitude of the response is considerably lower at dimensionless

frequencies greater than 1. The phase, when R/Q is small, has a wide frequency band of significant phase lag.

APPLICATION OF THEORETICAL RESPONSE

In Chapter 1 it was noted that water well response to atmospheric loading is strongly dependent on the surface loading efficiency of the aquifer. The above results also indicate that water well response to atmospheric loading will be strongly dependent on the three dimensionless fluid flow parameters: R, Q and W. If the response of a well can be fit to the theoretical solutions, it is possible to make estimates or place bounds on these 3 key parameters. Once these dimensionless parameters are estimated, it is then possible to make estimates of or place bounds on the fluid flow parameters that govern water well response: air diffusivity of the unsaturated zone, confining layer hydraulic diffusivity and aquifer permeability. The process of fitting well response as a function of frequency to dimensionless theoretical curves is analogous to the standard practice of fitting water level declines as a function of time in response to pumpage to "type curve" plots. The essential difference is that, because the solutions given here are a function of frequency, there are two "type curves" that are fit simultaneously: one for barometric efficiency and one for phase.

In order to compare a water well's response to the theoretical solutions, we need to determine its transfer function or barometric efficiency and phase as a function of frequency. The transfer function which relates atmospheric loading to water level can be found

using cross-spectral estimation (Bendat and Piersol, 1986). For the water well records examined here, the transfer functions were obtained by: 1) determining the power spectra and cross-spectra for the water well record, the local atmospheric pressure record and the theoretical areal strain produced by the earth tides; 2) solving the following system of complex linear equations for every frequency:

$$\begin{vmatrix} BB & BT \\ TB & TT \end{vmatrix} \begin{vmatrix} HB \\ HT \end{vmatrix} = \begin{vmatrix} BW \\ TW \end{vmatrix} \tag{21}$$

where BB and TT denote the power spectra of the atmospheric pressure and earth tides respectively, BT and TB denote the cross spectrum and complex conjugate of the cross spectrum, respectively, between atmospheric loading and earth tides, BW and TW denote the cross spectra between atmospheric loading and water level and earth tides and water level respectively, and HB and HT denote the transfer function between water level and atmospheric loading and water level and earth tides, respectively. The earth tides were included in the analysis because they have a strong influence on the response of the wells examined at diurnal and semi-diurnal frequencies. Further details on how the transfer functions were determined are given in Chapter 2.

A description of the wells examined in this paper is given in Table 3-1. Two of these wells, TF and JC, are located near Parkfield, California and the other well is located near Mammoth Lakes, California. The aquifer permeabilities given in Table 3-1 were determined from specific capacity data (TF) or slug tests (JC, SC2).

The aquifer permeabilities inferred from the slug tests as well as the thicknesses of the partial confining layers (depth from the water table to the top of the aquifer) at these wells indicate that the dimensionless ratio Q/W may be quite large; as a result, well response may take place in the three distinct bands noted above.

It is likely, however, that only a part of the complete theoretical response will be observed in any one well. The limited length of the data sets (about 150 days) and the lack of any large air pressure signal at frequencies greater than 2 cycles/day limit the band width over which we can estimate well response. For the wells examined here, we can obtain useful estimates of water well response in the frequency band of roughly 0.02 to 2 cycles/day. This band is only 2/5 of the frequency band detailed in Figure 3-3 and as a result, it is unlikely that the low frequency, intermediate frequency and high frequency response can all be observed. In the well responses examined below, only the low and intermediate frequency responses are observed. The lack of a high frequency response does serve, however, to place a lower bound on the aquifer permeabilities for these wells.

Well TF

The transfer function for the response of well TF to atmospheric loading is shown in Figure 3-8. Barometric efficiency peaks at 0.6 at a frequency of about 0.5 cycles/day. The phase which lags the atmospheric pressure at a frequency of 1 cycle/day, begins to cross over and show phase advance with decreasing frequency at about 0.6 cycles/day. The figure also shows the model fit to the observed

transfer function. The theoretical model indicates that the response in the frequency band of 0.02 to 2 cycles/day is dominated by water table influences. The confined response indicated by the model is only approached at the high end of the observed frequency band. The key parameters indicated by the model are a static-confined barometric efficiency of 0.37 and a value for both dimensionless frequencies R and Q of 2.2ω where frequency is in terms of cycles per day. The hydraulic and air diffusivities estimated from these values of R and Q are shown in Table 3-2. The specific storage for the aquifer under conditions of atmospheric loading is considered in Chapter 1 and is determined from the inferred static-confined barometric efficiency and dilatational efficiency for the well. Assuming that the specific storage of the confining layer is close to that of the aquifer, I can obtain an estimate of the vertical permeability of the confining layer. This permeability is 10 md, a value slightly less than the permeability of the aquifer of 20 md indicated by the specific capacity data. The lack of any observable response that can be attributed to limited groundwater flow between the borehole and the aquifer places a lower bound on aquifer permeability. Assuming that the dimensionless frequency W is less than 0.1, the permeability of the aquifer is greater than 1 md, a value consistent with the specific capacity data.

Well JC

Figure 3-9 shows the transfer function for the well response at JC. Barometric efficiency shows a nearly monotonic change with

decreasing frequency over the entire observed frequency band. The phase is nearly flat over the observed frequency band and indicates that the water level in the well lags slightly behind the atmospheric load. The fit to the theoretical model indicates that water well response is strongly governed by limited air flow between the earth's surface and the water table. Like the response at TF, the static-confined response is approached at a frequency of 2 cycles/day. The inferred static-confined barometric efficiency determined from the model is 0.67. The dimensionless parameters R and Q are 640ω and 6.4ω, respectively. The air and hydraulic diffusivities estimated from these parameters are shown in Table 3-2. The estimated hydraulic diffusivity of the partial confining layer is on the same order as that estimated at TF; the estimated pneumatic diffusivity is over two orders of magnitude less than that at TF. It should be noted that it is difficult to explain this difference on the basis of differences in site lithology. If the specific storage of the confining layer is close to that of the aquifer, the vertical permeability of the confining layer is about 3 md, a value which is one order of magnitude less than the permeability of the aquifer of 50 md estimated from a slug test.

Although phase lag increases slightly between between one and two cycles/day, nothing else suggests that any attenuation occurs due to limited groundwater flow between the aquifer and the borehole. Assuming that dimensionless frequency, W, is less than 0.1, the lower bound on permeability for the aquifer is 5 md, a value consistent with the slug test data of 50 md.

Well SC2

The response of SC2 to air pressure shown in Figure 3-10 indicates that both the barometric efficiency and phase are relatively flat over the observed frequency band. Because the response lacks any strong trend, it is somewhat ambiguous. The figure shows two interpretations of the response. In the first interpretation (Model 1), the static-confined response is observed over the entire frequency band. The barometric efficiency is a flat 0.78, Q is greater than 260ω and R is not indentifiable. Alternatively, water table effects begin to slightly influence water well response at the low end of the observable frequency (Model 2). In this interpretation, the static-confined barometric efficiency is 0.74 and the values for Q and R are 65ω and less than 6.5ω respectively.

Table 3-2 shows the air and hydraulic diffusivities inferred from Model 2. The lower bound on air diffusivity is nearly the same as the air diffusivity estimated at TF; the hydraulic diffusivity of the partial confining layer is considerably lower. If I assume that the specific storage of the confining layer and the aquifer are the same, the vertical permeability of the confining layer is estimated to be 2×10^{-2} md, indicating that the confining layer is composed of considerably different material than the aquifer. This inference is consistent with the lithology at the site: the well taps a fractured basalt overlain by glacial till (Farrar et al., 1985).

Once again, there is no observable attenuation of response due to limited hydraulic communication between the aquifer and the borehole.

The lack of observable attenuation indicates that aquifer permeability is greater than 7 md; the slug test data suggest that aquifer permeability is 2×10^7 md, a value much larger than this lower bound.

CONCLUSIONS

The response of water levels in wells which tap partially confined aquifers to atmospheric loading is dependent on the elastic and fluid flow properties of the aquifer as well as the material overlying the aquifer. Owing to the hydraulic properties of the aquifer and confining layer and the pneumatic properties of the unsaturated zone, water well response cannot be expected to be independent of frequency. Attenuation and amplification of the static-confined response to atmospheric loading can occur in theory and is observed in the wells examined here. Phase lags and advances observed in response to atmospheric loading also have a theoretical basis.

In many instances, the response of a well can be divided into three frequency bands. The response at low frequencies is independent of aquifer permeability and depends on the confining layer and unsaturated zone diffusivities. Attenuation and amplification as well as phase lags and phase advances are possible in this frequency band. The response at intermediate frequencies is dependent on the elastic properties of the aquifer and is independent of fluid flow properties; it is characterized by a flat barometric efficiency and phase. The response at high frequencies is independent of confining layer and unsaturated zone diffusivity and is strongly dependent on aquifer

permeability. It is characterized by increasing attenuation and phase lag with increasing frequency. The width of separation between the high frequency and low frequency response (ie. the width of the intermediate frequency band) is dependent on the well radius, the aquifer transmissivity, and the confining layer thickness and hydraulic diffusivity.

The theoretical response can be used in conjunction with the observed response of water wells as a function of frequency to yield estimates or place bounds on the fluid flow parameters within the aquifer, confining layer and unsaturated zone. For the wells examined, water well response to atmospheric loading does not yield much information on aquifer permeability; it is possible only to obtain a lower bound for this flow parameter. In low permeability environments, however, the response of water wells to atmospheric loading may prove useful in estimating aquifer permeability.

Water well response, for the wells examined here, does serve to yield useful estimates of confining layer hydraulic diffusivity and the air diffusivity of the unsaturated zone. If the site lithology indicates that the specific storage of the confining layer is close to the value of specific storage of the aquifer, it is also possible to make an estimate of the vertical permeability. Estimates of these parameters are usually difficult to obtain using conventional techniques and are valuable for purposes of water resource assessment and studies of contaminant migration in the near surface.

APPENDIX: SOLUTION TO THE DRAWDOWN IN A WELL WITH PERIODIC DISCHARGE TAPPING A PARTIALLY CONFINED AQUIFER

The drawdown within an aquifer which is partially confined in response to periodic discharge from a well is assumed to be governed by the following equation and boundary conditions:

$$\frac{\partial^2 s}{\partial r^2} + \frac{1}{r}\frac{\partial s}{\partial r} - \frac{K' s}{Kbb'} = \frac{S_s}{k}\frac{\partial s}{\partial t} \qquad \text{(A1a)}$$

$$s(\infty, t) = 0 \qquad \text{(A1b)}$$

$$\lim_{r \to 0} r\frac{\partial s}{\partial r} = \frac{\omega r_w^2 x_0 \sin\omega t}{2Kb} \qquad \text{(A1c)}$$

No initial condition is imposed because I seek the periodic steady-state solution. This problem is readily solved employing complex notation. Taking s to be complex:

$$s(r,t) = F(r)\exp(i\omega t) \qquad \text{(A2)}$$

and substituting in equation A1 I obtain:

$$F'' + \frac{F'}{r} - \left\{\frac{K'}{Kbb'} + \frac{S_s i\omega}{K}\right\}F = 0 \qquad \text{(A3a)}$$

$$F(\infty) = 0 \qquad \text{(A3b)}$$

$$\lim_{r \to 0} r\frac{\partial F}{\partial r} = \frac{-i\omega r_w^2 x_0}{2Kb} \qquad \text{(A3c)}$$

where, ', implies differentiation and all exponential terms have been divided out. Equation A3 is an ordinary differential equation with radial symmetry. Its general solution is given by (Tranter, 1968):

$$F=C_1 I_0(r) + C_2 K_0(r) \qquad (A4)$$

where C_1 and C_2 are constants determined by the boundary conditions and I_0 and K_0 are modified Bessel functions of the first and second kind respectively of order zero. The boundary condition A3b requires that C_1 equals zero. The solution for drawdown at the radius, r_w, is:

$$F_w = 10.5Wx_0K_0\left\{[W^2(S^2+1/q^2)]^{0.25}\exp[10.5(\tan^{-1}(qS))]\right\} \qquad (A5)$$

The complete solution is given in equation 13.

REFERENCES

Bendat, J. S., and A. G. Piersol, Random Data: Analysis and Measurement Procedures, John Wiley and Sons, New York, 566pp., 1986.

Bodvarsson, G., Confined fluids as strain meters, J. Geophys. Res., 75, 2711-2718, 1970.

Bredehoeft, J. D., Response of well-aquifer systems to earth tides, J. Geophys. Res., 72, 3075-3087, 1967.

Buckingham, E., Contributions to our knowledge of the aeration of soils, Bull. 25, 52pp., U. S. Dept. Agr. Soils Bur., Washington, D. C., 1904.

Carslaw, H. S., and J. C. Jaeger, Conduction of heat in solids, Oxford University Press, Oxford, England, 510pp., 1959.

Cooper, H. H. Jr., J. D. Bredehoeft, I. S., Papadopulos, and R. R. Bennett, The response of well-aquifer systems to seismic waves, J. Geophys. Res., 70, 3915-3926, 1965.

Farrar, C. D., M. L. Sorey, S. A. Rojstaczer, C. J. Janik, R. H. Mariner, T. L. Winnett, and M. D. Clark, Hydrologic and geochemical monitoring in Long Valley Caldera, Mono County, California, 1982-1984, U. S. Geological Survey Water Resources Investigations, 85-4183, 137pp., 1985.

Gambolati, G., Second-order theory of flow in three-dimensional deforming media, Water Resour. Res., 10, 1217-1228, 1974.

Gieske, A., On phase shifts and periodic well fluctuations, Geophys. J. R. Astr. Soc., 86, 789-799, 1986.

Hantush, M. S., Modification of the theory of leaky aquifers, J. Geophys. Res., 65, 3713-3725, 1960.

Hantush, M. S., and C. E. Jacob, Non-steady radial flow in an infinite leaky aquifer, Eos Trans AGU, 36, 95-100, 1955.

Hsieh, P. A., J. D. Bredehoeft, and J. M. Farr, Estimation of aquifer transmissivity from phase analysis of earth-tide fluctuations of water levels in artesian wells, Water Resour. Res., 23, 1824-1832, 1987.

Jacob, C. E., Radial flow in a leaky artesian aquifer, Eos Trans. AGU, 27, 198-205, 1946.

Jacob, C. E., The flow of water in an elastic artesian aquifer, Eos Trans. AGU, 21, 574-586, 1940.

Johnson, A. G., Pore pressure changes associated with creep events on the San Andreas Fault, Ph.D. thesis, Dept. of Geophysics, Stanford University, 177pp., 1973.

Morland. L. W., and E. C. Donaldson, Correlation of porosity and permeability of reservoirs with well oscillations induced by earth tides, Geophys. J. R. Astr. Soc., 79, 705-725, 1984.

Neuman, S. P., and P. A. Witherspoon, Theory of flow in a confined two-aquifer system, Water Resour. Res., 5, 803-816, 1969a.

Neuman, S. P., and P. A. Witherspoon, Applicability of current theories of flow in leaky aquifers, Water Resour. Res., 5, 817-829, 1969b.

Olver, F. W. J., Bessel functions of integer order, U. S. Nat. Bur. Stand. Appl. Math Ser., 55, 354-433, 1972.

Tranter, C. J., Bessel Functions with Some Physical Applications, English Universities Press, London, 148pp., 1968.

Van der Kamp, G. and J. E. Gale, Theory of earth tide and barometric effects in porous formations with compressible grains, Water Resour. Res., 19, 538-544, 1983.

Weeks, E. P., Barometric fluctuations in wells tapping deep unconfined aquifers, Water Resour. Res., 15, 1167-1176, 1979.

Yusa, Y., The fluctuation of the level of the water table due to barometric change, Geophys. Inst. Spec. Contrib. Kyoto Univ., 9, 15-28, 1969.

Table 3-1: Description of wells.

Well Id.	Permeability (millidarcies)	Open Interval (meters)	Depth to water table (meters)	Casing diameter (meters)	Aquifer lithology	Partial confining layer lithology
TF	2×10^{1}	152-177	18	.10	Marine sediments	Marine sediments
JC	5×10^{1}	147-153	14	.10	Diatomaceous sandstone	Largely fine to medium grained sandstone
SC2	2×10^{7}	66-70	32	.10	Fractured basalt	Basalt and glacial till

Table 3-2: Estimate of fluid flow properties of wells. Estimates for SC2 are from 'Model 2' in Figure 3-10.

Well Id.	Aquifer permeability (millidarcies)	Confining layer hydraulic diffusivity (cm^2/sec)	Unsaturated zone air diffusivity (cm^2/sec)
TF	>1	5×10^{2}	9×10^{0}
JC	>5	2×10^{2}	2×10^{-2}
SC2	>7	1×10^{0}	$>1 \times 10^{1}$

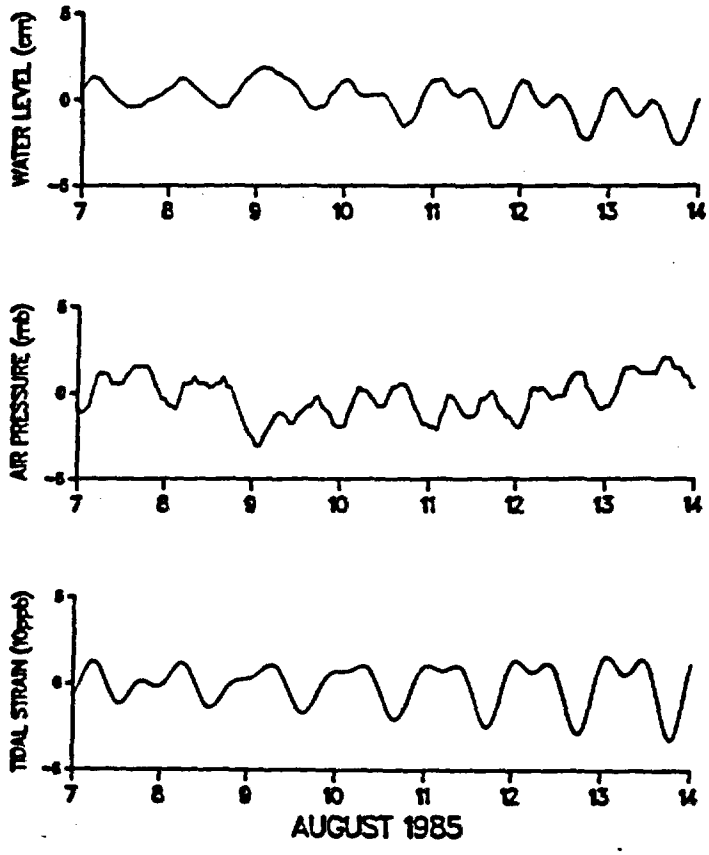

Figure 3-1: Hydrograph of TF during the second week of August, 1985, with corresponding barograph and theoretical tidal strain.

a

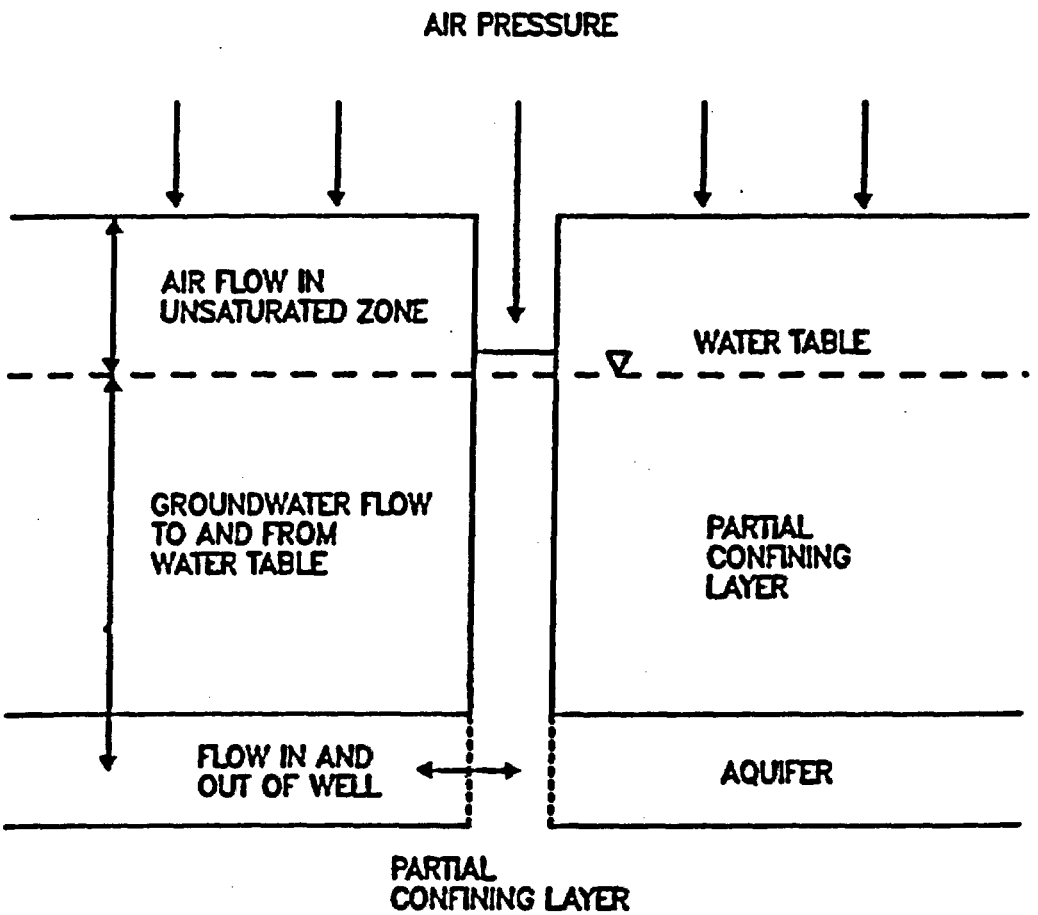

Figure 3-2: Cross-section of well responding to atmospheric loading and principal sources of attenuation and amplification of well response (a); idealized response of a well to a step change in atmospheric load (b); profile of pressure response due to step change in atmospheric load at four time periods (c).

b

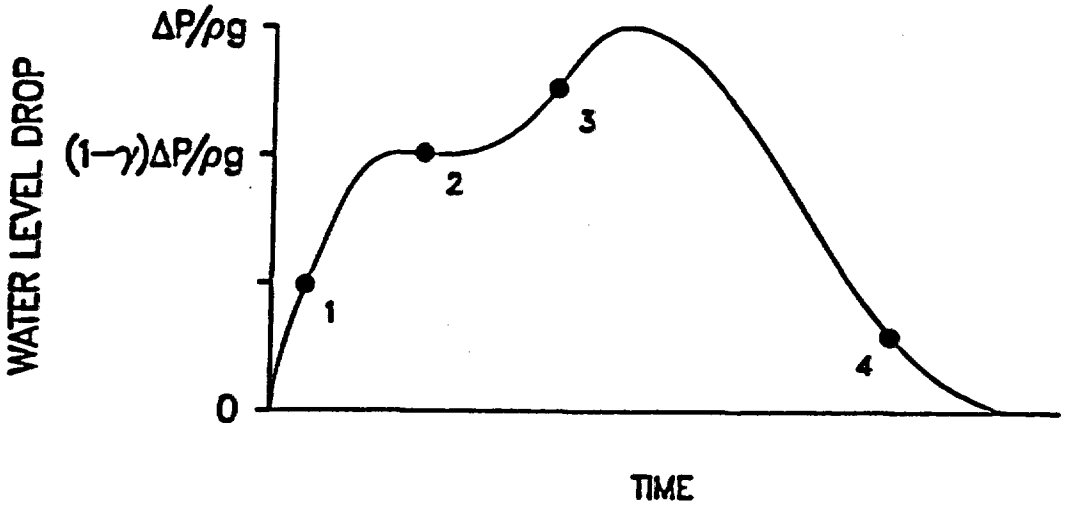

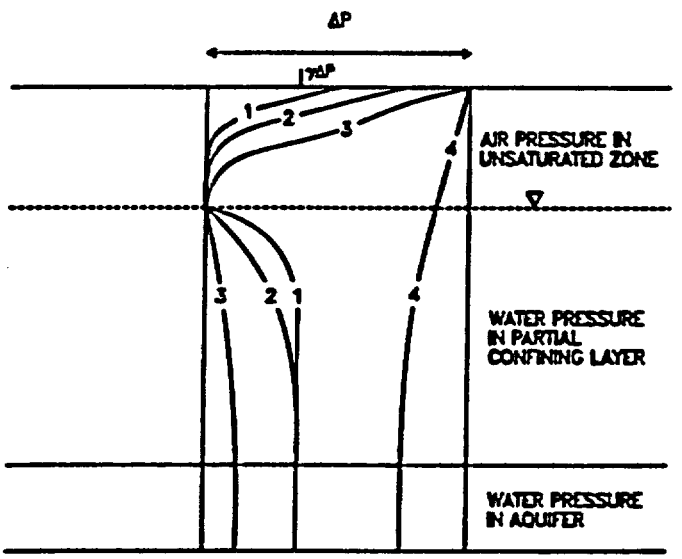
ΔP
1
2
3
4
AIR PRESSURE IN UNSATURATED ZONE
3
2
1
4
WATER PRESSURE IN PARTIAL CONFINING LAYER
WATER PRESSURE IN AQUIFER

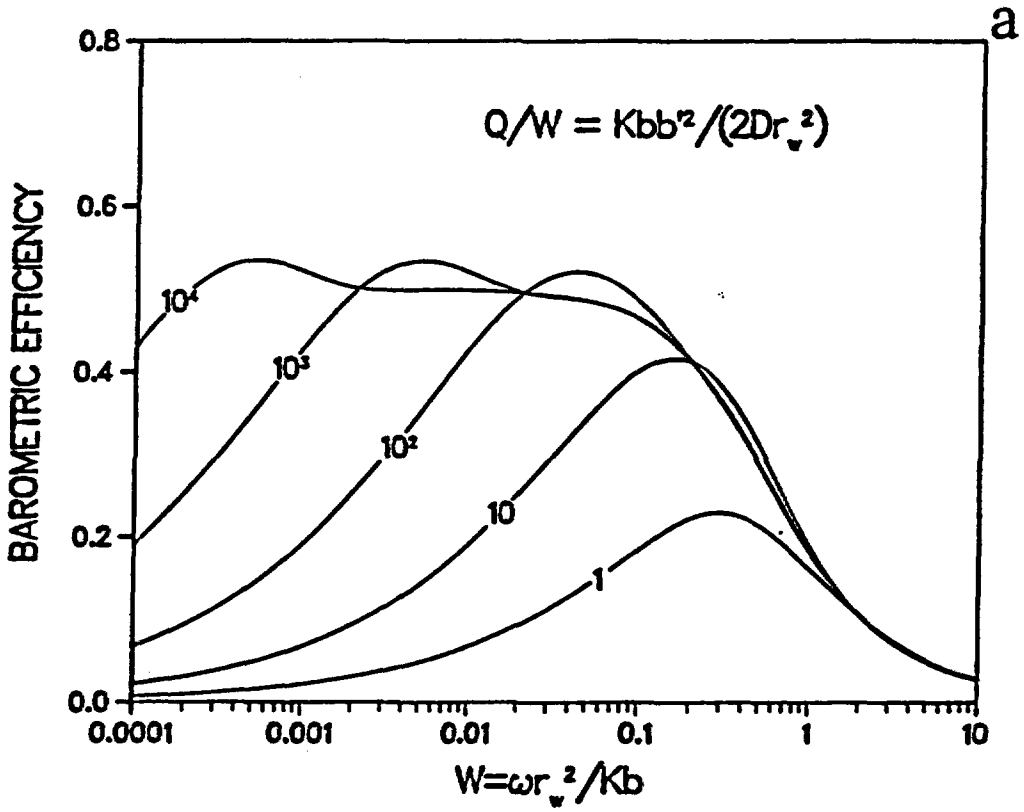

Figure 3-3: Barometric efficiency (a) and phase (b) of response of a well to atmospheric loading as a function of Q/W when S and S' equal 0.0001. Static-confined barometric efficiency is 0.5.

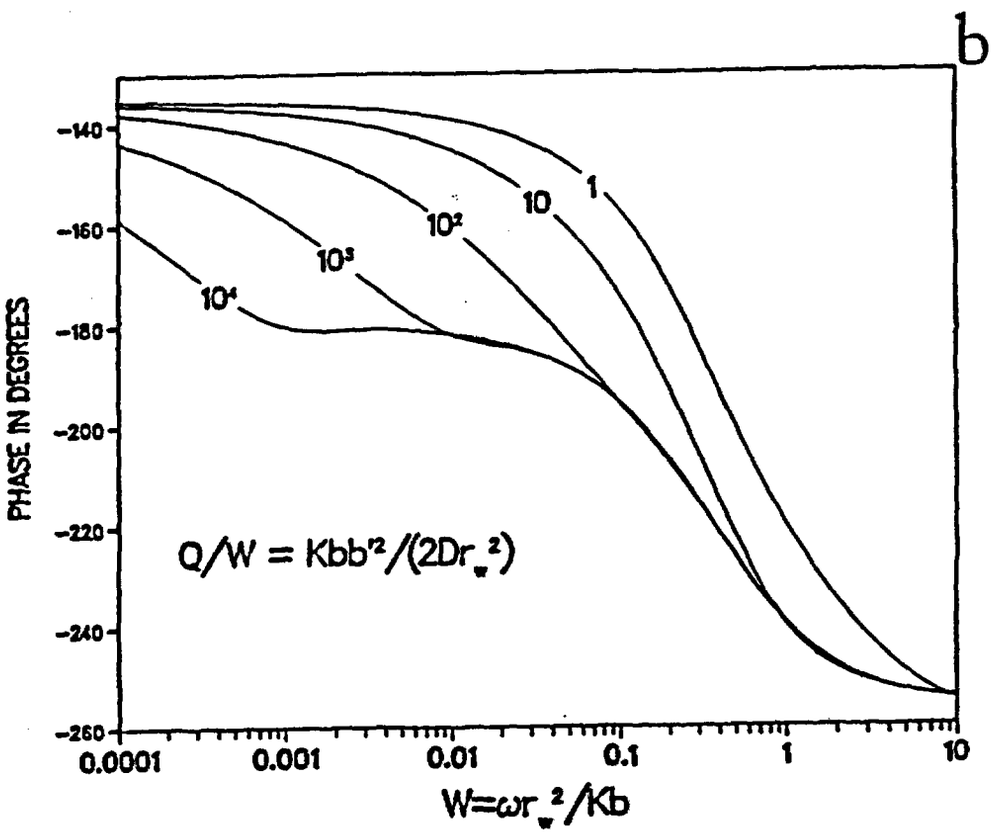
b
PHASE IN DEGREES
-140
-160
-180
-200
-220
-240
-260
1
10
10²
10³
10⁴
Q/W = Kbb'²/(2Dr_w²)
0.0001
0.001
0.01
0.1
1
10
W=ωr_w²/Kb

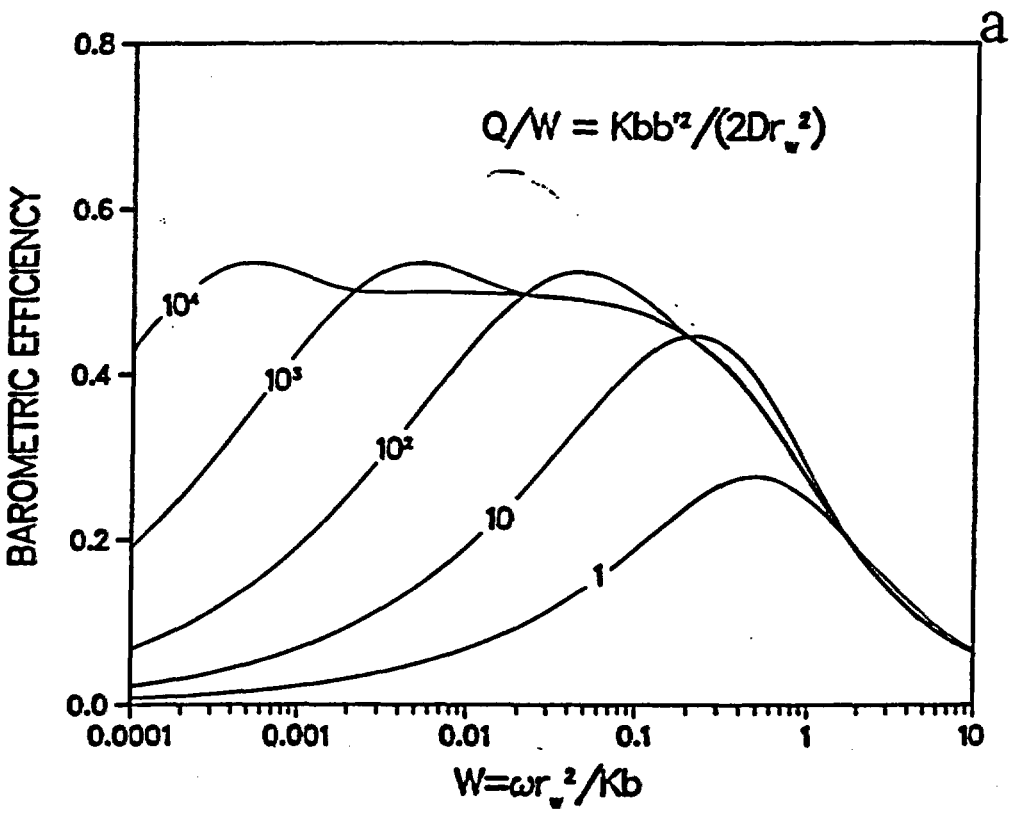

Figure 3-4: Barometric efficiency (a) and phase (b) of response of a well to atmospheric loading as a function of Q/W when S and S' equal 0.01. Barometric efficiency (c) and phase (d) when S and S' equal 1 x 10^{-6}. Static-confined barometric efficiency is 0.5.

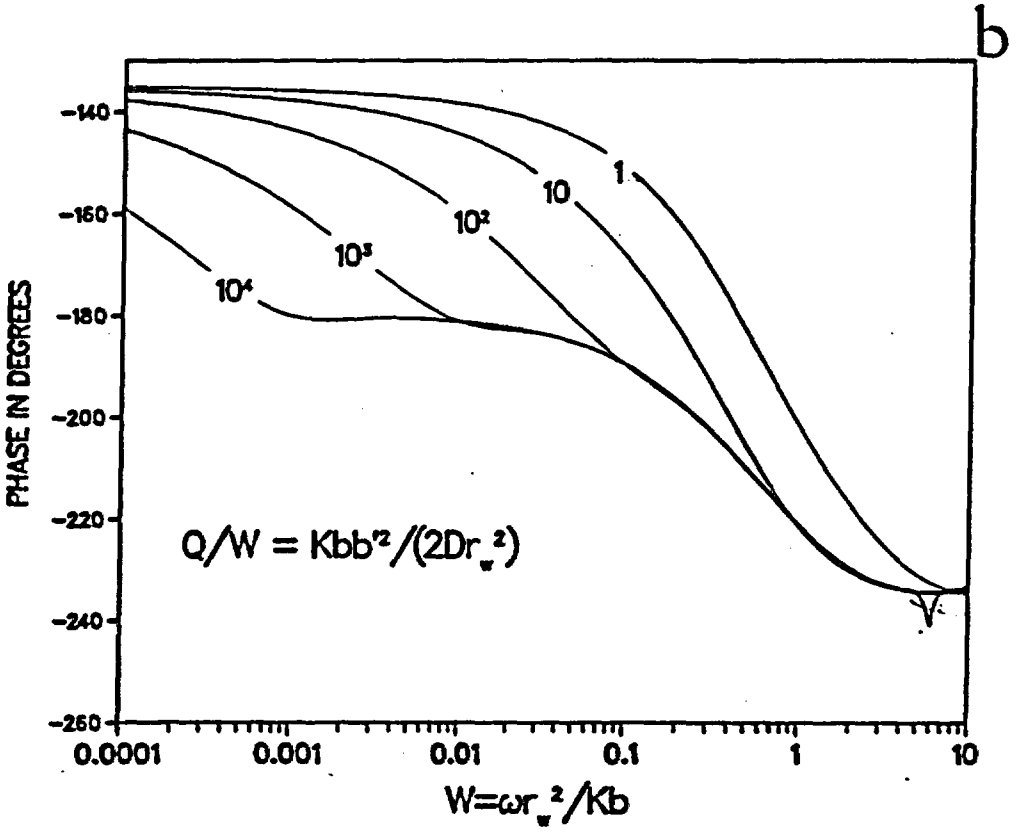
b
-140
-160
-180
-200
-220
-240
-260
PHASE IN DEGREES
1
10
10²
10³
10⁴
Q/W = Kbb'²/(2Dr_w²)
0.0001
0.001
0.01
0.1
1
10
W=ωr_w²/Kb

C

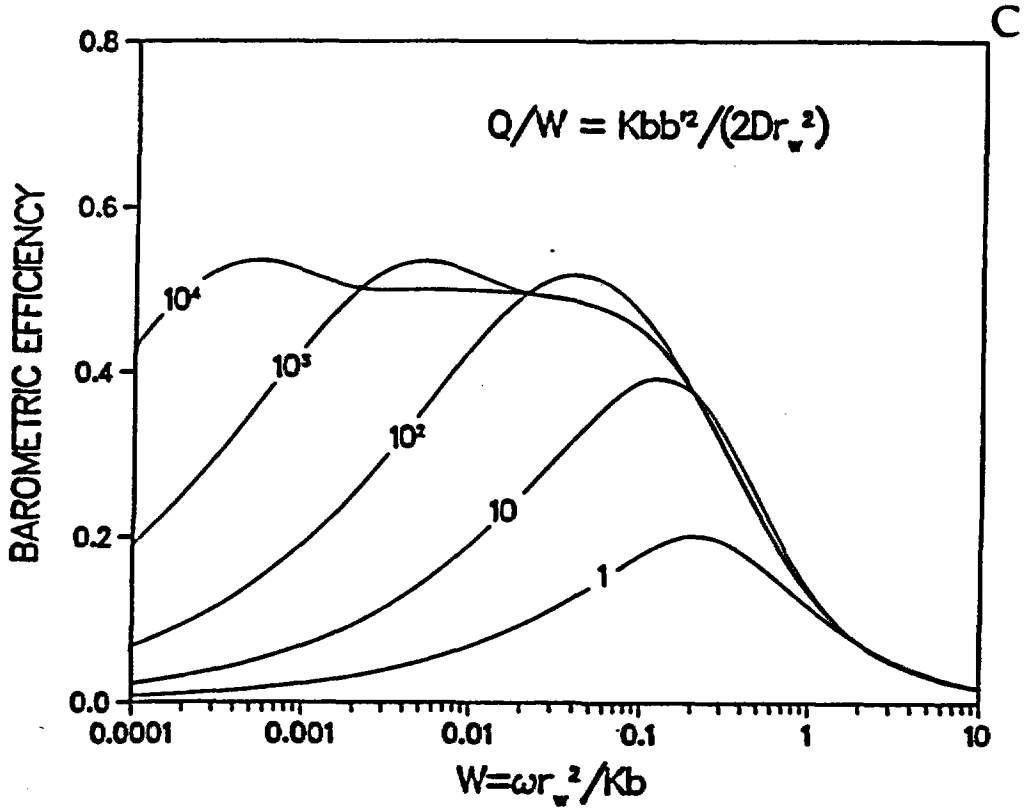
Q/W = Kbb'²/(2Dr_w²)
BAROMETRIC EFFICIENCY
0.8
0.6
0.4
0.2
0.0
10⁴
10³
10²
10
1
0.0001
0.001
0.01
0.1
1
10
W=ωr_w²/Kb

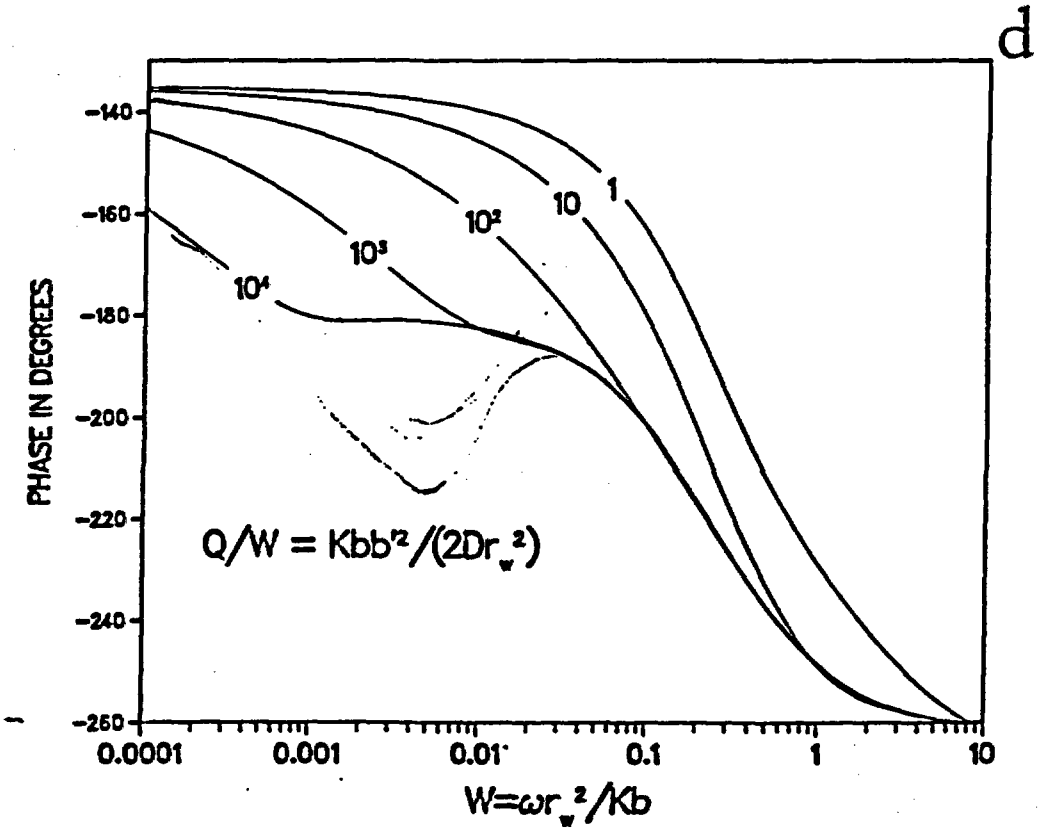
d
PHASE IN DEGREES
-140
-160
-180
-200
-220
-240
-260
1
10
10²
10³
10⁴
Q/W = Kbb'²/(2Dr_w²)
0.0001
0.001
0.01
0.1
1
10
W=ωr_w²/Kb

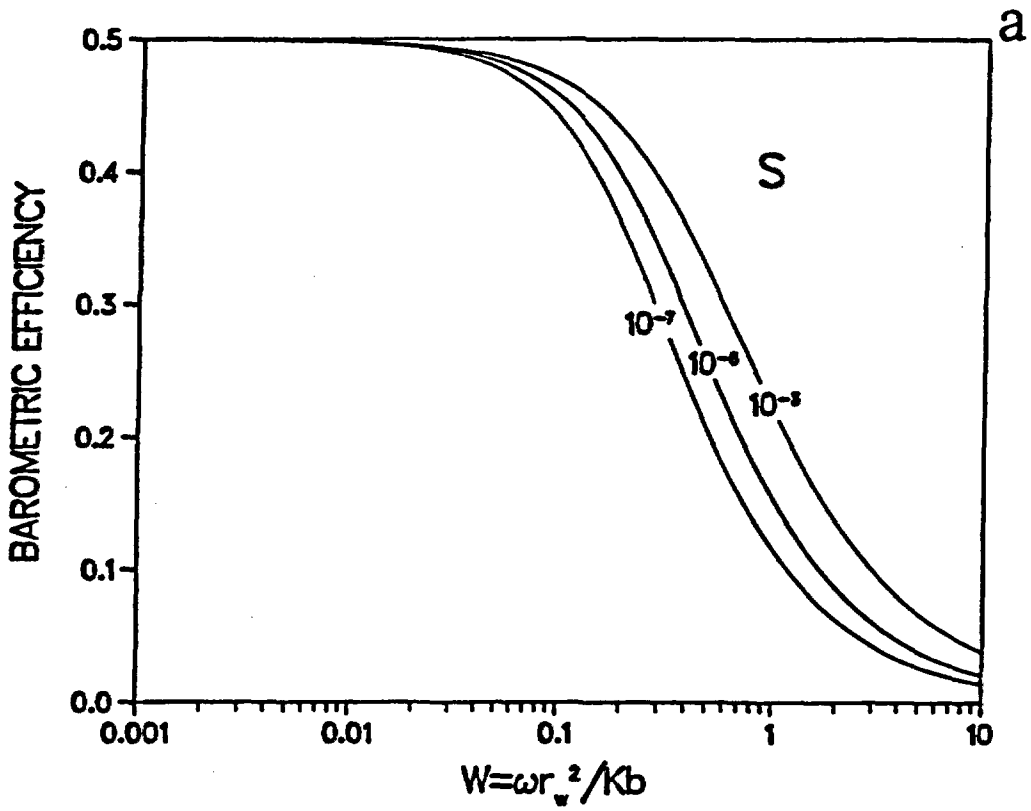

Figure 3-5: High frequency response in terms of barometric efficiency (a) and phase (b) as a function of S. Static-confined barometric efficiency is 0.5.

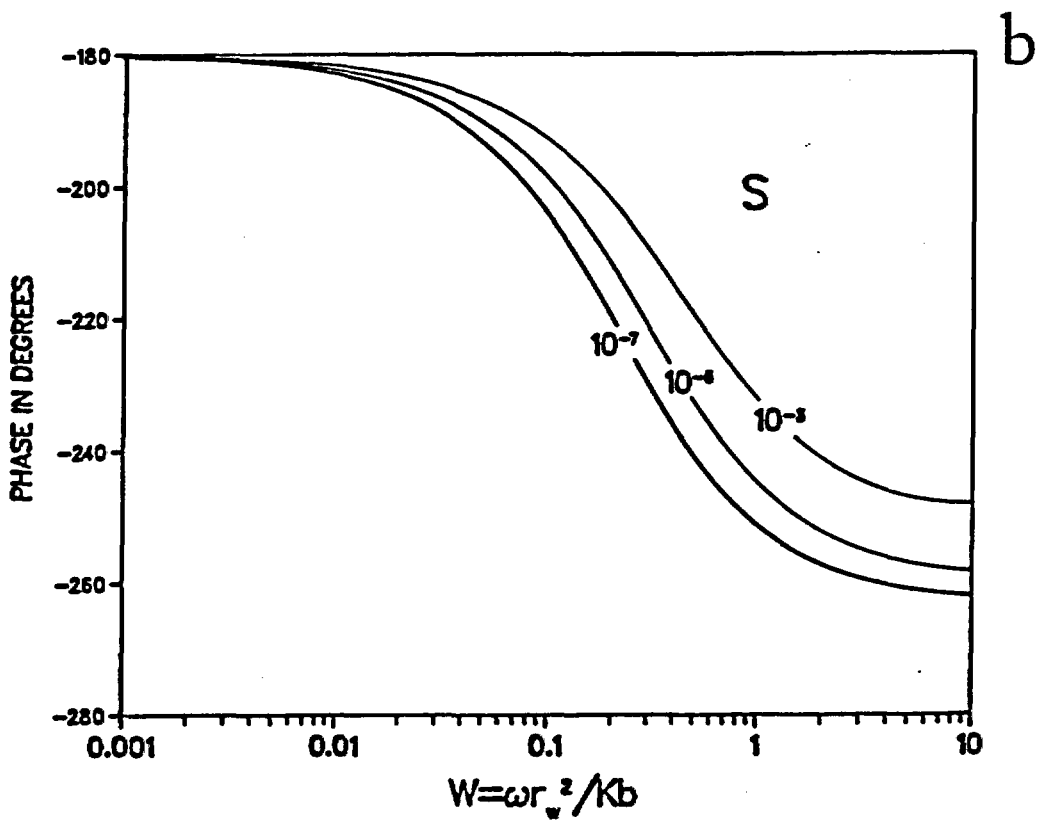
b
-180
-200
-220
-240
-260
-280
PHASE IN DEGREES
S
10⁻⁷
10⁻⁶
10⁻⁵
0.001
0.01
0.1
1
10
W=ωr_w²/Kb

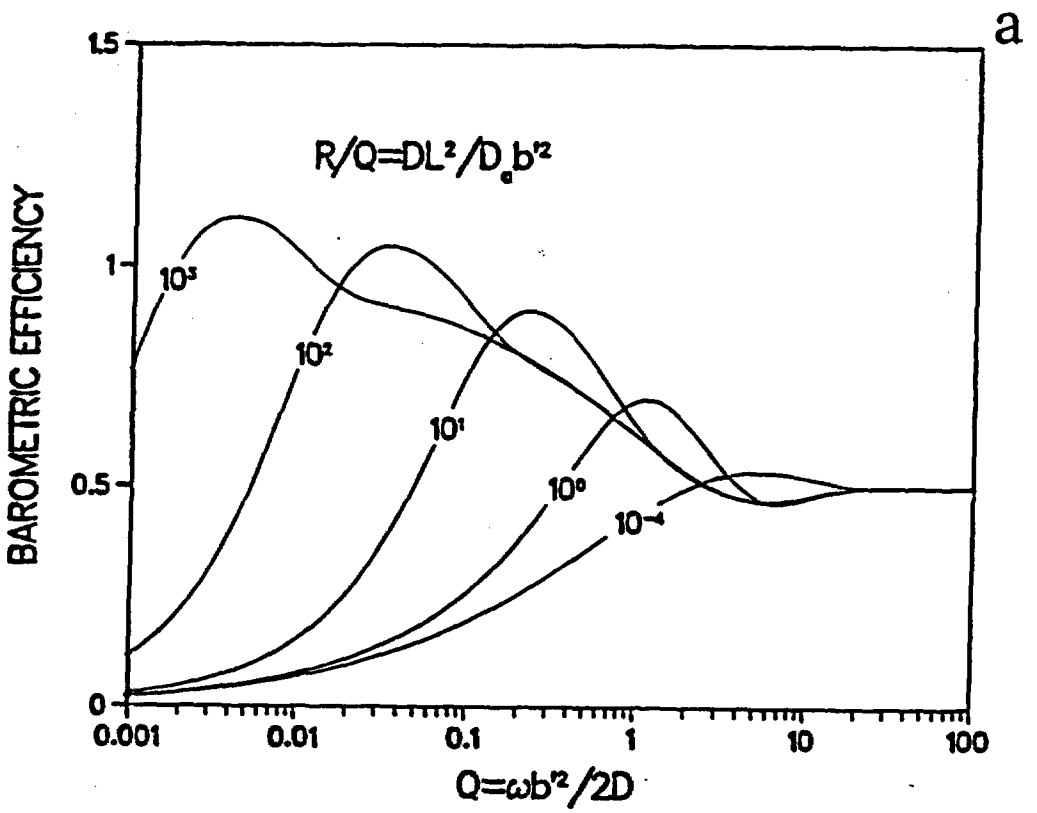

Figure 3-6: Low frequency response in terms of barometric efficiency (a) and phase (b) as a function of R/Q. Static-confined barometric efficiency is 0.5.

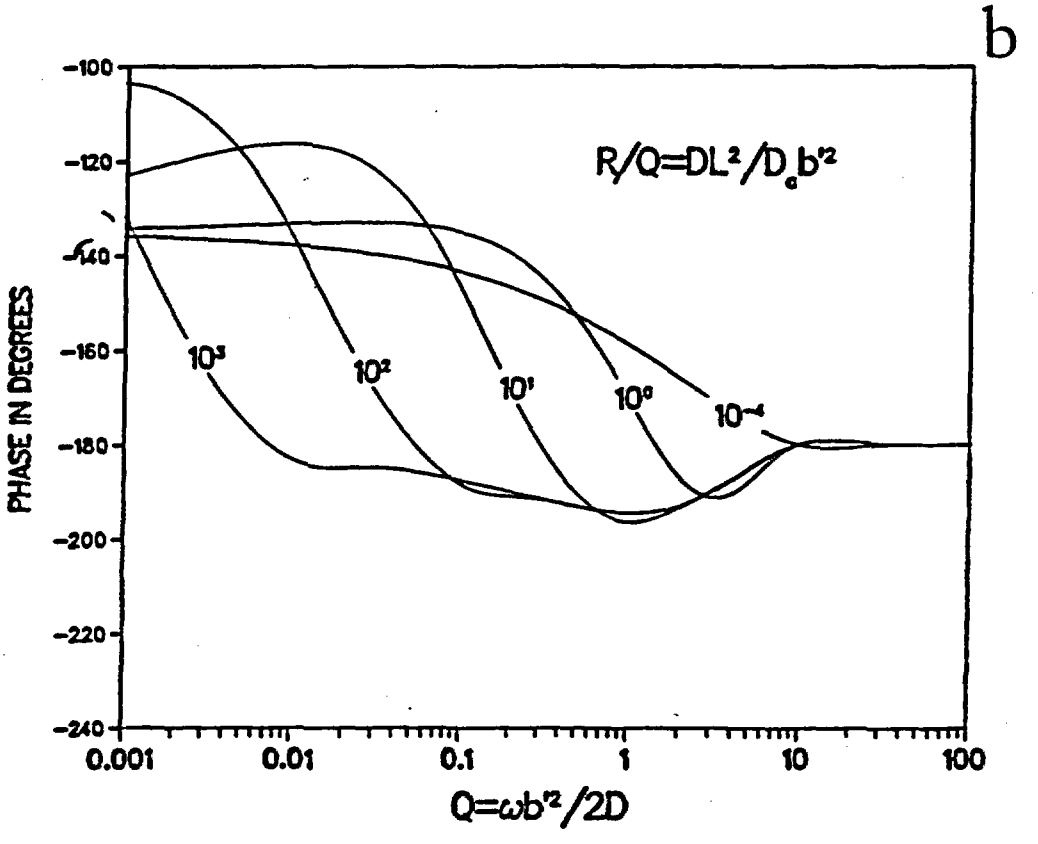
b
R/Q=DL²/D_eb^1/2
10³
10²
10¹
10⁰
10⁻¹
PHASE IN DEGREES
-100
-120
-140
-160
-180
-200
-220
-240
0.001
0.01
0.1
1
10
100
Q=ωb^1/2/2D

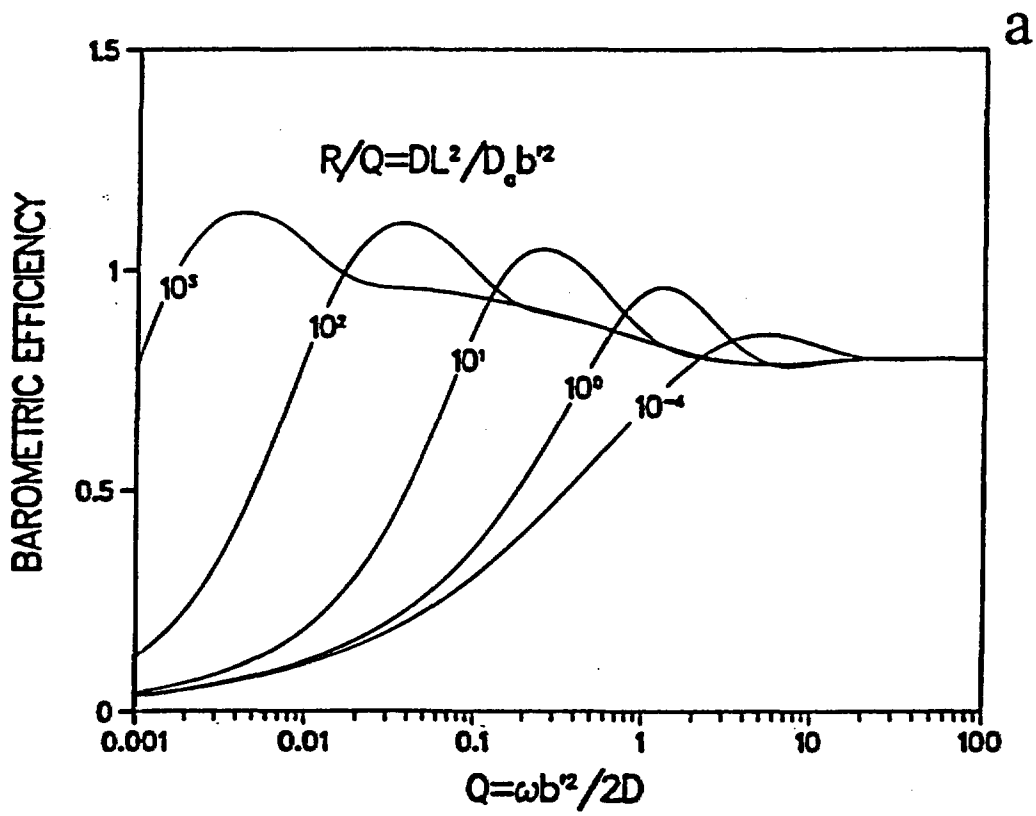

Figure 3-7: Effect of surface loading efficiency on low frequency response. Barometric efficiency (a) and phase (b) when the surface loading efficiency is 0.2. Barometric efficiency (c) and phase (d) when the surface loading efficiency is 0.8.

b

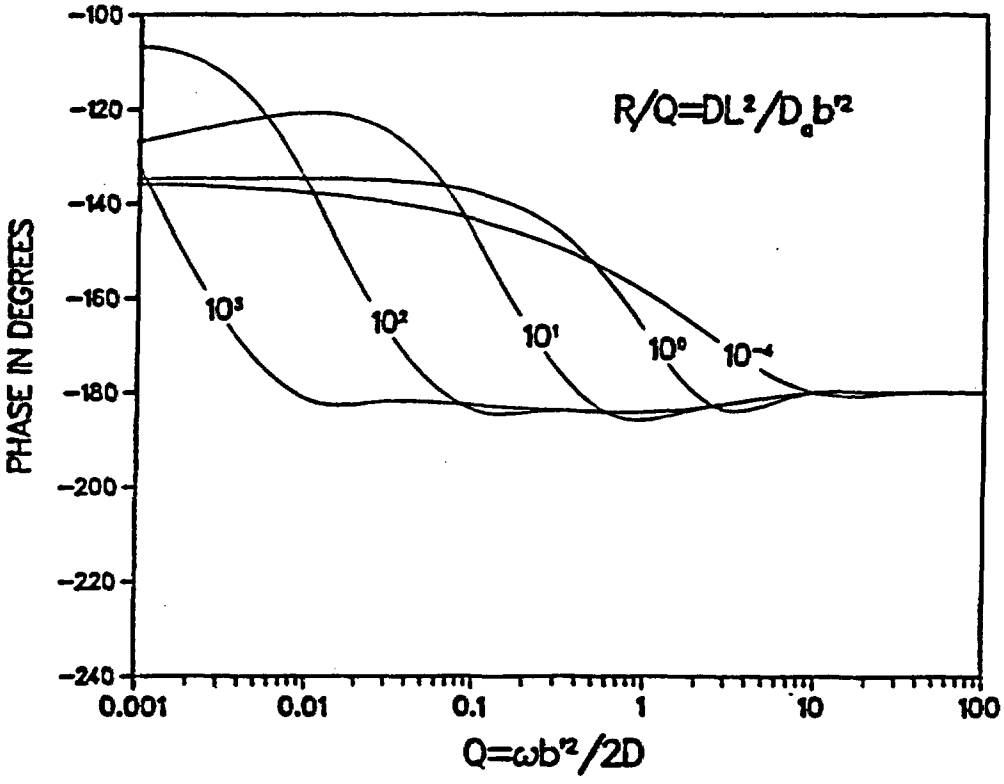
-100
-120
-140
-160
-180
-200
-220
-240
PHASE IN DEGREES
R/Q=DL²/D_eb^1/2
10³
10²
10¹
10⁰
10⁻¹
0.001
0.01
0.1
1
10
100
Q=ωb^1/2/2D

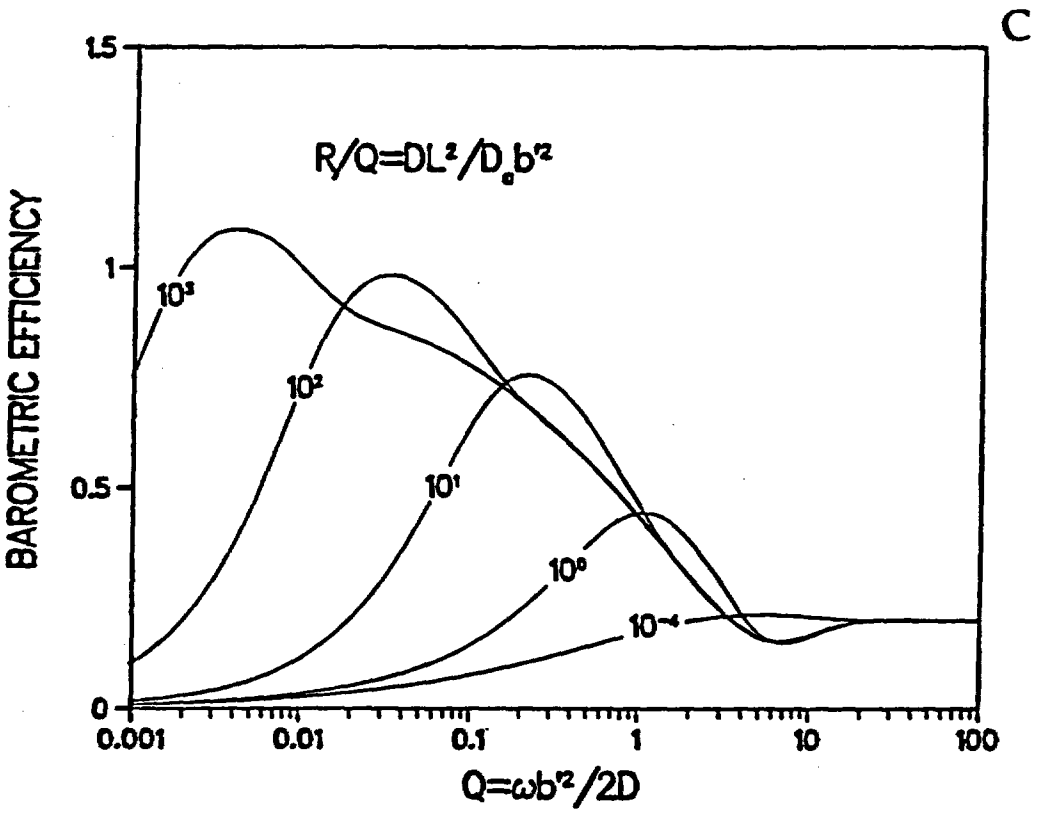
C
1.5
1
0.5
0
BAROMETRIC EFFICIENCY
R/Q=DL²/D_e b'²
10³
10²
10¹
10⁰
10⁻¹
0.001
0.01
0.1
1
10
100
Q=ωb'²/2D

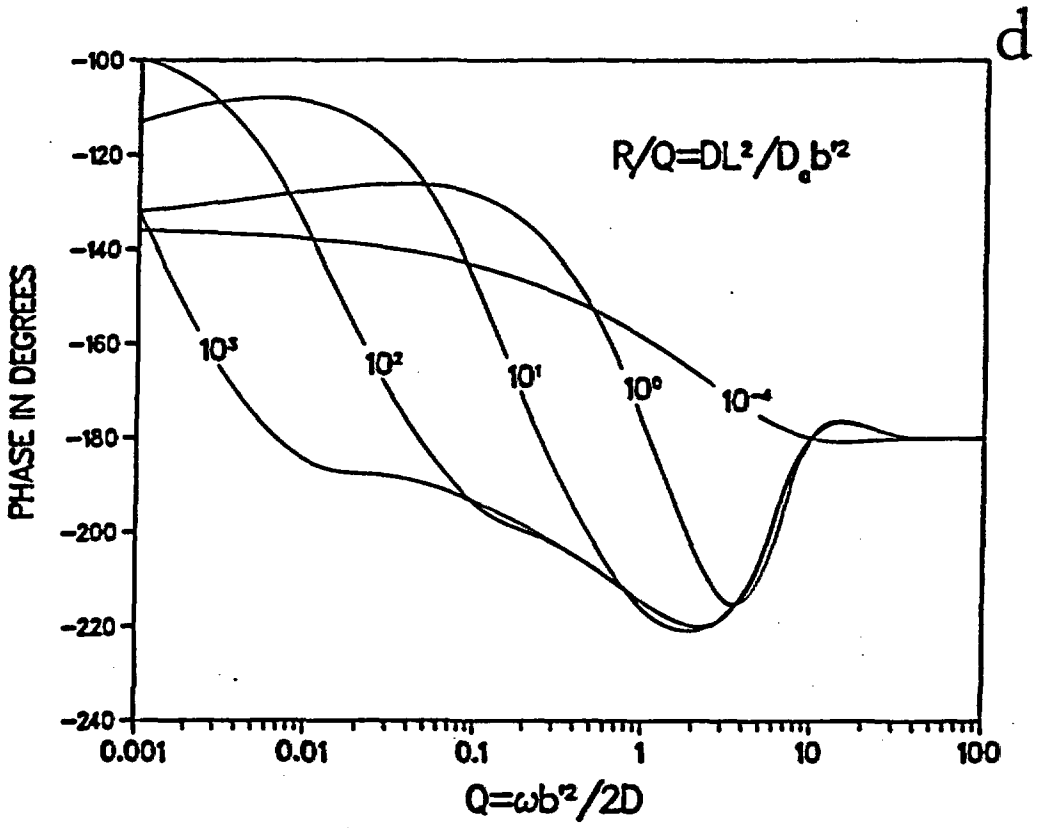
d
-100
-120
-140
-160
-180
-200
-220
-240
PHASE IN DEGREES
R/Q=DL²/D_eb^1/2
10³
10²
10¹
10⁰
10⁻¹
0.001
0.01
0.1
1
10
100
Q=ωb^1/2/2D

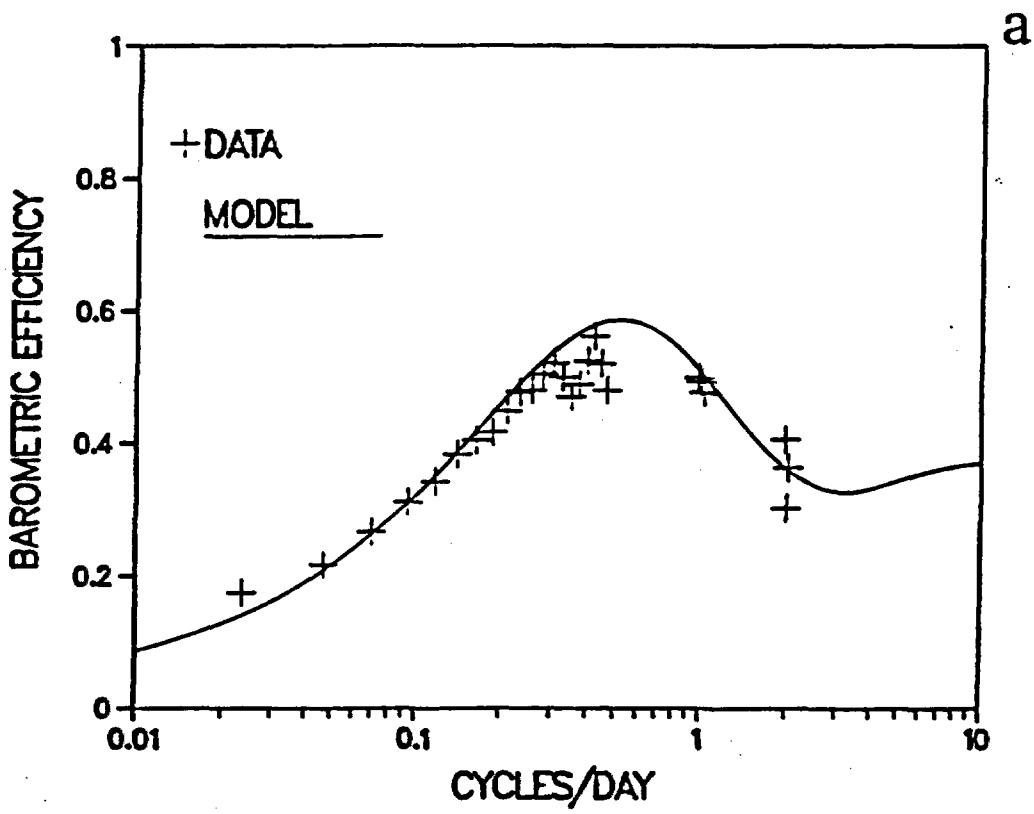

Figure 3-8: Response of TF to atmospheric pressure in terms of barometric efficiency (a) and phase (b). Fit to data is solid line denoted as 'MODEL'.

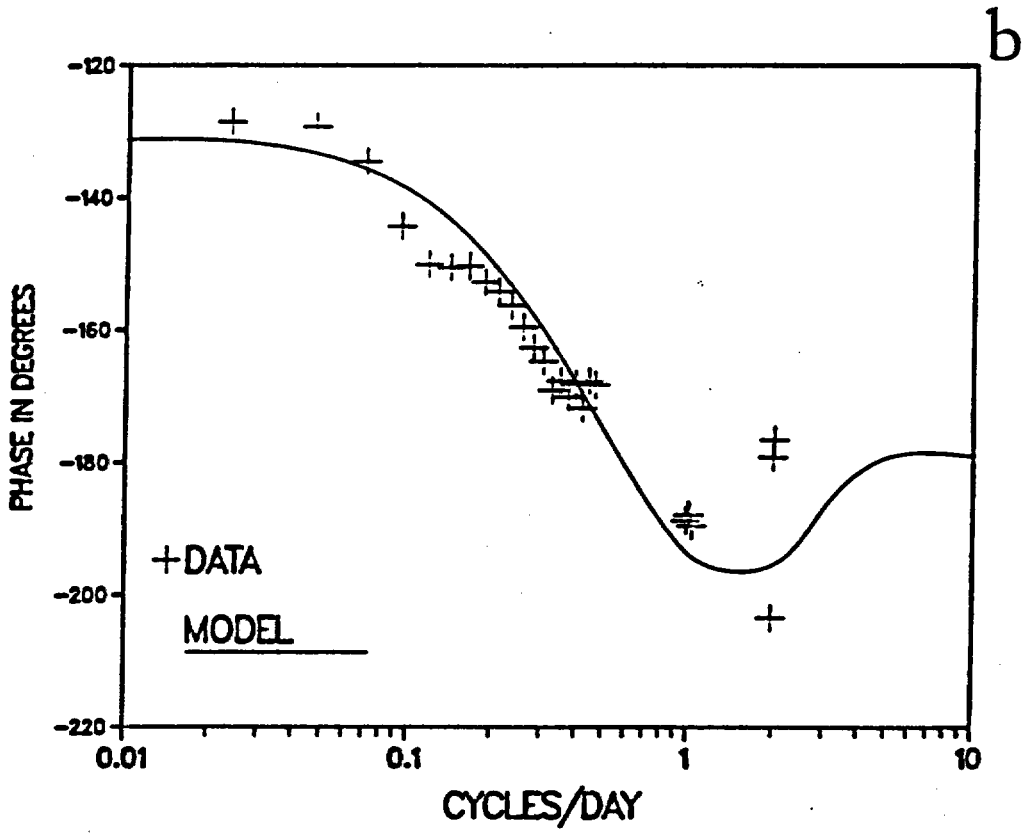
b
-120
-140
-160
-180
-200
-220
PHASE IN DEGREES
+DATA
MODEL
0.01
0.1
1
10
CYCLES/DAY

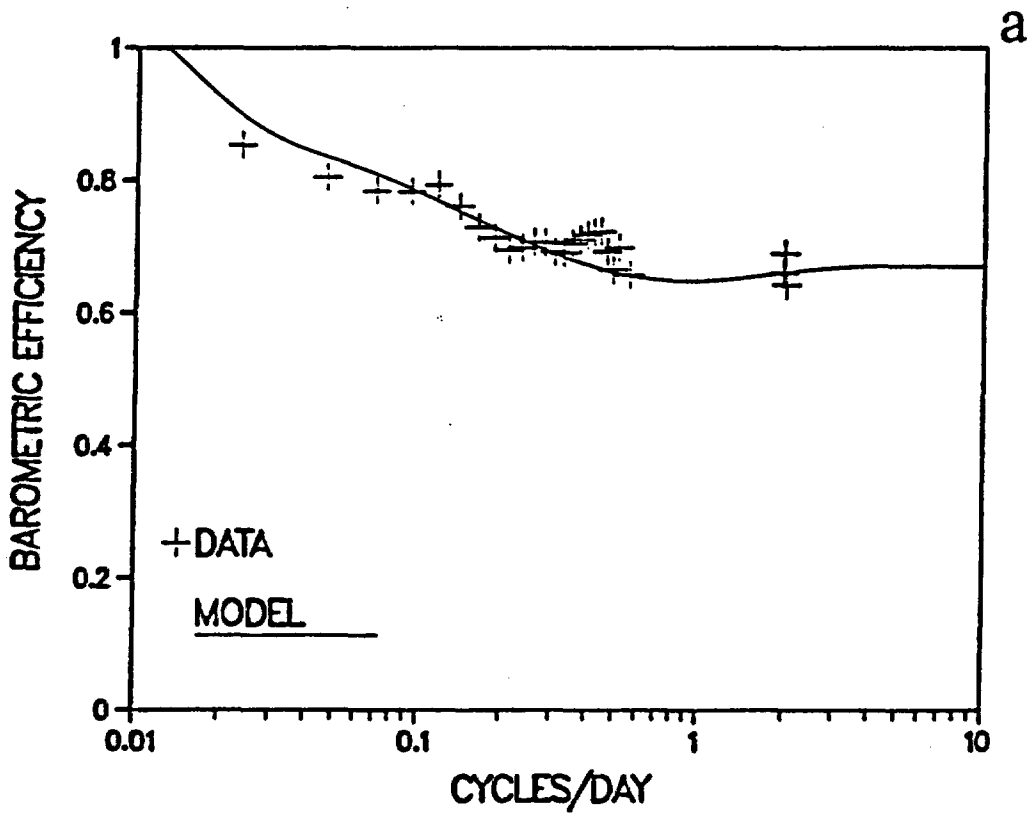

Figure 3-9: Response of JC to atmospheric pressure in terms of barometric efficiency (a) and phase (b). Fit to data is solid line denoted as 'MODEL'.

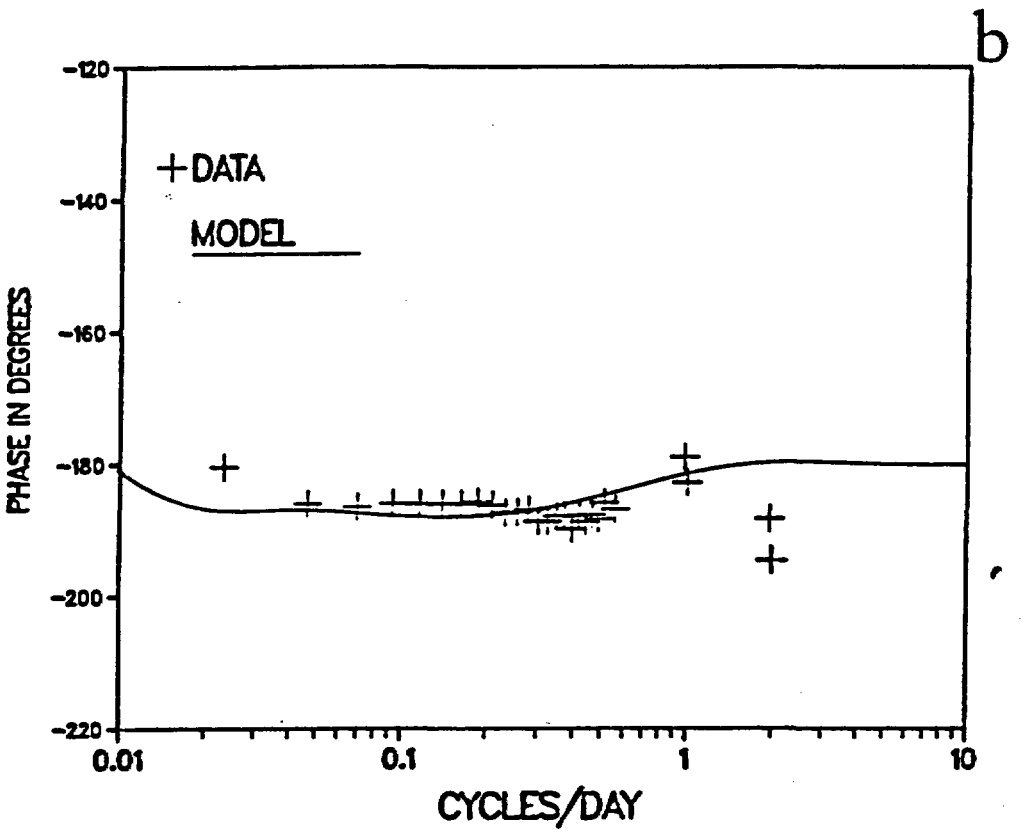
b
+DATA
MODEL
PHASE IN DEGREES
-120
-140
-160
-180
-200
-220
0.01
0.1
1
10
CYCLES/DAY

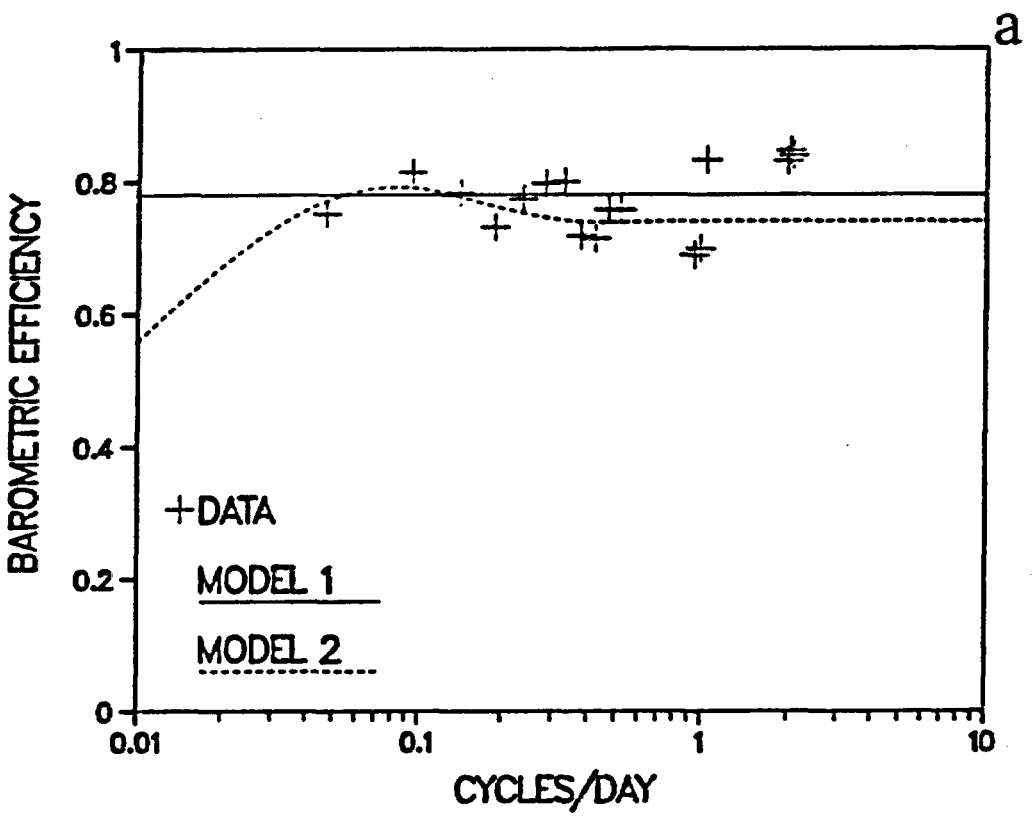

Figure 3-10: Response of SC2 to atmospheric pressure in terms of barometric efficiency (a) and phase (b). Fit to data is solid line denoted as 'MODEL'.

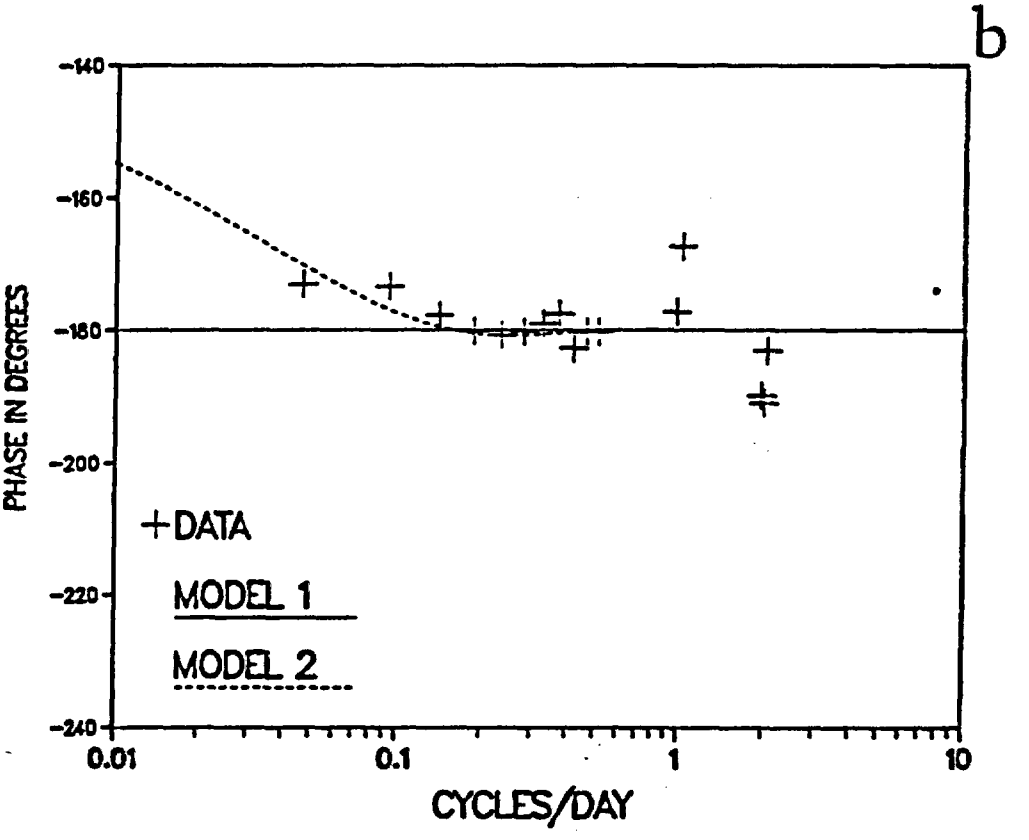
b
-140
-160
-180
-200
-220
-240
PHASE IN DEGREES
+DATA
MODEL 1
MODEL 2
0.01
0.1
1
10
CYCLES/DAY

It moved and moved, and took at last
A certain shape...

Samuel Taylor Coleridge

CHAPTER 4

THE INFLUENCE OF VERTICAL FLUID FLOW ON THE RESPONSE OF THE WATER LEVEL IN A WELL TO ATMOSPHERIC LOADING UNDER UNCONFINED CONDITIONS

ABSTRACT

The response of the water level in a well to atmospheric loading under unconfined conditions can be explained if the response is controlled by the aquifer response averaged over the saturated depth of the well. Because vertical averaging tends to diminish the influence of the water table, the response is qualitatively similar to the response of a well under partially confined conditions. At frequencies when the influence of well bore storage can be ignored, the response is strongly governed by two dimensionless vertical fluid flow parameters: a dimensionless unsaturated zone frequency, R, and a dimensionless aquifer frequency Q_u. When Q_u is large, the response of the well approaches the static response of the aquifer under confined conditions. When R is large relative to Q_u the response is strongly influenced by attenuation and phase shift of the air pressure signal in the unsaturated zone. At small values of Q_u, the well response is strongly influenced by the presence of the water table. The theoretical response of a phreatic well can be fit to the well

response inferred from cross-spectral estimation to yield estimates of the air diffusivity of the unsaturated zone and (if the specific storage of the aquifer is known) the vertical permeability of the aquifer.

INTRODUCTION

In some wells which tap unconfined aquifers, the water level in the well sensibly responds to rock deformation induced by both atmospheric loading and earth tides (e.g. Bower and Heaton, 1973; 1978). For these wells, the water level change cannot be a direct reflection of the water table response. While water table response to atmospheric loading may be influenced by unsaturated zone effects (Yusa, 1969; Weeks, 1979), the water table can be expected to be largely insensitive to earth-tide induced deformation (Bredehoeft, 1967).

Water level fluctuations in phreatic wells produced by changes in both earth tides and atmospheric loading can be explained if we assume that the water level in the well reflects the response of the aquifer averaged over the saturated depth of the well. While the water table is largely insensitive to rock deformation, the aquifer at depth can be largely isolated from water table influences if the vertical hydraulic diffusivity of the aquifer is low. For thick unconfined aquifers, the average response will at least be partially influenced by the response of the aquifer under conditions where the water table has little influence; the response will be qualitatively similar to the response of wells under partially confined conditions (see Chapter

2). As in the partially confined case, the barometric and tidal response will be a function of the length of time or frequency over which the deformation takes place. Water well response due to rapid changes in deformation will be weakly influenced by the water table response; the response will approach that which would occur if the aquifer were confined (Jacob, 1940; Bredehoeft, 1967; Van der Kamp and Gale, 1983; see Chapter 1). Water level response to slow changes in deformation will be strongly influenced by the water table response. Since atmospheric loading operates over a much wider frequency band than tidal forcing, this paper focuses on the barometric response of phreatic water wells.

Figure 4-1a shows an idealized cross section of a phreatic well and Figure 4-1b shows qualitatively the response of a phreatic well to a step change in atmospheric load. As suggested in the figure, fluid flow is an intrinsic part of water well response. A step change in atmospheric load will introduce three pressure potential imbalances in the well-aquifer system which induce fluid flow. The aquifer is pressurized instantaneously by an amount $\gamma\Delta P$ due to the surface load via grain to grain contact, where γ is the surface loading efficiency of the aquifer (see Chapter 1). The pressure change at the water surface of the open well is ΔP and the pressure change at the water table (due to its high storage) is, at least initially, negligible.

The pressure imbalance ΔP for the air between the earth's surface and the water table induces vertical flow of the air phase of the unsaturated zone. The pressure potential imbalance $\gamma\Delta P$ between the initial response of the water table and the instantaneous response of the aquifer induces vertical groundwater flow. Lateral and vertical

groundwater flow in the aquifer are induced by the pressure potential imbalance $(1-\gamma)\Delta P$ between the instantaneous response of the open well and the aquifer. If the well radius is small and the horizontal transmissivity of the aquifer is high, the well and the aquifer will quickly be in quasi-static equilibrium. The radial component of groundwater flow, although substantial near the well bore, will not significantly influence the aquifer head and the depth-averaged aquifer head will be influenced by vertical fluid flow alone. In this paper, I assume that the well is in quasi-static equilibrium with the aquifer.

The response of a well under conditions of quasi-static equilibrium to a step change in atmospheric load will (under certain conditions which will be examined below) take place in three stages (Figure 4-1b). During stage 1, well response strongly reflects the instantaneous compression of the aquifer due to the surface load. Fluid flow to the water table has only just begun to depressurize the aquifer. The water level in the well initially drops by an amount which is slightly greater than the static-confined response (i.e. the response that would occur if the aquifer were completely isolated from the water table) and only gradually continues to drop. Following stage 1, the average response of the aquifer is increasingly influenced by fluid flow to the water table; over this time interval (stage 2), the water table height is essentially static and insulated from air flow through the unsaturated zone. The water level in the well continues to drop and the well response eventually asymptotically approaches the negative of the atmospheric load (ie. the barometric efficiency approaches unity). Finally (stage 3), air flow causes the

water table to pressurize and, since (during this stage) the depth-averaged aquifer pressure change is the same as the water table pressure change, the barometric efficiency of the well approaches 0.

The response of phreatic wells to atmospheric loading has been examined by other workers. Bower and Heaton (1973) examined the response under the assumption that the well was open only at the bottom of the hole and that unsaturated zone and well bore storage effects were negligible. Johnson (1973) examined the theoretical response in a spherically shaped aquifer under the assumptions that unsaturated zone effects were negligible and that the water table was a fixed boundary. Yusa (1969) and Weeks (1979) examined the influence of the unsaturated zone on well response and assumed that: well bore storage effects were negligible; the water table was a fixed boundary; and the water table pressure change due to the atmospheric load represented the pressure change throughout the monitored depth of the aquifer.

This study extends the work of Yusa (1969) and Weeks (1979) by examining the theoretical response of water wells to atmospheric loading under conditions where: (1) the water table is a moving boundary; (2) the water well responds to the vertically averaged aquifer pressure change over the saturated depth of the well. As in the analysis of Yusa (1969) and Weeks (1979), I assume that well bore storage effects are negligible. Comparison is made with the theoretical results given in Chapter 3 for water well response under partially confined conditions. The theoretical model is then applied to the response of a phreatic well to atmospheric loading to yield

estimates of the air diffusivity of the unsaturated zone and the vertical hydraulic diffusivity of the unconfined aquifer.

SOLUTION TO THE RESPONSE OF A WELL IN AN UNCONFINED AQUIFER TO PERIODIC ATMOSPHERIC LOADING

The response of a phreatic water well to atmospheric loading can be broken up into five processes: 1) mechanical loading of the aquifer due to the surface load; 2) pressurization at the water surface of the open well due to the air load; 3) diffusion of air pressure between the earth's surface and the water table; 4) vertical diffusion of groundwater pressure through the aquifer; 5) diffusion of groundwater pressure between the aquifer and the borehole. As noted in Chapter 3, these processes also influence the response of well-aquifer systems under partially confined conditions. I can readily obtain a closed form solution to the response of a phreatic well to atmospheric loading if I assume that: (1) the well bore is in quasi-static equilibrium with the vertically-averaged aquifer pressure (i.e. well bore storage effects are negligible); (2) the aquifer has uniform material properties; and (3) that air flow between the earth's surface and the water table is predominantly vertical. The solution can be obtained by combining the solutions to two separate fluid flow problems: 1) vertical air flow between the earth's surface and the water table; and 2) vertical diffusion of the atmospheric pressure signal through the unconfined aquifer with concomitant loading. As is noted in detail below, the response given by this solution is

analogous to the 'low frequency' response for wells under partially confined conditions given in Chapter 3.

Vertical air flow between the earth's surface and the water table

As in the response under partially confined conditions, I assume that periodic vertical flow of air between the earth's surface and the water table is governed by a simple diffusion equation given elsewhere (Weeks, 1979). If I assume that the fluctuation of the water table is small relative to the thickness of the unsaturated zone (an assumption examined below) then, the solution for air pressure at the mean height of the water table (z=0), P_a, is (see Chapter 2):

$$P_a = (M-iN)A\exp(i\omega t) \qquad (1)$$

where M and N are:

$$M = \frac{2\cosh(\sqrt{\bar{R}})\cos(\sqrt{\bar{R}})}{\cosh(2\sqrt{\bar{R}})+\cos(2\sqrt{\bar{R}})} \qquad (2a)$$

$$N = \frac{2\sinh(\sqrt{\bar{R}})\sin(\sqrt{\bar{R}})}{\cosh(2\sqrt{\bar{R}})+\cos(2\sqrt{\bar{R}})} \qquad (2b)$$

and R is a dimensionless frequency referenced to air diffusivity, D_a, and the depth, L, from the earth's surface to the water table:

$$R = L^2\omega/2D_a \qquad (3)$$

Vertical diffusion of the atmospheric pressure signal through the aquifer: first order approximation

In the absence of well bore drainage effects, the response of the unconfined aquifer to periodic atmospheric loading is governed by (see Chapter 1):

$$D\frac{\partial^2 P}{\partial z^2} = \frac{\partial P}{\partial t} + \gamma A\omega \sin\omega t \qquad (4)$$

where D is the vertical hydraulic diffusivity of the unconfined aquifer under conditions where the principal components of horizontal strain are 1/2 the vertical strain, P is pore pressure and γ is the surface loading efficiency. The source term in equation 4 accounts for the deformation of the aquifer due to the imposed surface load. It should be noted that I take compression to be positive.

The appropriate boundary conditions should take into account the possible effect of any periodic fluctuations in water table height. If the water table boundary condition is imposed at the mean height of the water table (z=0), I obtain the following first-order, linearized approximation of the boundary conditions:

$$\partial P(0,t)/\partial z = -(S_y/K_z)\partial P(0,t)/\partial t + (S_y/K_z)[\,MA\sin(\omega t) - NA\cos(\omega t)] \qquad (5a)$$

$$P(\infty,t) = A\gamma\cos(\omega t) \qquad (5b)$$

where K_z and S_y are the vertical hydraulic conductivity and specific yield of the aquifer respectively. The first term on the right hand side of the water table boundary condition is identical to the first order approximation used by Neuman (1972) in his analysis of the response of phreatic wells to constant pumpage. The second term on the right hand side of the water table boundary condition is obtained from the solution given by equation 1 and accounts for the influence of air diffusion on the well response. Equation 5b states that at infinite depth, the aquifer pressure change due to atmospheric loading is isolated from water table influences. This boundary condition assumes that the aquifer is very thick and its appropriateness is discussed below. The solution of equation 4 subject to boundary conditions given in equation 5 is given in Appendix A:

$$P = \frac{(M-iN-\gamma)}{\Omega} A\exp(-(i+1)\sqrt{Q_v})\exp(i\omega t) + A\gamma\exp(i\omega t) \qquad (6)$$

where Ω is a dimensionless parameter which which governs the movement of the water table:

$$\Omega = \left\{1 - (1-i)\frac{\sqrt{Q_v}\, S_s z}{2Q_v S_y}\right\} \qquad (7)$$

and Q_v is a dimensionless frequency referenced to the saturated thickness at the depth of interest, z (the depth from the mean height of the water table to the observation point), the specific storage of

the aquifer under conditions of surface loading (see Chapter 1), S_s, and the vertical hydraulic conductivity of the aquifer, K_z:

$$Q_v = \frac{\omega S_s z^2}{2K_z} = \frac{\omega z^2}{2D} \tag{8}$$

It should be noted that equation 6 is nearly the same as the solution given in Chapter 3 for diffusion of the air pressure signal through a partial confining layer. The difference here is that I have allowed the water table to periodically fluctuate. The significance of water table fluctuations is discussed in detail in the following section.

Since water well response is driven by the depth averaged pressure change in the aquifer, $\bar{P}$, I vertically average the solution in equation 6 over the saturated well depth to obtain:

$$\bar{P} = \left[\frac{(\bar{U} + i\bar{V})}{\Omega_u} - \gamma \right] A \exp(i\omega t) \tag{9}$$

where $\bar{U}$ and $\bar{V}$ are:

$$\bar{U} = (-M + \gamma)\exp-\lfloor\bar{Q}_u[-\cos\lfloor\bar{Q}_u + \sin\lfloor\bar{Q}_u]/2\lfloor\bar{Q}_u + N\exp-\lfloor\bar{Q}_u[-\cos\lfloor\bar{Q}_u - \sin\lfloor\bar{Q}_u]/2\lfloor\bar{Q}_u + (-M+\gamma+N)/2\lfloor\bar{Q}_u \tag{10a}$$

$$\bar{V} = (M - \gamma)\exp-\lfloor\bar{Q}_u[-\cos\lfloor\bar{Q}_u - \sin\lfloor\bar{Q}_u]/2\lfloor\bar{Q}_u + N\exp-\lfloor\bar{Q}_u[-\cos\lfloor\bar{Q}_u + \sin\lfloor\bar{Q}_u]/2\lfloor\bar{Q}_u + (M-\gamma+N)/2\lfloor\bar{Q}_u \tag{10b}$$

and Q_u and Ω_u are a dimensionless aquifer frequency and dimensionless water table parameter respectively, both of which are referenced to the saturated thickness of the well, b:

$$Q_u = \frac{\omega S_s b^2}{2K_z} = \frac{\omega b^2}{2D} \tag{11a}$$

$$\Omega_u = \left\{1 - (1-i)\frac{\sqrt{Q_u}\, S_s b}{2Q_u S_y}\right\} \tag{11b}$$

The solutions given in equations 6 and 9 assume that the aquifer is of infinite vertical extent. They are appropriate at frequencies where the depth of significant pressure diffusion is less than the thickness of the aquifer. By analogy to heat flow (Carslaw and Jaeger, p. 66, 1959), this diffusive depth, d, can be estimated from the vertical hydraulic diffusivity of the material, K_z/S_s:

$$d = \sqrt{\frac{4\pi K_z}{S_s \omega}} \tag{12}$$

For rock with a hydraulic conductivity typical for the crust of 1×10^{-5} cm/sec (Brace, 1980; 1984) and a specific storage of 1×10^{-8} cm^{-1}, an atmospheric cycle with a period of 1 day would cause significant pressure diffusion down to depths of about 350 meters. Use of the solution given in equation 9 would be appropriate for analysis of this atmospheric cycle with this moderate hydraulic conductivity and specific storage if the aquifer were thick.

Response of a phreatic well to atmospheric loading

The response of a well to atmospheric loading can be obtained, in the absence of well bore storage effects, through the use of equation 9. Because I assume that in the frequency range of interest well bore storage effects are negligible, the relation between the amplitude of the water level change in the well, x_0, and the amplitude of the atmospheric load wave, A, is:

$$x_0 = -A/\rho g + \bar{P}_0/\rho g \qquad (13)$$

where $\bar{P}_0$ is the far-field depth-averaged pore pressure within the aquifer, $\bar{P}$, divided by $\exp(i\omega t)$:

$$\bar{P}_0 = \bar{P}\exp(-i\omega t) \qquad (14)$$

Equation 13 describes the response of the well in the frequency domain and states that the change in water level in the well plus the atmospheric load (in terms of equivalent change of water level) equals the far-field, depth-averaged pore pressure change (in terms of equivalent water level).

The barometric efficiency, BE, and phase, θ, of the response are:

$$BE(\omega) = \left|\frac{x_0 \rho g}{A}\right| = \left|\bar{P}_0/A - 1\right| \qquad (15a)$$

$$\theta(\omega) = \arg(x_0 \rho g / A) \qquad (15b)$$

where the vertical bars in equation 15a denote the modulus of the complex function; and 'arg' in equation 15b denotes the inverse tangent of the ratio of the imaginary component to the real component of the complex function. Equations 9 and 15 indicate that the barometric efficiency, BE, and phase, θ, of the response are a function of 5 dimensionless parameters: 1) R, the dimensionless unsaturated frequency; 2) Q_u, the dimensionless frequency of the aquifer; 3) $S_s b$, the specific storage of the aquifer under conditions of surface loading multiplied by the saturated well depth; 4) S_y, the specific yield of the aquifer; and 5) γ, the surface loading efficiency of the aquifer.

Figure 4-2 shows the response of a water well as a function of dimensionless aquifer frequency Q_u and dimensionless unsaturated zone frequency R. The static-confined barometric efficiency of the well is 0.5 (γ=0.5). The water table is assumed to be fixed (ie. the ratio of S_y to $S_s b$ is assumed to be infinite and the dimensionless parameter Ω_u is unity), an assumption which will be relaxed below. The response is qualitatively similar to the 'low frequency' response of a partially confined well given in Chapter 3. Water well response is a strong function of both R and Q_u. When the ratio R/Q_u is 10^{-4} or less, attenuation of air flow has little influence on response and the barometric efficiency gradually attenuates (relative to the static-confined response) with decreasing frequency; the phase shows a monotonic advance with decreasing frequency. The increasing phase advance and attenuation with decreasing frequency shown for the case

when R/Q_u is 10^{-4} is analogous to the long period response to the step load (stage 3) shown in Figure 4-1b. The water table, which is fully pressurized by the atmospheric load, increasingly influences the depth-averaged aquifer response and causes the barometric efficiency to asymptotically approach 0. For larger values of R/Q_u, however, the water table response to periodic atmospheric loading is attenuated by unsaturated zone influences. As a result, the barometric efficiency curves exceed the confined response over much of the frequency band analyzed and the phase curves show a slight lag. The increasing barometric efficiency with decreasing frequency when R/Q_u is large is qualitatively analogous to stage 2 in Figure 4-1b. When R/Q_u is large, the water table can be effectively isolated from the atmospheric load at the soil surface and the barometric efficiency can approach unity. It should be noted that when R/Q_u is greater than 10, the barometric efficiency at the resonance frequency of the system actually exceeds unity.

For comparison with the unconfined response, I show the solution to the 'low frequency', partially confined response given in Chapter3 as a function of R/Q in Figure 4-3. The parameter Q represents a dimensionless frequency referenced to the vertical hydraulic diffusivity, D', and thickness, b', of the partial confining layer:

$$Q = \frac{\omega b'^2}{2D'} \qquad (16)$$

The results shown in Figure 4-3 represent the response at the base of the partial confining layer. Under conditions where Q_u equals Q and

the geometry and air flow parameters of the unsaturated zone for both unconfined and partially confined conditions are identical, the difference between Figures 4-2 and 4-3 strictly reflects the difference between the vertically averaged unconfined aquifer response and the response of a thin partially confined aquifer. Comparison of Figure 4-2 with Figure 4-3 indicates that when R/Q_u and R/Q are greater than 100, there is little difference in the responses; for both cases, unsaturated zone influences strongly control the response throughout the frequency band examined. When R/Q_u and R/Q are less than 100, however, there is a substantial difference between the responses; attenuation and phase shift due to water table drainage occur significantly more rapidly under unconfined conditions.

The effect of allowing the water table to fluctuate is shown in Figure 4-4 by allowing S_y to be less than infinite. The response when the ratio $S_y/S_s b$ equals 10^8 (Figures 4-4a and 4-4b) indicates that in comparison to the response which ignores water table fluctuations, there are relatively rapid changes in phase at low values of dimensionless frequency Q_u and high ratios of R/Q_u; the response of the barometric efficiency, however, is indistinguishable from the curves shown in Figure 4-2. Decreasing the ratio $S_y/S_s b$ to 10 (Figures 4-4c and 4-4d), causes distinguishable changes in response in both the barometric efficiency and phase curves. The barometric efficiency curves show a rise with decreasing frequency at low values of Q_u (less than 0.01). This increase has no analog in Figure 4-1b and is due to significant water table fluctuations at low frequencies. Phase relations, when the ratio $S_y/S_s b$ is 10, show increasingly less phase shift with decreasing frequency at low values of Q_u.

It is worth examining whether the influence of a fluctuating water table can be expected to be identifiable in a well's response to atmospheric loading. Noting that significant water table fluctuation occurs when Q_u is less than 0.01 and $S_y/S_s b$ is 10 or less, the highest frequency at which water table fluctuations might be observable is given by:

$$\omega = \frac{S_s K_v}{5 S_y^2} \qquad (17)$$

Water table fluctuations at a given frequency are thus enhanced when rock is highly compressible and has high hydraulic conductivity and low specific yield. If we limit our analysis to atmospheric cycles with period less than 50 days, an aquifer with a compressibility typical of rock of 10^{-11} cm^2/dyne (Haas, 1981) and a specific yield of 0.1 will show significant water table fluctuations only if the vertical hydraulic conductivity of the aquifer exceeds 1 cm/sec. Such a value for hydraulic conductivity is very high compared to typical crustal values (Brace, 1980). Furthermore, the depth of diffusive penetration for an atmospheric cycle with period of 50 days would (by equation 11) have to be nearly 800 km under such hydraulic conditions. This depth is well beyond the thickness of the crust of the earth. Thus significant water table fluctuations due to atmospheric loading cannot be expected to occur.

APPLICATION OF THEORETICAL RESPONSE

The theoretical results given above indicate that water well response to atmospheric loading will be strongly dependent on two dimensionless parameters: R and Q_u. If the response of a well can be fit to the theoretical solutions, it is possible to make estimates of or place bounds on these these dimensionless parameters. The parameters R and Q_u can then be used to estimate the air diffusivity of the unsaturated zone and the vertical aquifer diffusivity respectively. As is noted in Chapter 3, the process of fitting well response as a function of frequency to dimensionless theoretical curves is analogous to the standard practice of fitting water level declines as a function of time in response to pumpage to 'type curve' plots. The essential difference is that because the solutions given here are a function of frequency, there are two 'type curves' which are fit simultaneously: one for barometric efficiency and one for phase.

A description of the well (GD) examined in this paper is given in Table 4-1. Well GD taps an unconfined granodiorite aquifer of unknown but presumably considerable vertical extent. The lateral aquifer permeability at GD was determined from its response to an earthquake (Evelyn Roeloffs, personal communication). If it is assumed that the influence of well bore storage on the response of unconfined wells can be approximated by the theoretical response of confined or partially confined aquifers to periodic loading (Hsieh et al., 1987; see Chapter 3), the lateral permeability of this well indicates that well bore storage effects will be small or negligible at frequencies less than 2 cycles/day. Under these conditions, the response given by equation 9 will be valid if the aquifer is relatively thick.

In order to compare a water well's response to the theoretical solutions, we need to determine its transfer function: the estimated barometric efficiency and phase as a function of frequency. The transfer function for the well was determined from cross-spectral estimation (Bendat and Piersol, 1986) and details are discussed in Appendix B. Application of the theoretical results over a wide frequency band is limited by the length of the data sets and the magnitude of the atmospheric pressure signal. For GD, the length of the water level record examined is roughly 5 months. As shown in Chapter 2, atmospheric loading has a small signal at frequencies greater than 2 cycles/day and we limit our analysis to frequencies no higher than this bound. The low end of the frequency band analyzed for each well was determined from the coherence squared, Γ^2, of the relationship between water level and atmospheric loading where the coherence squared is defined as (Bendat and Piersol, 1986):

$$\Gamma^2(\omega) = \frac{|BW(\omega)|^2}{BB(\omega)WW(\omega)} \qquad (16)$$

It should be noted that BW is the cross spectrum between air pressure and water level and BB and WW are the power spectra of the atmospheric load and the water level respectively. The coherence squared is analogous to r^2 in linear regression and represents the ability of a linear relationship between atmospheric load and water level to account for the water level signal at a given frequency. For the well response analyzed here, I excluded frequencies at which the coherence squared was less than 0.7; this limited analysis to frequencies

greater than 0.09 cycles/day. I also excluded frequencies at which the value of the water level power spectrum was less than 0.1 cm^2days/cycle because transfer function estimates at frequencies where the value of the water level spectrum was below this limit were implausible: the barometric efficiency and phase appeared to be a random function of frequency and sometimes had values which had no theoretical basis.

The transfer function for the response of well GD to atmospheric loading is shown in Figure 4-5. Barometric efficiency is a strong function of frequency and ranges from 0.3 to 0.6 in the frequency band examined. The phase indicates that the water level lags the atmospheric load over much of the frequency band analyzed, but this phase lag diminishes with decreasing frequency. The figure also shows the model fit to the observed transfer function. The theoretical model indicates that the response in the observed frequency band is dominated by water table influences. The depth-averaged response of the aquifer never approaches the static-confined response. The key parameters indicated by the model are a static-confined barometric efficiency of 0.10 and a value for both dimensionless frequencies R and Q_u of 4.5ω where frequency is in terms of cycles per day. The air and hydraulic diffusivities estimated from these values of R and Q_u are shown in Table 4-2. The specific storage for the aquifer under conditions of surface loading is estimated in Chapter 1 and is determined from the inferred static-confined barometric efficiency and dilatational efficiency for the well. The specific storage is used in conjunction with the hydraulic diffusivity to estimate the aquifer's vertical permeability. The vertical permeability is a factor of 30

less than the inferred lateral permeability of the aquifer, suggesting that the rock tapped by the well possesses moderate hydraulic anisotropy.

CONCLUSIONS

The water level response of wells which tap water table aquifers to atmospheric loading is qualitatively similar to the partially confined response detailed in Chapter 3; it is dependent on the elastic and fluid flow properties of the aquifer as well as the air flow properties of the material overlying the aquifer. Water well response can be dependent on the frequency of the excitation and reflects the response of the unconfined aquifer averaged over the saturated depth of the well. As in the partially confined response, attenuation and amplification relative to the static-confined response of the aquifer can occur in theory and is observed in the wells examined; phase lags and advances observed in response to atmospheric loading also have a theoretical basis.

Comparison of the theoretical response given here with the theoretical solution given elsewhere for the response of wells under partially confined conditions indicates that the responses are virtually identical when the dimensionless ratio R/Q_u is large. When R/Q_u is small (less than 100), however, we can expect the water table to have a significantly greater influence on water well response under unconfined conditions. The influence of water table fluctuations on well response can be expected to be negligible, regardless of the frequency band observed and the hydraulic properties of the aquifer.

The theoretical response can be used in conjunction with the observed response of water wells as a function of frequency to yield estimates of or place bounds on the vertical fluid flow properties of the aquifer and the air diffusivity of the unsaturated zone. The response of the well examined here to atmospheric loading indicates that the vertical permeability of the aquifer is less than the lateral permeability. Partial isolation from the water table in the aquifer at the observed frequencies is achieved because its vertical permeability is relatively low.

For the well examined, the barometric response is a strong function of frequency and estimates of the controlling parameters can be readily made. It should be noted that the parameters which control response may not always be identifiable. When the depth to the water table is shallow, it may be possible to place only an lower bound on the air diffusivity. Under conditions where the vertical hydraulic conductivity of the aquifer is relatively high and the saturated depth of the well is relatively thin, the depth averaged response of the aquifer may only be weakly influenced by the static-confined response of the aquifer in the frequency band analyzed; for these situations it may only be possible to place a lower bound on the vertical hydraulic diffusivity of the aquifer. Under conditions where the vertical conductivity of the aquifer is very low and the saturated well depth is very thick, the barometric response may be largely independent of water table influences throughout the frequency band of interest; for these situations it may be possible to place only an upper bound on the vertical hydraulic diffusivity. Although cross-spectral estimation of the response of wells to atmospheric loading may not

have universal application, the results given here indicate that it can yield some useful information about the material properties of unconfined aquifers and the unsaturated zone.

APPENDIX A: SOLUTION TO THE RESPONSE OF AN UNCONFINED AQUIFER TO PERIODIC ATMOSPHERIC LOADING

The response of an unconfined aquifer to periodic atmospheric loading is governed by (Chapter 1):

$$D\frac{\partial^2 P}{\partial z^2} = \frac{\partial P}{\partial t} + \gamma A\omega \sin\omega t \qquad \text{(A1)}$$

where compression is taken to be positive. The solution to the aquifer response can be obtained by combining the solutions to two separate boundary value problems. The sum of the boundary conditions in the two problems is equivalent to the boundary conditions given in equation 5. In the first problem, the boundary conditions are:

$$P(0,t) = (M-iN)A\exp(i\omega t) \qquad \text{(A2a)}$$

$$P(\infty,t) = (M-iN)A\exp(i\omega t) \qquad \text{(A2b)}$$

the taking of the real parts being understood. The solution of equation A1 subject to the boundary conditions of equation A2 is trivially satisfied by:

$$P(z,t) = (M-iN)A\exp(i\omega t) \qquad \text{(A3)}$$

In the second problem, the boundary conditions are:

$$\partial P(0,t)/\partial z = -(S_y/K_z)\partial P(0,t)/\partial t \qquad \text{(A4a)}$$

$$P(\infty,t) = (\gamma - M + iN)A\exp(i\omega t) \qquad \text{(A4b)}$$

Taking P to be complex:

$$P(z,t) = F(z)\exp(i\omega t)$$

and substituting in equations A1 and A4 I obtain:

$$F'' - \frac{i\omega F}{D} = \frac{i\omega A\gamma}{D} \qquad \text{(A5a)}$$

$$F'(0) = \frac{-i\omega S_y F(0)}{K_z} \qquad \text{(A5b)}$$

$$F(\infty) = A(\gamma - M + iN) \qquad \text{(A5c)}$$

Equation A5a is an ordinary differential equation and its particular solution subject to the boundary conditions is:

$$F_p(z) = A(\gamma - M + iN) \qquad \text{(A6)}$$

Its homogeneous solution is:

$$F_h(z) = \frac{(M-iN-\gamma)}{\Omega} A\exp(-(i+1)\sqrt{Q_u}) \qquad (A7)$$

Summing A6 and A7 and multiplying by exp(iωt) yields:

$$P(z,\omega) = \frac{(M-iN-\gamma)}{\Omega} A\exp(-(i+1)\sqrt{Q_u})\exp(i\omega t) + A(\gamma-M+iN)\exp(i\omega t) \qquad (A8)$$

The solution to the response of an unconfined aquifer to periodic atmospheric loading can be obtained by summing equations A3 and A8 and is given in equation 6.

APPENDIX B: METHOD BY WHICH THE TRANSFER FUNCTION OF WATER LEVEL TO ATMOSPHERIC LOAD WAS DETERMINED

The transfer function between water level and atmospheric loading was found using cross-spectral estimation (Bendat and Piersol, 1986). For the water well records examined here, the transfer functions were obtained by: 1) removing the mean and the long term trend from the water level and atmospheric loading time series; 2) determining the power spectra and cross-spectra for the water well record, the local atmospheric pressure record and the theoretical areal strain produced by the earth tides; 3) solving the following system of complex linear equations for every frequency:

$$\begin{vmatrix} BB & BT \\ TB & TT \end{vmatrix} \begin{vmatrix} HB \\ HT \end{vmatrix} = \begin{vmatrix} BW \\ TW \end{vmatrix} \qquad (B1)$$

where BB and TT denote the power spectra of the atmospheric pressure and earth tides respectively, BT and TB denote the cross spectrum and complex conjugate of the cross spectrum respectively between atmospheric loading and earth tides, BW and TW denote the cross spectra between atmospheric loading and water level and earth tides and water level respectively, and HB and HT denote the transfer function between water level and atmospheric loading and water level and earth tides respectively. The earth tides were included in the analysis because they have a strong influence on the response of the wells examined at diurnal and semi-diurnal frequencies. Further details on how the transfer functions were determined can be found in Chapter 2.

REFERENCES

Bendat, J. S., and A. G. Piersol, Random Data: Analysis and Measurement Procedures, John Wiley and Sons, New York, 566pp., 1986.

Bower, D. R., and K. C. Heaton, Response of an aquifer near Ottawa to tidal forcing and the Alaskan earthquake of 1964, Can. J. Earth Sci., 15, 331-340, 1978.

Bower, D. R. and K. C. Heaton, Response of an unconfined aquifer to atmospheric pressure, earth tides and a large earthquake, in Szadeczky-Kardoss, G., ed., Proceedings of the seventh international symposium on earth tides, Akademiai Kiado, Budapest, Hungary, 155-164, 1973.

Neuman, S. P., Theory of flow in unconfined aquifers considering delayed response of the water table, Water Resour. Res., 8, 1031-1045, 1972.

Van der Kamp, G., and J. E. Gale, Theory of earth tide and barometric effects in porous formations with compressible grains, Water Resour. Res., 19, 538-544, 1983.

Weeks, E. P., Barometric fluctuations in wells tapping deep unconfined aquifers, Water Resour. Res., 15, 1167-1176, 1979.

Yusa, Y., The fluctuation of the level of the water table due to barometric change, Geophys. Inst. Spec. Contrib., Kyoto Univ., 9, 15-28, 1969.

Table 4-1: Description of well GD.

Location	Rock type	Horizontal permeability (millidarcies)	Open Interval (meters)	Depth to water table (meters)
Parkfield, CA	Granodiorite	3×10^{1}	18-88	18

Table 4-2: Estimate of fluid flow properties of well GD.

Vertical aquifer hydraulic diffusivity (cm^2/sec)	Unsaturated zone air diffusivity (cm^2/sec)	Specific storage under surface loading (cm^{-1})	Vertical aquifer permeability (millidarcies)
6×10^{1}	4×10^{0}	2×10^{-8}	1×10^{0}

a

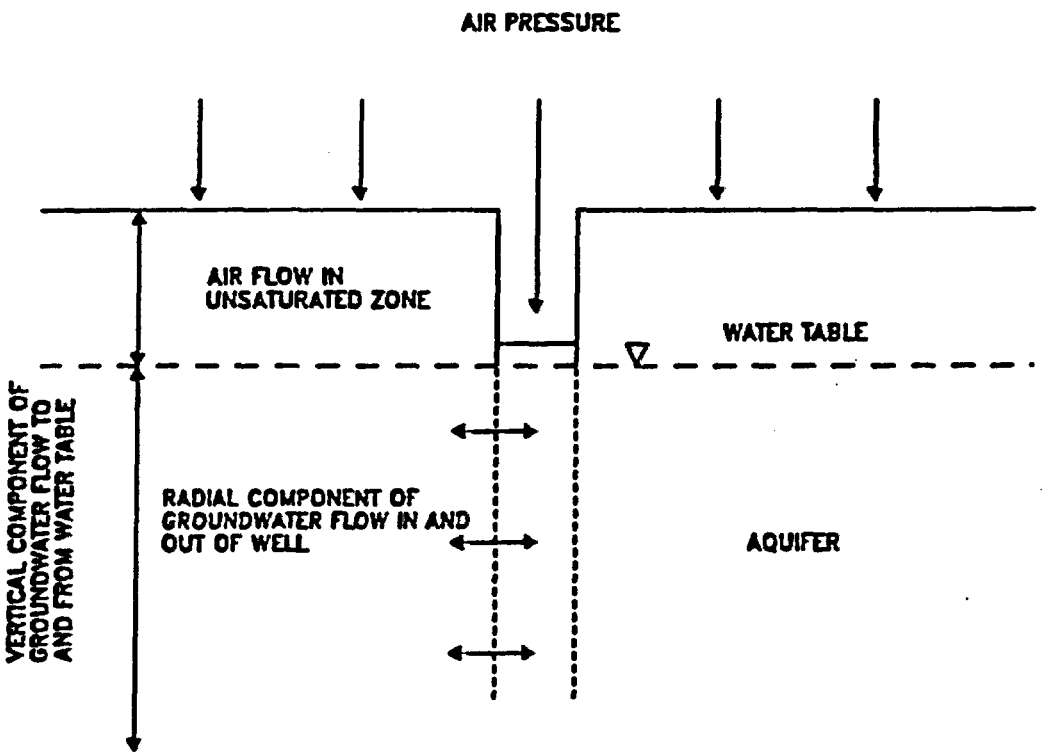

Figure 4-1: Cross-section of a phreatic well and influences of fluid flow on well response to atmospheric loading (a); idealized response of a well to a step change in atmospheric load ignoring the influence of well bore storage (b).

b

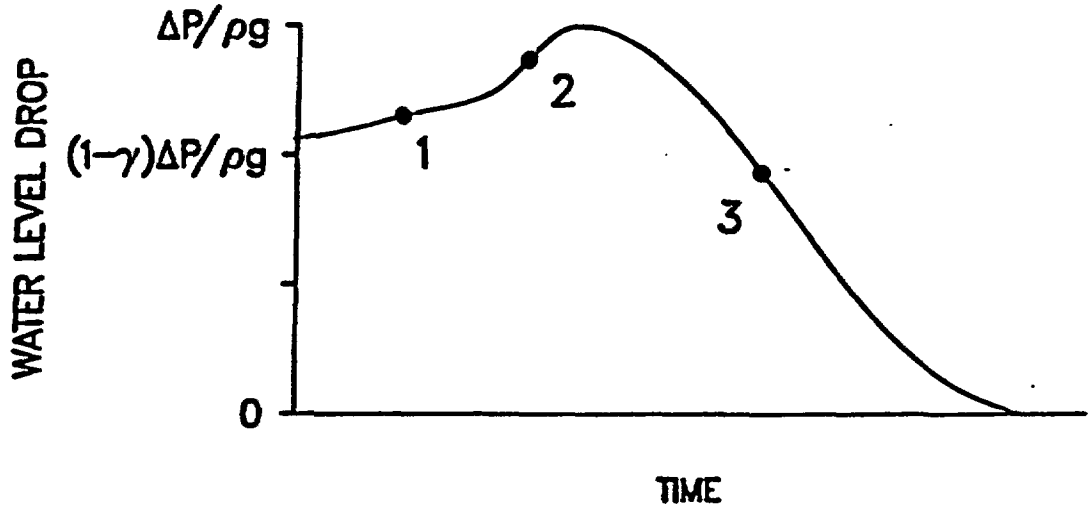

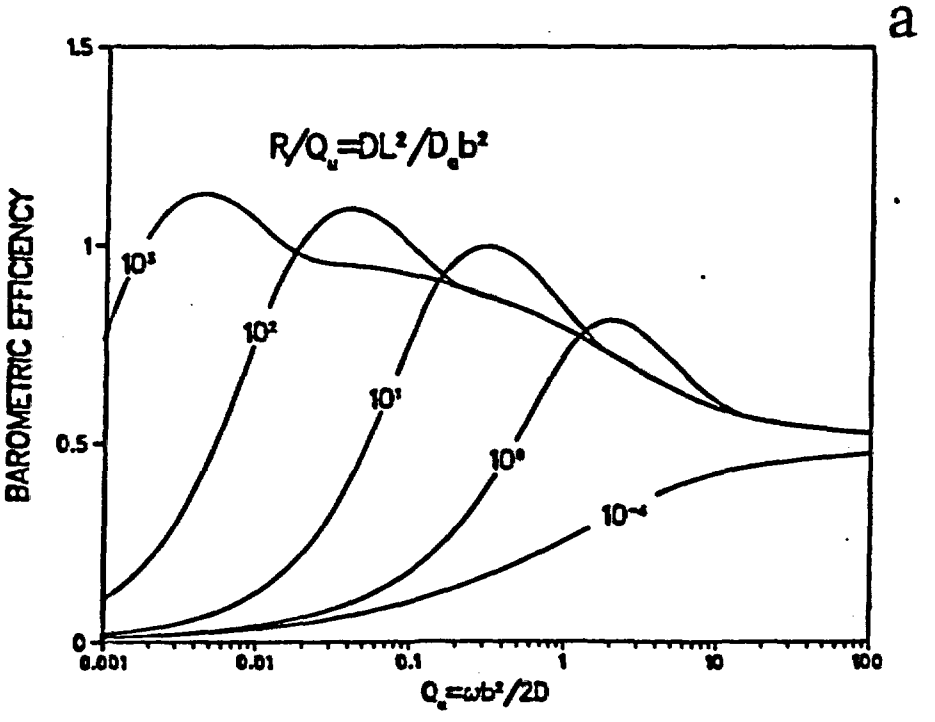

Figure 4-2: Barometric efficiency (a) and phase (b) of response of a phreatic well to atmospheric loading as a function of R/Q_u when $S_y/S_s b$ is infinite. Static-confined barometric efficiency of the well is 0.5.

b

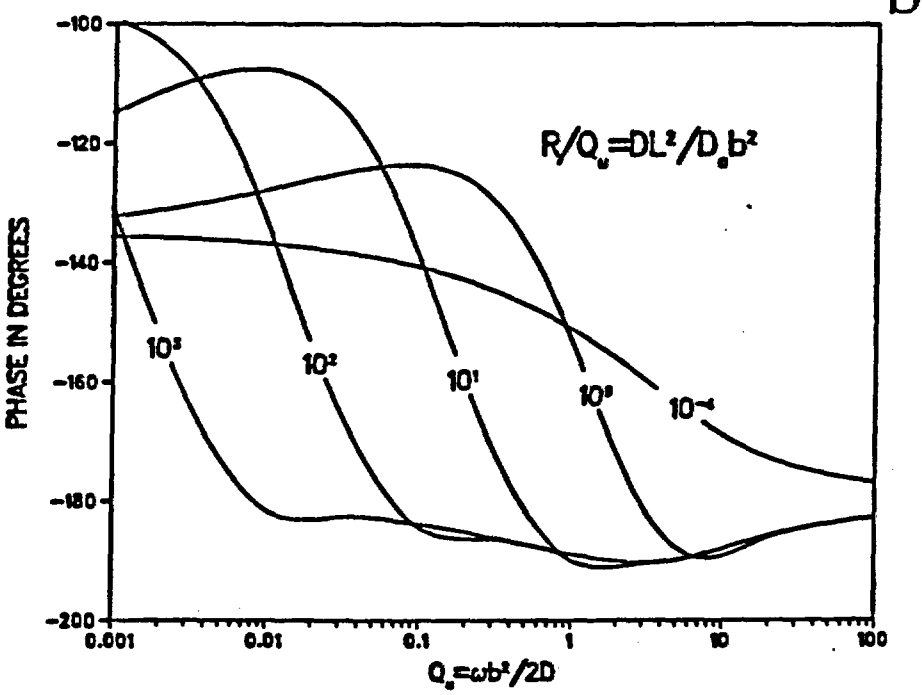
-100
-120
-140
-160
-180
-200
PHASE IN DEGREES
0.001
0.01
0.1
1
10
100
$Q_a=\omega b^2/2D$
$R/Q_u=DL^2/D_a b^2$
10^3
10^2
10^1
10^0
10^{-1}

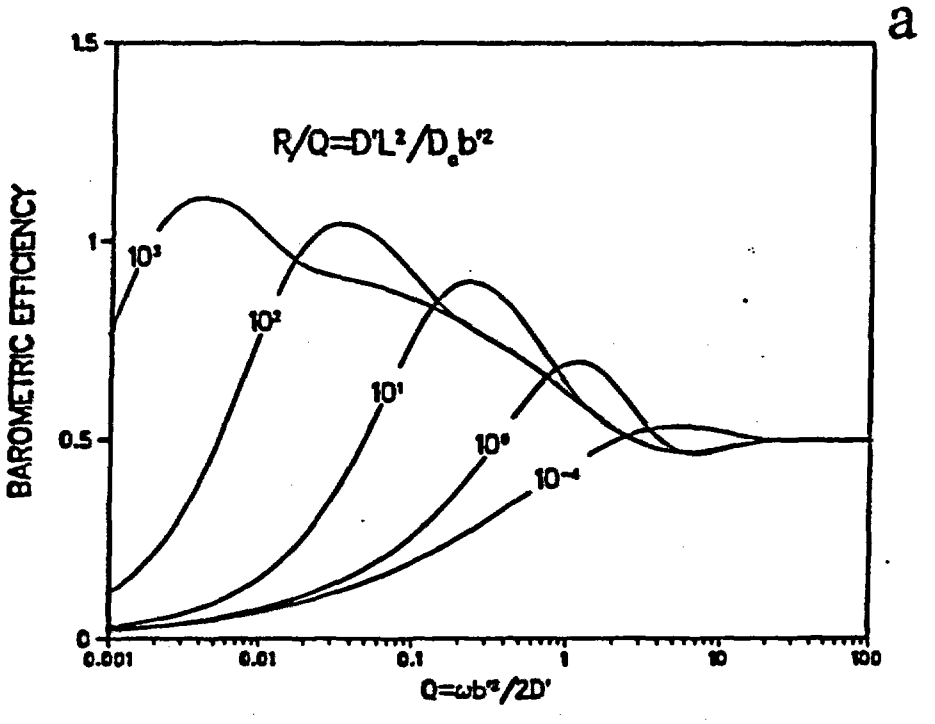

Figure 4-3: Barometric efficiency (a) and phase (b) of response of a partially confined well to atmospheric loading as a function of R/Q ignoring the influence of well bore storage. Static-confined barometric efficiency of the well is 0.5.

b

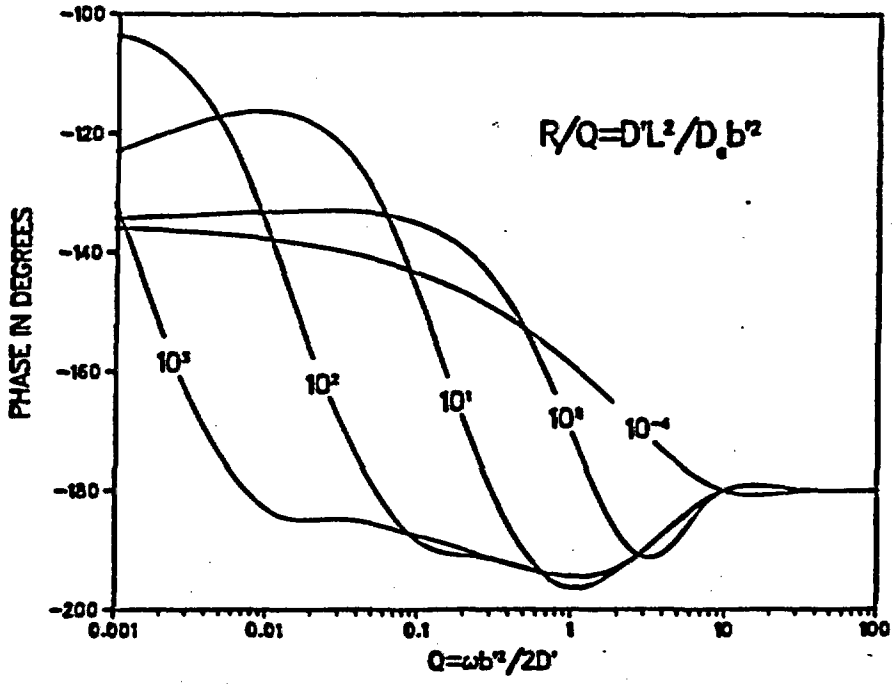
-100
-120
-140
-160
-180
-200
PHASE IN DEGREES
R/Q=D'L²/D_eb'²
10³
10²
10¹
10⁰
10⁻¹
0.001
0.01
0.1
1
10
100
Q=ωb'²/2D'

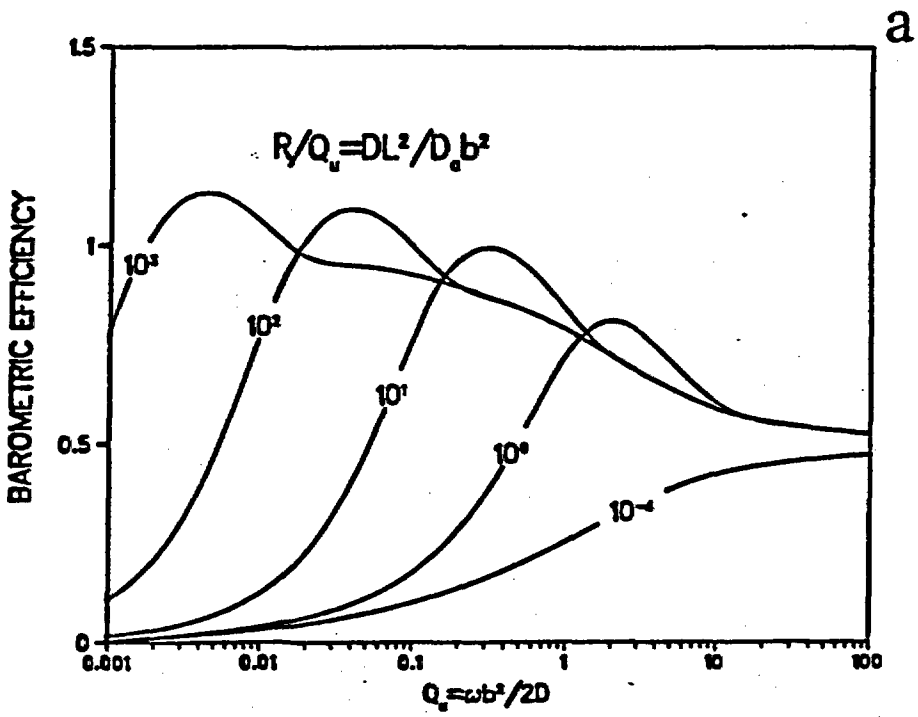

Figure 4-4: Barometric efficiency (a) and phase (b) of response of a phreatic well to atmospheric loading as a function of R/Q_u when $S_y/S_s b$ is 10^3; when $S_y/S_s b$ is 10 (c and d). Static-confined barometric efficiency of the well is 0.5.

C

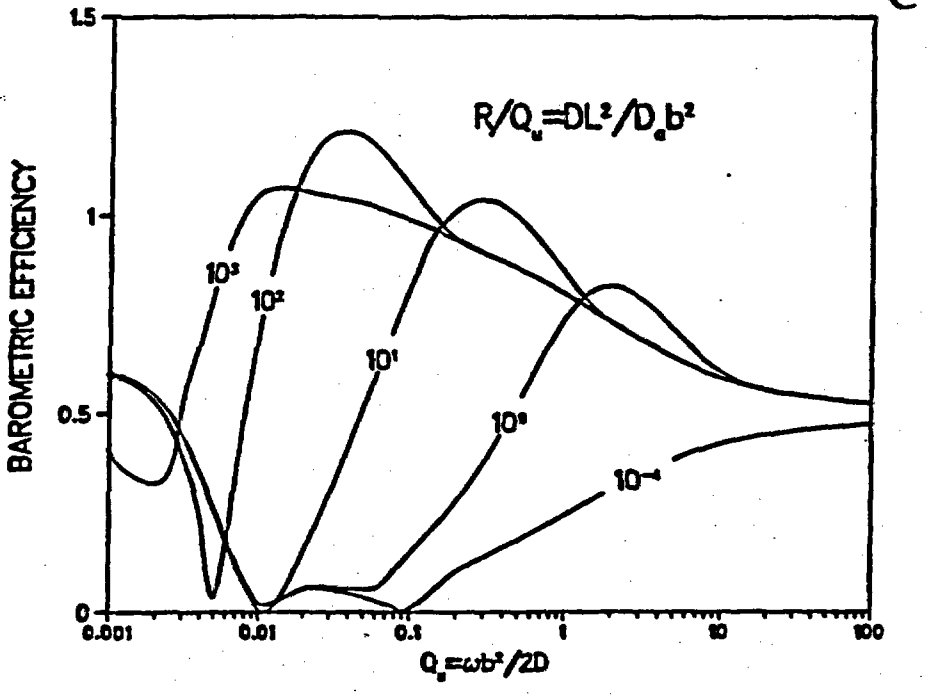
1.5
1
0.5
0
BAROMETRIC EFFICIENCY
$R/Q_u = DL^2/D_e b^2$
10^3
10^2
10^1
10^0
10^{-1}
0.001
0.01
0.1
1
10
100
$Q_e = \omega b^2/2D$

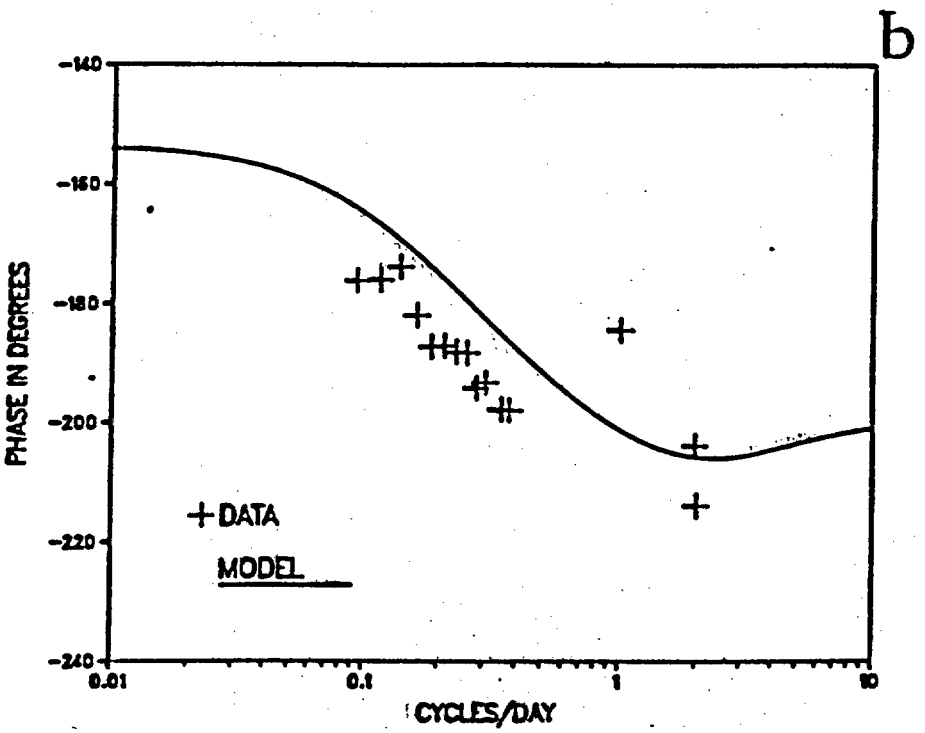
b
-140
-160
-180
-200
-220
-240
PHASE IN DEGREES
+ DATA
MODEL
0.01
0.1
1
10
CYCLES/DAY